

## DISCLAIMER

This contractor document was prepared for the U.S. Department of Energy (DOE), but has not undergone programmatic, policy, or publication review, and is provided for information only.

The document provides preliminary information that may change based on new information or analysis, and represents a conservative treatment of parameters and assumptions to be used specifically for Total System Performance Assessment analyses. The document is a preliminary lower level contractor document and is not intended for publication or wide distribution.

Although this document has undergone technical reviews at the contractor organization, it has not undergone a DOE policy review. Therefore, the views and opinions of authors expressed may not state or reflect those of the DOE. However, in the interest of the rapid transfer of information, we are providing this document for your information per your request.

NM5507

**OFFICE OF CIVILIAN RADIOACTIVE WASTE MANAGEMENT  
ANALYSIS/MODEL COVER SHEET**

1. QA: QA

Page: 1 of: 81

*Complete Only Applicable Items*

<p>2. <input type="checkbox"/> Analysis      Check all that apply</p> <table border="1" style="width:100%; border-collapse: collapse;"> <tr> <td style="width:20%;">Type of Analysis</td> <td><input type="checkbox"/> Engineering</td> </tr> <tr> <td></td> <td><input type="checkbox"/> Performance Assessment</td> </tr> <tr> <td></td> <td><input type="checkbox"/> Scientific</td> </tr> </table> <table border="1" style="width:100%; border-collapse: collapse;"> <tr> <td style="width:20%;">Intended Use of Analysis</td> <td><input type="checkbox"/> Input to Calculation</td> </tr> <tr> <td></td> <td><input type="checkbox"/> Input to another Analysis or Model</td> </tr> <tr> <td></td> <td><input type="checkbox"/> Input to Technical Document</td> </tr> <tr> <td></td> <td><input type="checkbox"/> Input to other Technical Products</td> </tr> </table> <p>Describe use:</p>	Type of Analysis	<input type="checkbox"/> Engineering		<input type="checkbox"/> Performance Assessment		<input type="checkbox"/> Scientific	Intended Use of Analysis	<input type="checkbox"/> Input to Calculation		<input type="checkbox"/> Input to another Analysis or Model		<input type="checkbox"/> Input to Technical Document		<input type="checkbox"/> Input to other Technical Products	<p>3. <input checked="" type="checkbox"/> Model      Check all that apply</p> <table border="1" style="width:100%; border-collapse: collapse;"> <tr> <td style="width:20%;">Type of Model</td> <td><input type="checkbox"/> Conceptual Model</td> <td><input checked="" type="checkbox"/> Abstraction Model</td> </tr> <tr> <td></td> <td><input type="checkbox"/> Mathematical Model</td> <td><input type="checkbox"/> System Model</td> </tr> <tr> <td></td> <td colspan="2"><input type="checkbox"/> Process Model</td> </tr> </table> <table border="1" style="width:100%; border-collapse: collapse;"> <tr> <td style="width:20%;">Intended Use of Model</td> <td><input checked="" type="checkbox"/> Input to Calculation</td> </tr> <tr> <td></td> <td><input checked="" type="checkbox"/> Input to another Model or Analysis</td> </tr> <tr> <td></td> <td><input checked="" type="checkbox"/> Input to Technical Document</td> </tr> <tr> <td></td> <td><input checked="" type="checkbox"/> Input to other Technical Products</td> </tr> </table> <p>Describe use: Abstraction of waste form colloid source term process models.</p>	Type of Model	<input type="checkbox"/> Conceptual Model	<input checked="" type="checkbox"/> Abstraction Model		<input type="checkbox"/> Mathematical Model	<input type="checkbox"/> System Model		<input type="checkbox"/> Process Model		Intended Use of Model	<input checked="" type="checkbox"/> Input to Calculation		<input checked="" type="checkbox"/> Input to another Model or Analysis		<input checked="" type="checkbox"/> Input to Technical Document		<input checked="" type="checkbox"/> Input to other Technical Products
Type of Analysis	<input type="checkbox"/> Engineering																															
	<input type="checkbox"/> Performance Assessment																															
	<input type="checkbox"/> Scientific																															
Intended Use of Analysis	<input type="checkbox"/> Input to Calculation																															
	<input type="checkbox"/> Input to another Analysis or Model																															
	<input type="checkbox"/> Input to Technical Document																															
	<input type="checkbox"/> Input to other Technical Products																															
Type of Model	<input type="checkbox"/> Conceptual Model	<input checked="" type="checkbox"/> Abstraction Model																														
	<input type="checkbox"/> Mathematical Model	<input type="checkbox"/> System Model																														
	<input type="checkbox"/> Process Model																															
Intended Use of Model	<input checked="" type="checkbox"/> Input to Calculation																															
	<input checked="" type="checkbox"/> Input to another Model or Analysis																															
	<input checked="" type="checkbox"/> Input to Technical Document																															
	<input checked="" type="checkbox"/> Input to other Technical Products																															

4. Title:  
Waste Form Colloid-Associated Concentrations Limits: Abstraction And Summary

5. Document Identifier (including Rev. No. and Change No., if applicable):  
ANL-WIS-MD-000012 REV00

Total Attachments: 16	7. Attachment Numbers - No. of Pages in Each: I-3, II-2, III-2, IV-2, V-2, VI-2, VII-2, VIII-2, IX-2, X-2, XI-2, XII-2, XIII-2, XIV-2, XV-1, XVI-14
--------------------------	--

	Printed Name	Signature	Date
8. Originator	Stephen Alcorn	<i>Robert MacKinnon for SA</i>	4/28/00
9. Checker	Hans Papenguth	<i>Robert MacKinnon for HP</i>	4/28/00
10. Lead/Supervisor	Rob P. Rechar	<i>Robert MacKinnon for RR</i>	4/28/00
11. Responsible Manager	Bob MacKinnon	<i>Robert MacKinnon</i>	4/28/00

12. Remarks:  
00 INITIAL ISSUE

**INFORMATION COPY**

**LAS VEGAS DOCUMENT CONTROL**

OFFICE OF CIVILIAN RADIOACTIVE WASTE MANAGEMENT  
ANALYSIS/MODEL REVISION RECORD

*Complete Only Applicable Items*

1. Page: 2 of: 81

2. Analysis or Model Title:

Colloid-Associated Concentration Limits: Abstraction and Summary

3. Document Identifier (including Rev. No. and Change No., if applicable):

ANL-WIS-MD-000012 REV00

4. Revision/Change No.

5. Description of Revision/Change

00

Initial issue



## CONTENTS (Continued)

	Page
6.3.3.1	Waste-Form (Smectite) Colloids ..... 56
6.3.3.2	Corrosion (Iron-[Hydr]oxide) Colloids ..... 59
6.3.3.3	Groundwater (Smectite) Colloids ..... 61
6.3.3.4	Colloid-Associated Radionuclide Source Term in Waste Package ..... 63
6.4	ASSESSMENT OF ABSTRACTION ..... 63
6.4.1	Validity of Abstraction and Comparison to Data ..... 63
6.4.2	Alternative Models ..... 64
6.4.2.1	Rate-of-Colloid-Generation Model ..... 64
6.4.3	Issues and Comments from the NRC IRSRs ..... 73
7.	CONCLUSIONS ..... 75
8.	INPUTS AND REFERENCES ..... 77
8.1	DOCUMENTS CITED ..... 77
8.2	CODES, STANDARDS, REGULATIONS, AND PROCEDURES ..... 80
8.3	SOURCE DATA ..... 81
ATTACHMENT I - YMP NO. 2.1.09.14.00 NEA NO. 2.1.09AO-COLLOID FORMATION IN WASTE AND EBS ..... 1	
I.1	YMP PRIMARY FEP DESCRIPTION ..... 1
I.2	SCREENING DECISION ..... 1
I.3	SCREENING ARGUMENT ..... 1
I.4	TSPA DISPOSITION ..... 2
I.5	BASIS FOR SCREENING DECISION ..... 2
ATTACHMENT II - YMP NO. 2.1.09.15.00 NEA NO. 2.1.09C-FORMATION OF TRUE COLLOIDS IN WASTE AND EBS ..... 1	
II.1	YMP PRIMARY FEP DESCRIPTION ..... 1
II.2	SCREENING DECISION ..... 1
II.3	SCREENING ARGUMENT ..... 1
II.4	TSPA DISPOSITION ..... 1
II.5	BASIS FOR SCREENING DECISION ..... 1
ATTACHMENT III - YMP NO. 2.1.09.16.00 NEA NO. 2.1.09D-FORMATION OF PSEUDO- COLLOIDS (NATURAL) IN WASTE AND EBS ..... 1	
III.1	YMP PRIMARY FEP DESCRIPTION ..... 1
III.2	SCREENING DECISION ..... 1
III.3	SCREENING ARGUMENT ..... 1
III.4	TSPA DISPOSITION ..... 1
III.5	BASIS FOR SCREENING DECISION ..... 1
ATTACHMENT IV - YMP NO. 2.1.09.16.01 NEA NO. 2.1.09A-COLLOID PHASES PRODUCED BY CO-PRECIPITATION (IN WASTE AND EBS) (SECONDARY TO YMP 2.1.09.16.00 [NEA 2.1.09D]) ..... 1	
IV.1	YMP PRIMARY FEP DESCRIPTION ..... 1
IV.2	SCREENING DECISION ..... 1
IV.3	SCREENING ARGUMENT ..... 1
IV.4	TSPA DISPOSITION ..... 1

## CONTENTS (Continued)

	Page
IV.5 BASIS FOR SCREENING DECISION .....	1
ATTACHMENT V - YMP NO. 2.1.09.17.00 NEA NO. 2.1.09E-FORMATION OF PSEUDO-COLLOIDS (DEPENDENT ON CORROSION PRODUCTS) (IN WASTE AND EBS)	1
V.1 YMP PRIMARY FEP DESCRIPTION.....	1
V.2 SCREENING DECISION .....	1
V.3 SCREENING ARGUMENT .....	1
V.4 TSPA DISPOSITION.....	1
V.5 BASIS FOR SCREENING DECISION .....	2
ATTACHMENT VI - YMP NO. 2.1.09.18.00 NEA NO. 3.2.04AA-MICROBIAL COLLOID TRANSPORT IN THE WASTE AND EBS.....	1
VI.1 YMP PRIMARY FEP DESCRIPTION.....	1
VI.2 SCREENING DECISION .....	1
VI.3 SCREENING ARGUMENT .....	1
VI.4 TSPA DISPOSITION.....	1
VI.5 BASIS FOR SCREENING DECISION .....	1
ATTACHMENT VII - YMP NO. 2.1.09.19.00 NEA NO. 3.2.04Z-COLLOID TRANSPORT AND SORPTION.....	1
VII.1 YMP PRIMARY FEP DESCRIPTION.....	1
VII.2 SCREENING DECISION .....	1
VII.3 SCREENING ARGUMENT .....	1
VII.4 TSPA DISPOSITION.....	1
VII.5 BASIS FOR SCREENING DECISION .....	1
ATTACHMENT VIII - YMP NO. 2.1.09.20.00 NEA NO. 3.2.04Y-COLLOID FILTRATION..	1
VIII.1 YMP PRIMARY FEP DESCRIPTION.....	1
VIII.2 SCREENING DECISION .....	1
VIII.3 SCREENING ARGUMENT .....	1
VIII.4 TSPA DISPOSITION.....	1
VIII.5 BASIS FOR SCREENING DECISION .....	1
ATTACHMENT IX - YMP NO. 2.1.09.21.00 NEA NO. 3.2.08C-SUSPENSIONS OF PARTICLES LARGER THAN COLLOIDS.....	1
IX.1 YMP PRIMARY FEP DESCRIPTION.....	1
IX.2 SCREENING DECISION .....	1
IX.3 SCREENING ARGUMENT .....	1
IX.4 TSPA DISPOSITION.....	1
IX.5 BASIS FOR SCREENING DECISION .....	1
ATTACHMENT X - YMP NO. 2.1.10.01.00 NEA NO. 2.1.10D-BIOLOGICAL ACTIVITY IN WASTE AND EBS .....	1
X.1 YMP PRIMARY FEP DESCRIPTION.....	1
X.2 SCREENING DECISION .....	1
X.3 SCREENING ARGUMENT .....	1
X.4 TSPA DISPOSITION.....	1
X.5 BASIS FOR SCREENING DECISION .....	1

## CONTENTS (Continued)

	Page
ATTACHMENT XI - YMP NO. 2.1.13.03.00 NEA NO. 2.1.13A-MUTATION .....	1
XI.1 YMP PRIMARY FEP DESCRIPTION.....	1
XI.2 SCREENING DECISION .....	1
XI.3 SCREENING ARGUMENT .....	1
XI.4 TSPA DISPOSITION .....	1
XI.5 BASIS FOR SCREENING DECISION .....	1
ATTACHMENT XII - YMP NO. 2.1.09.22.00 COLLOID SORPTION AT THE AIR-WATER INTERFACE.....	1
XII.1 YMP PRIMARY FEP DESCRIPTION.....	1
XII.2 SCREENING DECISION .....	1
XII.3 SCREENING ARGUMENT .....	1
XII.4 TSPA DISPOSITION .....	1
XII.5 BASIS FOR SCREENING DECISION .....	1
ATTACHMENT XIII - YMP NO. 2.1.09.23.00 COLLOID STABILITY AND CONCENTRATION DEPENDENCE ON AQUEOUS CHEMISTRY.....	1
XIII.1 YMP PRIMARY FEP DESCRIPTION.....	1
XIII.2 SCREENING DECISION .....	1
XIII.3 SCREENING ARGUMENT .....	1
XIII.4 TSPA DISPOSITION .....	1
XIII.5 BASIS FOR SCREENING DECISION .....	1
ATTACHMENT XIV - YMP NO. 2.1.09.24.00 COLLOID DIFFUSION .....	1
XIV.1 YMP PRIMARY FEP DESCRIPTION.....	1
XIV.2 SCREENING DECISION .....	1
XIV.3 SCREENING ARGUMENT .....	1
XIV.4 TSPA DISPOSITION .....	1
XIV.5 BASIS FOR SCREENING DECISION .....	1
ATTACHMENT XV - YMP NO. 2.1.09.24.00 COLLOID GRAVITATIONAL SETTLING .....	1
XV.1 YMP PRIMARY FEP DESCRIPTION.....	1
XV.2 SCREENING DECISION .....	1
XV.3 SCREENING ARGUMENT .....	1
XV.4 TSPA DISPOSITION .....	1
XV.5 BASIS FOR SCREENING DECISION .....	1
ATTACHMENT XVI - RADIONUCLIDE UPTAKE MECHANISMS.....	1
XVI.1 RADIONUCLIDE UPTAKE MECHANISMS.....	1
XVI.1.1 REVERSIBLE UPTAKE .....	1
XVI.1.1.1 NAGRA Results .....	3
XVI.1.1.2 EPA Results .....	3
XVI.1.1.3 LANL Results .....	3
XVI.1.1.4 Recommendations.....	4
XVI.1.2 Irreversible Uptake .....	4

## FIGURES

		<b>Page</b>
Figure 1.	Several Types of Radionuclide-Bearing Colloids .....	23
Figure 2.	Schematic of Colloid Formation from Waste Form Corrosion .....	24
Figure 3.	The Cumulative Normalized Release of the Elements B, Np, Pu, and Am.....	25
Figure 4.	Plutonium Release Rate versus Cumulative Boron Release.....	27
Figure 5.	Experimental Determination of Montmorillonite Stability as a Function of pH and Ionic Strength.....	34
Figure 6.	Experimentally Derived Stability Ratio, $W_{exp}$ , of a Hematite Suspension Plotted as a Function of pH for Differing Ionic Strengths.....	35
Figure 7.	Plutonium-Bearing Colloids as a Function of Ionic Strength in Corrosion Tests.....	37
Figure 8.	Colloid Concentrations Versus Alkali and Alkaline-Earth Concentration for Groundwaters from Around the World.....	38
Figure 9.	Colloid Concentration Versus Ionic Strength for Groundwaters from Around the World .....	39
Figure 10.	Concentration of Pu Colloids as a Function of HLW Corrosion Test Duration..	49
Figure 11.	Schematic Representation of Iron-(Hydr)oxide Colloid Stability as a Function of pH and Ionic Strength.....	50
Figure 12.	Schematic Representation of Smectite Stability as a Function of pH and Ionic Strength.....	51
Figure 13.	Schematic Relationship Between Radionuclide-Bearing Colloid Concentration and Ionic Strength.....	52
Figure 14.	Schematic Relationship between Groundwater Colloid Concentration and Ionic Strength.....	53
Figure 15a.	Flow Chart and Logic Statements: Effect of Ionic Strength on the Concentration of Waste-form Colloids Generated during HLW Glass Degradation Based on Experiments Conducted at ANL (see Figure 13).....	56
Figure 15b.	Flow Chart and Logic Statements: Effect of pH and Ionic Strength on Waste- form Colloid Stability Based on Stability Behavior of Montmorillonite Colloids (see Figure 12).....	57
Figure 15c.	Flow Chart and Logic Statements: Determination of Mobile Mass of Waste- form Colloids .....	57
Figure 15d.	Flow Chart and Logic Statements: Sorption of Radionuclides on Waste-form Colloids.....	58
Figure 15e.	Flow Chart and Logic Statements: Effect of Ionic Strength and pH on Stability of Iron-(Hydr)oxide Colloids (see Figure 11).....	59
Figure 15f.	Flow Chart and Logic Statements: Sorption of Radionuclide RN on Iron- (Hydr)oxide Colloids .....	60
Figure 15g.	Flow Chart and Logic Statements: Effect of Ionic Strength on Mobile Mass of Groundwater Colloids. ....	61
Figure 15h.	Flow Chart and Logic Statements: Effect of pH and Ionic Strength on Groundwater Colloids Stability Based on Stability Behavior of Montmorillonite Colloids .....	62
Figure 15i.	Flow Chart and Logic Statements: Radionuclide Sorption on Groundwater Colloids.....	62

FIGURES (Continued)

	Page
Figure 15j. Flow Chart and Logic Statements: Calculation of Colloid-associated Radionuclide Source Term from Summation of Calculated Colloid and Radionuclide Masses .....	63
Figure 16. Ratio of Normalized Mass Loss of Plutonium to Normalized Mass Loss of Boron, $NL(Pu)/NL(B)$ .....	65
Figure 17. Fractional Release Rate of Pu as a Function of Cumulative Fractional Tc Release for the ATM-103 and ATM-106 High-drip-rate Tests.....	67
Figure 18. Flow Chart Illustrating Alternative Abstraction Logic.....	69

## TABLES

		Page
Table 1.	Summary of Parameters Used in Abstraction.....	14
Table 2.	Assumptions Used in the Analysis and Model Development.....	18
Table 3.	Features, Events, and Processes (FEPs) Included in AMR .....	21
Table 4.	Sorption Data for Colloid Transport.....	43
Table 5.	Ranges and bounds for the constants, <i>a</i> and <i>b</i> , in Equation 7.....	66
Table 6.	Summary of Parameters for Prospective Alternative Abstraction.....	70
Table 7.	NRC IRSR Issues .....	73
Table XVI-1.	Sorption Behavior of Key Radionuclides as a Function of Aqueous Chemical Conditions .....	XVI-6
Table XVI-2.	YMP Groundwater Compositions, Compared to NAGRA Groundwater (and Porewater) Compositions .....	XVI-8
Table XVI-3.	Summary of Sorption Data Developed by NAGRA for Bentonite, Crystalline Rock, and Marl.....	XVI-8
Table XVI-4.	Summary of Sorption Data Developed by EPA (1999).....	XVI-9
Table XVI-5.	YMP-specific Data for Sorption of Plutonium and Americium on Colloidal Hematite, Goethite, Ca-montmorillonite, and Silica: (a) Pu(IV), (b) Pu(V), (c) Am(III) .....	XVI-10
Table XVI-6.	Summary of Sorption Data .....	XVI-13
Table XVI-7.	Recommendations for PA.....	XVI-14

## ACRONYMS AND ABBREVIATIONS

AMR	Analysis/Model Report
ANL	Argonne National Laboratory
c.c.c.	critical coagulation concentration
CLST	Container Life and Source Term
CRWMS	Civilian Radioactive Waste Management System
CSNF	commercial spent nuclear fuel
DHLW	defense high-level radioactive waste
DIRS	Document Input Reference System
DLVO	theory of particle stability in terms of surface charges and potentials, independently developed by Derjaguin and Landau and Verney and Overbeek
DOE	U.S. Department of Energy
DOE-SNF	DOE-owned spent nuclear fuel
EBS	engineered barrier system
EDL	electric double layer
eq/L	equivalence (equivalents/liter)
EPA	Environmental Protection Agency
FEP	feature, event, or process
HLW	high-level radioactive waste
IRSR	Issue Resolution Status Report
KTI	Key Technical Issues
LANL	Los Alamos National Laboratory
QAP	Quality Assurance Plan
M	molarity (moles/liter)
m	molality (moles/kilogram)
MIC	microbial influenced corrosion
M&O	Management and Operating Contractor
µm	micron, or micrometer ( $10^{-6}$ meter)
NAGRA	National Cooperative for the Disposal of Radioactive Waste (Switzerland)
nm	nanometer ( $10^{-9}$ meter)
NRC	U.S. Nuclear Regulatory Commission
pH <sub>ZPC</sub>	pH at zero point of charge
pt	number of particles
PZNPC	point of zero net proton charge

## ACRONYMS AND ABBREVIATIONS (Continued)

REE	rare earth element
RN	radionuclide
SA	surface area
SNF	spent nuclear fuel
SRL	Savannah River Laboratory
SZ	saturated zone
TEM	transmission electron microscopy
TSPAI	Total System Performance Assessment and Integration
TSPA-SR	Total System Performance Assessment-Site Recommendation
TSPA-VA	Total System Performance Assessment-Viability Assessment
UZ	unsaturated zone
V	volume of fluid used
VA	Viability Assessment
WVDP	West Valley Demonstration Project
YMP	Yucca Mountain Project
ZPC	zero point of charge

## 1. PURPOSE

The purpose of this Analysis/Model Report (AMR) is to present and describe the abstraction of process models and data developed primarily by Argonne National Laboratory (ANL) and Los Alamos National Laboratory (LANL) for the Total System Performance Assessment-Site Recommendation (TSPA-SR) calculations to be performed with the TSPA code, GoldSim. The process models describe the observed types, formation, and stability of radionuclide-bearing colloids that result from degradation and decomposition of the waste forms contained in failed waste packages. In addition, contaminant-colloid attachment/detachment mechanisms and transport characteristics anticipated in the repository are discussed for colloids formed from degradation of the waste forms, colloids formed from man-made materials introduced into the repository, and naturally occurring colloids. The abstraction of the process models is intended to capture the most important characteristics of radionuclide-colloid behavior for use in predicting the potential impact on repository performance of colloid-facilitated radionuclide transport.

It is anticipated that quantities of colloids will be mobilized as a result of alteration of both the high-level radioactive waste (HLW) and spent nuclear fuel (SNF) waste forms. The abundance of colloids within the breached waste package will depend on the extent of waste form alteration and the alteration products formed. Colloid abundance and stability also depend on many environmental factors, including the ionic strength, pH, cation concentrations, colloid content of groundwater entering the waste package from the drift, presence of fulvic and humic acids, and microbe fragments. Suspended colloids may subsequently flocculate and settle by gravity, be chemically or mechanically filtered, or dissolve. If the environmental factors change, colloids may be peptized; colloid-sized particles may precipitate; or other natural processes may occur. In addition, colloids may sorb readily at the interfaces between air and water in rocks and engineered barriers and, depending upon the degree of saturation of the porous medium as well as its configuration, may be retarded, even immobilized or transported. These issues are relevant to colloid transport, which is of primary concern within the engineered barrier system (EBS) in the drift and in the near- and far-fields. They are relevant as well to transport, which also may occur to some extent within the waste package.

Colloid source term is defined here as the total of those radionuclides associated in some manner with colloids that: (1) are mobilized at the surface of the waste form, (2) are transported within the waste package to the waste package wall, (3) leave the waste package at a breach or breaches in the waste package wall, and (4) enter the drift. This abstraction analysis is restricted to this in-package portion of the repository system.

Colloidal systems are defined here as those in which the component phases are dispersed in an aqueous medium (groundwater, leachate) ranging in size from approximately 1 nm to 1  $\mu$ m. Much has been learned about environmental behavior of colloids over the past few decades, but due largely to their small size and unique surface-dominated chemical and physical characteristics, they have proven to be difficult to study. Therefore, the approach taken in this analysis was to bound the probable behavior of colloid-associated radionuclides. The lack of certain data can be mitigated as well by comparing these bounding predictions with relevant laboratory and field studies and with analog sites in which environmental conditions are analogous in critical respects to conditions used in experiments and anticipated in the repository. These approaches have been used to the extent possible to reduce the uncertainties associated

with predictions of colloid-associated radionuclide concentrations, stability, and transport characteristics.

In accordance with AP-2.13Q, *Technical Product Development Planning*, a development plan, *Waste Form Colloid-Associated Concentration Limits—Abstraction and Summary*, was developed, issued, and utilized in the preparation of this AMR (CRWMS M&O 2000c).

## 2. QUALITY ASSURANCE

The Quality Assurance (QA) program applies to this AMR. All types of WPs were classified (per QAP-2-3) as Quality Level-1. CRWMS M&O (1999a, p. 7) in *Classification of the MGR Uncanistered Spent Nuclear Fuel Disposal Container System* is cited as an example of a WP type. The Performance Assessment Operations responsible manager has evaluated this technical document activity in accordance with QAP-2-0, *Conduct of Activities*. The activity evaluation, *Conduct of Performance Assessment*, determined that this activity is subject to the *Quality Assurance Requirements and Description* (DOE 2000) requirements.

## 3. COMPUTER SOFTWARE AND MODEL USAGE

No computer software was used for calculations and/or modeling in support of this AMR. No codes or routines were developed.

Reference to parameters used in calculations by GoldSim is made in this AMR. The parameters are provided for use by the TSPA-SR team in GoldSim, but no GoldSim calculations were performed for this AMR.

Graphs and figures were prepared with Microsoft Excel 97, Microsoft PowerPoint 97, and Adobe Illustrator 8.0.1. Excel was used for tabular presentation of data only in Attachment XVI, Table XVI-5.

## 4. INPUTS

The rationale for the approach used in the waste form colloid source term abstraction for TSPA-SR is based largely on the observation and characterization of radionuclide-bearing colloids formed during waste form degradation tests conducted at ANL. The general approach used in the analysis was extended and developed from that used in the TSPA Viability Assessment (VA). Additional data and improved process models from ongoing and recently completed laboratory and field testing programs at ANL and LANL are incorporated into this AMR. The data and models were developed according to AP-3.10Q and the respective Quality Assurance Plans (QAPs) for Yucca Mountain Project activities performed at ANL and LANL. Results of these activities enabled reduction in uncertainties through the refinement of parameter ranges and a better understanding of fundamental mechanisms of colloid formation, stability, and behavior and the association of radionuclides with colloids.

## 4.1 DATA AND PARAMETERS

Technical product inputs and sources are listed in Table 1 and on the Document Input Reference System as stipulated by AP-3.10Q. Primary technical inputs have been taken from CRWMS M&O (2000a).

Table 1. Summary of Parameters Used in Abstraction

Data Tracking Number (DTN)	Parameter Name	Parameter Description	Units <sup>a</sup>	Basis for Value/ Source	Value and Distribution
<b>Waste Form Colloids</b>					
LL991109851021.095	CRNcoll,wf,irrev,max	Highest observed or expected concentration of Pu associated with both types of waste-form colloids	mol/L	Figures 7 and 13 (Pu only)	6E-8 mol/L <sup>b</sup>
MO0003SPALOW12.001	CRNcoll,wf,irrev,min	Lowest observed or expected concentration of Pu associated with both types of waste-form colloids	mol/L	Figures 7 and 13 (Pu only)	1E-11 mol/L <sup>b</sup>
LL991109851021.095	Mcoll,wf,both,max	Highest observed or expected mass of both types of waste-form colloids per unit volume or mass of water	mg/L	Figure 10	5 mg/L <sup>c</sup>
N/A, intermediate parameter resulting from development of TSPA in this AMR	CRNcoll,wf,irrev	Concentration of irreversibly attached (or engulfed as a solid inclusion) radionuclide element RN associated with waste-form colloids	mol/L	Determined in PA calculation; Flow-charts 1a, 1b	N/A
N/A, intermediate parameter resulting from development of TSPA in this AMR	CRNcoll,wf,rev	Concentration of reversibly attached radionuclide element RN associated with waste-form colloids	mol/L	Determined in PA calculation; Flow-chart 1d	N/A
N/A, intermediate parameter resulting from development of TSPA in this AMR	Mcoll,wf,both	Mass of waste-form colloids with reversibly sorbed or irreversibly attached (or engulfed) radionuclide element RN per unit volume or mass of water	mol/L	Determined in PA calculation; Flow-chart 1c	N/A
MO0003SPAION02.003	llo-thresh,coll,wf	Ionic strength below which waste-form colloids are stable	mol/L	Figures 7 and 13; Figures 5 and 12	0.01 mol/L
MO0003SPAION02.003	lhi-thresh,coll,wf	Ionic strength above which waste-form colloids are unstable	mol/L	Figures 7 and 13; Figures 5 and 12	0.05 mol/L
MO0004SPAKDS42.005	Kd,RNcoll,wf,rev	Distribution coefficient for reversible sorption of radionuclide element RN onto waste-form colloids	mL/g colloid	Data developed from LANL data; CRWMS M&O (2000c)	Geometric mean values: Pu = 1e+4 Am = 1e+5 log-normal distributions; geometric std. dev. = 10
N/A, intermediate function resulting from development of TSPA in this AMR	STcoll,wf,is	Function relating stability of waste-form colloids to ionic strength, based on results of HLW glass degradation experiments (based on Pu concentration)	mol/L	Figures 7 and 13	[Pu colloid] = -1.25E-6 × I +7.25E-8

Data Tracking Number (DTN)	Parameter Name	Parameter Description	Units <sup>a</sup>	Basis for Value/ Source	Value and Distribution
N/A, intermediate functions resulting from development of TSPA in this AMR	ST <sub>coll,wf,pH</sub>	Function relating stability of waste-form colloids to ionic strength and pH, over limited pH range, based on results of montmorillonite stability experiments	mol/L	Figures 5 and 12	$I = \text{pH}/200$
<b>Iron-(hydr)oxide Colloids</b>					
N/A, intermediate parameter resulting from development of TSPA in this AMR	CRN <sub>coll,FeOx</sub>	Concentration of reversibly attached radionuclide element RN associated with iron-(hydr)oxide colloids	mol/L	Determined in PA calculation; Flow-chart 2b	N/A
N/A, intermediate parameter resulting from development of TSPA in this AMR	M <sub>coll,FeOx</sub>	Mass of iron-(hydr)oxide colloids per unit volume or mass of water	mg/L	Determined in PA calculation; Flow-chart 2a	N/A
MO0003SPA HIG12.002	M <sub>coll,FeOx,max</sub>	Highest observed or expected mass of iron-(hydr)oxide colloids per unit volume or mass of water	mg/L	Reasonable conservative estimate	1 mg/L
MO0003SPA HIG12.002	M <sub>coll,FeOx,min</sub>	Lowest observed or expected mass of iron-(hydr)oxide colloids per unit volume or mass of water	mg/L	Reasonable conservative estimate	1E-3 mg/L
MO0003SPA ION02.003	I <sub>lo-thresh, coll, FeOx</sub>	Ionic strength below which iron-(hydr)oxide colloids are stable	mol/L	Figures 6 and 11	0.01 mol/L
MO0003SPA ION02.003	I <sub>hi-thresh, coll, FeOx</sub>	Ionic strength above which iron-(hydr)oxide colloids are unstable	mol/L	Figures 6 and 11	0.05 mol/L
MO0004PAKDS42.005	K <sub>d,RNcoll,FeOx</sub>	Distribution coefficient for reversible sorption of radionuclide element RN onto iron-(hydr)oxide colloids	mL/g colloid	Data developed from LANL data; CRWMS M&O (2000c)	Geometric mean values: Pu, Am = 1e+4 log-normal distributions; geometric std. dev. = 10
N/A, intermediate function resulting from development of TSPA in this AMR	ST <sub>coll,FeOx,pHlo</sub>	Function relating stability of iron-(hydr)oxide colloids to pH and ionic strength at relatively low pH values	mol/L	Figure 6 and 11	$I = -0.02 \times \text{pH} + 0.17$
N/A, intermediate function resulting from development of TSPA in this AMR	ST <sub>coll,FeOx,pHhi</sub>	Function relating stability of iron-(hydr)oxide colloids to pH and ionic strength at relatively high pH values	mol/L	Figure 6 and 11	$I = +0.02 \times \text{pH} - 0.17$
N/A, intermediate function resulting from development of TSPA in this AMR	ST <sub>coll,FeOx,pHint</sub>	Function relating stability of iron-(hydr)oxide colloids to pH and ionic strength at intermediate pH values	Boolean	Figure 6 and 11	Boolean (pH ≥ 8 AND pH ≤ 9)
<b>Groundwater Colloids</b>					
N/A, intermediate parameter resulting from development of TSPA in this AMR	CRN <sub>coll,gw</sub>	Concentration of reversibly attached radionuclide element RN associated with groundwater colloids	mol/L	Determined in PA calculation; Flow-chart 3b	N/A

Data Tracking Number (DTN)	Parameter Name	Parameter Description	Units <sup>a</sup>	Basis for Value/ Source	Value and Distribution
N/A, intermediate parameter resulting from development of TSPA in this AMR	$M_{coll,gw}$	Mass of groundwater colloids per unit volume or mass of water	mg/L	Determined in PA calculation; Flow-chart 3a	N/A
MO0003SPAHLO12.004	$M_{coll,gw,max}$	Highest observed or expected mass of groundwater colloids per unit volume or mass of water	mg/L	Figures 9 and 14	3E-2 mg/L
MO0003SPAHLO12.004	$M_{coll,gw,min}$	Lowest observed or expected mass of groundwater colloids per unit volume or mass of water	mg/L	Figures 9 and 14	3E-6 mg/L
MO0004SPAKDS42.005	$K_{d,RN,coll,gw}$	Distribution coefficient for reversible sorption of radionuclide element RN onto groundwater colloids	mL/g colloid	Data developed from LANL data; CRWMS M&O (2000c)	Geometric mean value: $P_u, A_m = 1e+3$ log-normal distribution; geometric std. dev. = 1 order-of-magnitude
MO0003SPAION02.003	$I_{lo-thresh,coll,gw}$	Ionic strength below which groundwater colloids are stable	mol/L	Figures 9 and 14	0.01 mol/L
MO0003SPAION02.003	$I_{hi-thresh,coll,gw}$	Ionic strength above which groundwater colloids are unstable	mol/L	Figures 9 and 14	0.05 mol/L
N/A, intermediate function resulting from development of TSPA in this AMR	$ST_{coll,gw}$	Function relating stability of groundwater colloids to ionic strength at intermediate ionic strengths	mg/L	Figures 9 and 14	Function in Section 6.3.3.3, Figure 15g
<b>Other output</b>					
N/A, intermediate parameter resulting from development of TSPA in this AMR	$C_{RNcoll}$	Concentration of mobile colloidal radionuclide element RN per unit volume or mass of water	mol/L	Determined in PA calculation; Figure 15j	N/A
N/A, intermediate parameter resulting from development of TSPA in this AMR	$C_{RNdiss}$	Concentration of dissolved radionuclide element RN per unit volume or mass of water	mol/L	Input parameter and determined in PA calculation	N/A
N/A, intermediate parameter resulting from development of TSPA in this AMR	$M_{coll}$	Total mass of all mobile colloids per unit volume or mass of water	mg/L	Determined in PA calculation; Figure 15j	N/A
<b>Input parameters</b>					
N/A, parameter provided by GoldSim calculation	I	Ionic strength	mol/L	Input parameter	N/A
N/A, parameter provided by GoldSim calculation	pH	pH	pH units	Input parameter	N/A

Data Tracking Number (DTN)	Parameter Name	Parameter Description	Units <sup>a</sup>	Basis for Value/ Source	Value and Distribution
N/A, parameter provided by GoldSim calculation	C <sub>RNdiss</sub>	Concentration of dissolved radionuclide element RN per unit volume or mass of water	mol/L	Input parameter and determined in PA calculation	N/A
LA0003NL831352.002 LA0003NL831352.003	[referred to in AMR]	Distribution coefficients and forward and reverse adsorption/desorption rates for element RN onto waste-form colloids—source data	Various	LANL laboratory data	Various

NOTE: <sup>a</sup> mol/L is actually moles per liter of dispersion and is not molarity in the strict sense

<sup>b</sup> uncertainty is linked to uncertainty for ionic strength, which is an input parameter; no additional uncertainty is added

<sup>c</sup> mass is correlated with irreversible radionuclide concentration

## 4.2 CRITERIA

The NRC Total System Performance Assessment and Integration (TSPA) IRSR (NRC 1998a) establishes generic technical acceptance criteria considered by the NRC staff to be essential to a defensible, transparent, and comprehensive assessment methodology for the repository system. These regulatory acceptance criteria address five fundamental elements of the DOE TSPA model for the Yucca Mountain site, namely:

1. Data and model justification (focusing on sufficiency of data to support the conceptual basis of the process model and abstractions)
2. Data uncertainty and verification (focusing on technical basis for bounding assumptions and statistical representations of uncertainties and parameter variabilities)
3. Model uncertainty (focusing on alternative conceptual models consistent with available site data)
4. Model verification (focusing on testing of model abstractions using detailed process-level models and empirical observations)
5. Integration (focusing on appropriate and consistent coupling of model abstractions).

Relevant to the topic of this AMR, elements (1) through (4) of the acceptance criteria are addressed herein and/or in the supporting Calculation document(s). Element (5) of the NRC acceptance criteria, which strictly applies to the completed synthesis of process-level models and abstractions, will be addressed separately in the TSPA-SR. As well, this AMR addresses relevant KTIs raised in the NFE IRSR Revision 2 (NRC 1999a) and CLST IRSRs Revisions 1 (NRC 1998b) and 2 (NRC 1999b).

### 4.3 CODES AND STANDARDS

This AMR was prepared to comply with the above NRC TSPAI acceptance criteria, as well as the DOE interim guidance (Dyer 1999) which requires the use of specified subparts/sections of the proposed NRC high-level waste rule, 10 CFR Part 63 (64 FR 8640). Subparts of this proposed rule that are particularly applicable to data include Subpart B, Section 15 (Site Characterization) and Subpart E, Section 114 (Requirements for Performance Assessment). Subparts applicable to models are outlined in Subpart E, Sections 114 (Requirements for Performance Assessment) and 115 (Characteristics of the Reference Biosphere and Critical Group).

### 5. ASSUMPTIONS

Assumptions made as a part of the analysis and model development are presented in Table 2 and incorporated into the discussion in Section 6.3, Abstraction and Implementation in GoldSim.

Table 2. Assumptions Used in the Analysis and Model Development

Category	Assumption	Rationale	Section Used
Colloid Formation	The colloids produced from corrosion of HLW glass and SNF are predominantly smectite; a good approximation for abstraction is that all waste form colloids are smectite, or are irreversibly attached to smectite.	ANL experimental data indicate that preponderance of HLW glass-derived colloids is smectite, and that degradation of SNF produces smectite as well (CRWMS M&O 2000a).	6.3
	Metal (hydr)oxide colloids, large particles, and scale may form from degradation of the waste package and its internal components; a good approximation for abstraction is that all metal (hydr)oxides are iron-(hydr)oxides.	The preponderance of metal in the waste package steels is iron.	6.3
	Smectite colloids may form from spallation of alteration phases from HLW as well as precipitation from solution.	Based on observations and inferences in connection with ANL experimental program (CRWMS M&O 2000a)	6.3
	SNF produces colloids less readily under experimental conditions approximating repository conditions for reasons related to the mechanisms of alteration of the SNF.	Based on observations and inferences in connection with ANL experimental program (CRWMS M&O 2000a)	6.3
	DOE-SNF and commercial SNF (CSNF) are considered together as "generic" SNF and are not treated separately in the abstraction	The preponderance of SNF is CSNF. Metallic fuels may produce fine particulates as they degrade, but it is currently considered that DOE-SNF will not adversely affect repository performance (see Section 6.1.1.1)	6.3
	The waste form degrades according to in-package geochemistry process models and abstractions and are represented by a single GoldSim mixing cell	TSPA methodology (in progress)	6.3
Colloid Stability and Concentration	The stability of smectite colloids will depend to varying degrees on their concentration and the composition, ionic strength, and pH of the solution	Observed in experiments (e.g., Tombacz et al. 1990)	6.3

(continued on next page)

Category	Assumption	Rationale	Section Used
	The stability of smectite is less sensitive to pH (is increased) at higher values of pH, more sensitive to pH (is decreased) at lower values	Observed in experiments (Tombacz et al. 1990)	6.3
	Am is assumed to behave as does Pu in terms of mobilization from waste degradation and formation of irreversible association with smectite colloids and clay layers on HLW	Reasonable assumption based on chemical characteristics of Pu and Am	6.3
	The properties of colloidal smectite and iron-(hydr)oxides are well known and applicable to radionuclide-bearing colloids	Smectite and iron-(hydr)oxide colloid behavior (Tombacz et al. 1990; Liang and Morgan 1990)	6.3
	Iron-(hydr)oxide colloid stability and concentration depend upon both the pH and ionic strength that may be encountered in the repository	Generally acknowledged relationship (Liang and Morgan 1990)	6.3
	Waste form colloids produced at 90°C are stable at 25°C	Stability is considered to increase as T drops	6.3
Radionuclide Attachment to Colloids	Some radionuclides released from degraded fuel occur as aqueous (dissolved) species and are available to sorb reversibly to smectite and iron-(hydr)oxide colloids, forming pseudocolloids	Experimental results and solubility determinations indicate that radionuclides may dissolve, and colloids are available for sorption of radionuclides (CRWMS M&O 2000a)	6.3
	Smectite colloids contain entrained radionuclide-bearing phases; further, all discrete radionuclide-bearing colloid-sized phases (besides smectite) are entrained in smectite colloids	ANL experimental data indicate that smectite colloids contain entrained or embedded RN-bearing phases; conservative assumption made because reversibility of attachment was not analyzed (CRWMS M&O 2000a).	6.3
	Smectite colloids with or without entrained radionuclide-bearing phases may have adsorbed dissolved radionuclides.	Smectite colloids are considered to have the capability of sorbing dissolved radionuclides to form pseudocolloids (e.g., Kim 1994).	6.3
	Pu, Am, Th, Pa, Cs, and Sr are assumed to be the most significant radionuclides available for colloid association; data indicate that smectite colloids may contain Pu, Am, Th, U, Cm, Np, and rare earth elements (REEs), and that Pu generally behaves similarly to Th, Am and REEs	These are RNs of interest for several TSPA investigators. Smectite colloid RN compositions observed in ANL experiments (CRWMS M&O 2000a).	6.3
	Radionuclide association with colloids is irreversible within the waste package environment, except for dissolved radionuclides available for pseudocolloid formation.	A conservative assumption; transport times for colloids leaving the waste package are considered to be short in comparison with sorption-desorption times (DTNs: LA0003NL831352.002 and LA0003NL831352.003).	6.1
	Adsorption/desorption of radionuclides on colloids to form pseudocolloids is defined according to experimentally determined rates of adsorption and desorption of Pu and Am on several types of colloids, and consequently to an effective $K_d$ incorporating both the forward and reverse attachment rates.	Based on results of experiments performed at LANL (DTNs: LA0003NL831352.002 and LA0003NL831352.003)	6.1

Category	Assumption	Rationale	Section Used
	Desorption of Pu and Am from pseudocolloids is assumed to be slow relative to transport rates within the waste package, i.e., pseudocolloid sorptive attachment is effectively irreversible within the waste package	Estimates or over-estimates the consequences and is bounding	6.3
Physical Filtration of Colloids	Physical filtration of colloids may occur within the waste package but is not considered in the abstraction.	All stable colloids are considered to leave a failed waste package through the failure opening, which over-estimates the consequences and is considered bounding	6.3
Colloid Sorption at the Air-Water Interface	Colloid sorption at the air-water interface may occur within the waste package, but is not considered in the abstraction	This over-estimates the consequences and is considered bounding, as colloid sorption to stationary air-water interfaces would retard colloid transport	6.3
Gravitational Settling of Colloids	Gravitational settling of colloids may occur within the waste package, but is not considered in the abstraction.	This over-estimates the consequences and is considered bounding, as all stable colloids are assumed not to settle but to leave a failed waste package through the failure opening	6.3
Colloid Diffusion	Colloid diffusion may occur within the waste package, but is not considered in the abstraction.	This over-estimates the consequences and is considered bounding, as all stable colloids are assumed not to settle but to leave a failed waste package through the failure opening	6.3
Microbes and Colloidal Organic Components	Processes involving interactions between contaminants and microbes and organic components (such as humic and fulvic acids) are not considered in this abstraction	This is considered to over-estimate the consequences and is considered bounding, as biological influences have been known to encourage colloid agglomeration	6.3
Colloid Transport	All stable colloids are assumed to leave a failed waste package through the failure opening	This over-estimates the consequences and is considered bounding; processes such as sorption to in-package components, gravitational settling, and filtration would tend to retain colloids in the waste package.	6.3

## 6. ANALYSIS/MODEL

Colloids may affect repository performance if they are generated in significant quantities; are stable within the waste package, Engineered Barrier System (EBS), and unsaturated and saturated zones (UZ and SZ, respectively); carry a significant radionuclide load; and transport readily. Processes relevant to the waste package environment are discussed in this section in the context of conceptual models and process models and in the approach to abstraction used in this effort.

### 6.1 CONCEPTUAL MODELS AND BACKGROUND

Features, events, and processes (FEPs) relevant to colloid processes in the waste package are listed and summarized in Table 3. The complete FEPs are presented in Attachments I through XV.

Table 3. Features, Events, and Processes (FEPs) Included in this AMR

FEP YMP No.	FEP Title	FEP Summary	FEP Location in AMR
2.1.09.14.00	Colloid Formation in Waste and EBS	Colloids may form as true colloids, colloids formed by co-precipitation with waste alteration phases, pseudocolloids, and microbial colloids.	Sections 6.1.1, 6.2.1, 6.3
2.1.09.15.00	Formation of True Colloids in Waste and EBS	True colloids (radionuclide intrinsic colloids) are colloid-sized assemblages of hydrolyzed, polymerized dissolved radionuclides.	Sections 6.1.1, 6.2.1, 6.3
2.1.09.16.00	Formation of Pseudocolloids (Natural) in Waste and EBS	Pseudocolloids are colloid-sized particles with attached radionuclides. Natural pseudocolloids may include mineral fragments in groundwater, microbes and fragments, and organic acids.	Sections 6.1.3, 6.2.3, 6.3
2.1.09.16.01	Colloid Phases Produced by Co-precipitation (in Waste and EBS)	Colloidal phases containing embedded radionuclides and radionuclide phases occur at the waste form.	Sections 6.1.3, 6.2.3, 6.3
2.1.09.17.00	Formation of Pseudocolloids (Dependent on Corrosion Products) (in Waste and EBS)	Pseudocolloids are colloid-sized particles with attached radionuclides. Colloid-sized particles to which radionuclide may attach may form from the corrosion of materials introduced into the repository during construction and waste emplacement.	Sections 6.1.3, 6.2.3, 6.3
2.1.09.18.00	Microbial Colloid Transport in the Waste and EBS	Colloid-sized microbes and microbe fragments may form pseudocolloids. Microbes can also affect waste package corrosion rates, possibly affecting corrosion colloid production rates, as well as increasing colloid size, resulting in increased gravitational settling and filtration.	Sections 6.1.8, 6.2.8
2.1.09.19.00	Colloid Transport and Sorption	Interactions between radionuclide-bearing colloids and the waste form and EBS materials may result in retardation from sorption.	Sections 6.1.9, 6.2.9, 6.3
2.1.09.20.00	Colloid Filtration	Filtration processes may affect transport of radionuclide-bearing colloids in the	Sections 6.1.4, 6.2.4

FEP YMP No.	FEP Title	FEP Summary	FEP Location in AMR
		waste and EBS.	
2.1.09.21.00	Suspensions of Particles Larger Than Colloids	Groundwater flow through the waste could remove radionuclide-bearing particles larger than colloids by a rinse mechanism.	Not analyzed in AMR
2.1.10.01.00	Biological Activity in Waste and EBS	Biological activity in the waste and EBS may affect radionuclide transport through, for example, formation of colloids and biofilms.	Sections 6.1.8, 6.2.8
2.1.13.03.00	Mutation	Radiation fields could cause mutation of microorganisms, leading to unexpected chemical reactions and impacts.	Not analyzed in AMR
2.1.09.22.00 (proposed)	Colloid Sorption at the Air-Water Interface	Colloids may sorb irreversibly at the gas-water interface under partially saturated conditions.	Sections 6.1.5, 6.2.5
2.1.09.23.00 (proposed)	Colloid Stability and Concentration Dependence on Aqueous Chemistry	Colloid stability is determined in part by ionic strength, pH, and cation concentrations of the aqueous medium.	Sections 6.1.2, 6.2.2, 6.3
2.1.09.24.00 (proposed)	Colloid Diffusion	Colloids may diffuse into intercrystalline porosity and be physically retarded.	Sections 6.1.7, 6.2.7
2.1.09.25.00 (proposed)	Colloid Gravitational Settling	Larger colloids may experience gravitational settling, thereby inhibiting transport.	Sections 6.1.6, 6.2.6

### 6.1.1 Colloid Formation

Several types of colloids are expected to be generated within the Yucca Mountain repository system. Colloids will be present at the waste form and in the drift and the unsaturated and saturated zones. At the waste form, colloids are produced during the degradation of the waste form and waste package. In the repository, additional colloids may be produced from the degradation of steel and concrete components of the EBS. Several types of colloids (mineral and organic colloids) are present in the unsaturated zone, as well as the saturated zone, and may be introduced into the repository. Mineral colloids include clays, iron-(hydr)oxides (goethite, hematite), and silica; organic colloids include microbes and fragments as well as humic and fulvic acids. Formation and introduction of colloids to the waste form/waste package environment are discussed below in the context of the conceptual models considered in the abstraction.

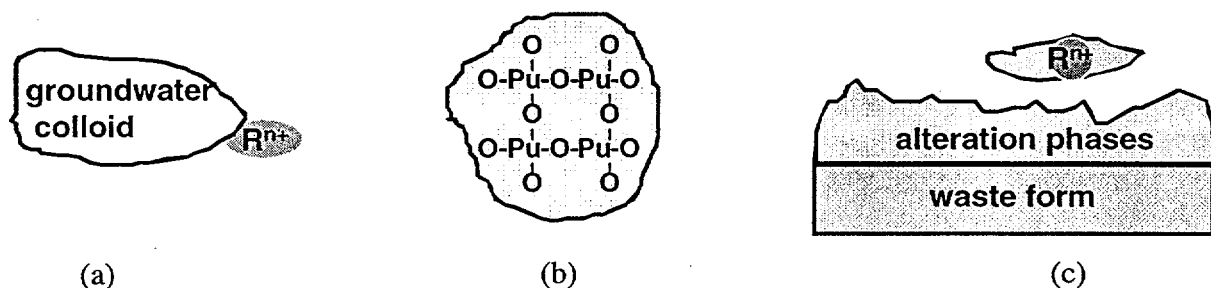
#### 6.1.1.1 Colloids Derived from Waste Form Degradation

Several types of radionuclide-bearing colloids may result from the degradation of waste forms. Formation of radionuclide-bearing colloids is discussed in this section; colloid stability and the nature of the attachment of radionuclides to colloids is discussed in Sections 6.1.2 and 6.1.3, respectively.

Real colloids are formed from polymerization of hydrolyzed radionuclide ions (Figure 1) (Kim 1994). For real colloids to form it is necessary that the fluid be saturated with respect to a solid phase, sometimes amorphous; thus, the formation of real colloids is solubility limited. No real colloids were detected in the experimental investigations at ANL (CRWMS M&O 2000a), and so they are not included here.

Pseudocolloids may be formed by the incorporation, adsorption, and ion exchange of dissolved radionuclides onto existing colloids, either formed from waste form degradation or introduced with groundwater (Figure 1) (Kim 1994). Thus, radionuclides, which might otherwise sorb to minerals in the rock or other immobile substrates, instead attach to mobile colloidal particles and, added to the dissolved radionuclides, increase the mobile radionuclide source term. Colloids may facilitate migration within the repository system and potentially the far-field.

Waste form colloids, or primary colloids, may provide the most significant contribution to colloid-facilitated radionuclide transport. These colloids form from nucleation of colloids from waste form dissolution and spallation of colloid-sized waste form alteration products that contain radionuclides and have the potential for increasing mobile concentration to levels higher than achievable with real colloids or pseudocolloids (Figures 1 and 2) (CRWMS M&O 2000a).

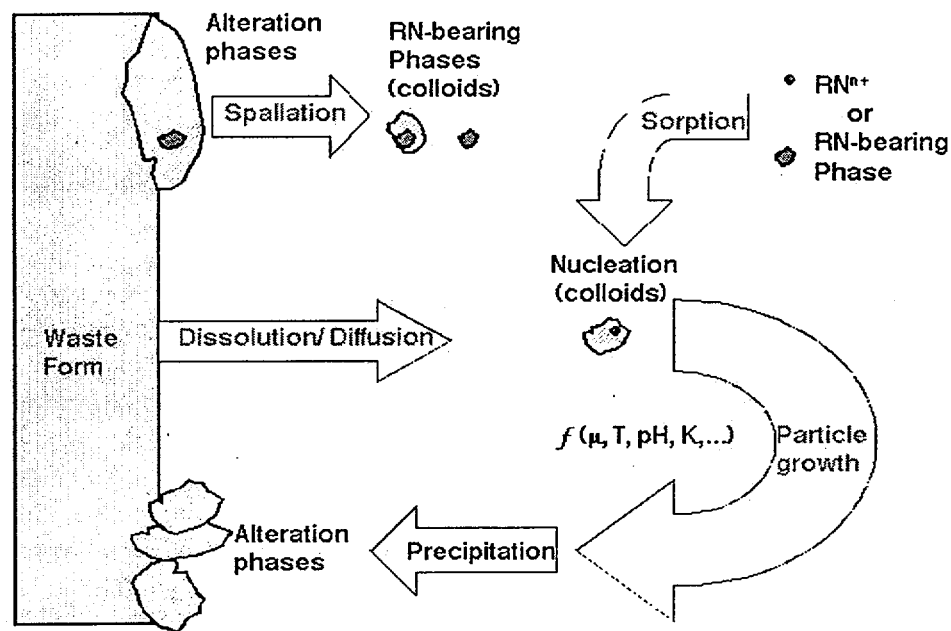


NOTE: Several types of radionuclide-bearing colloids are depicted: (a) pseudo-colloids, (b) real colloids, and (c) waste form colloids. The radionuclide ( $Rn^{+}$ ) associated with the pseudo and waste form colloids can be an ionic species, a real colloid, or a discrete radionuclide-bearing phase. The size range for the colloids is approximately 1 to 1000 nm. (CRWMS M&O 2000a, Fig. 1)

Figure 1. Several Types of Radionuclide-Bearing Colloids

Three broad categories of waste form are to be placed in the repository. The most abundant waste type is commercial spent nuclear fuel (CSNF) from commercially owned and operated electric power reactors. DOE spent nuclear fuel (DOE-SNF) is a diverse collection of waste from reactors at U.S. Department of Energy (DOE) nuclear complex sites. Defense high-level radioactive waste (DHLW) is a borosilicate glass-based waste form containing radionuclides. In the following descriptions, CSNF and DOE-SNF are treated together.

**Corrosion of DHLW**—Testing on corrosion of DHLW has gone on for over ten years in the case of static tests in which glass samples are immersed in fluid and for over four years in the case of drip tests in which fluid is dripped at specified rates onto the glass sample. In the static tests, surface area (SA) of the sample was varied relative to the volume (V) of fluid used; this proportion is referred to as SA/V. SA was determined using geometric estimates of crushed materials, not by a gas adsorption method. Glass waste forms tested include Savannah River Laboratory (SRL) and West Valley Demonstration Project (WVDP) glasses. Fluids used were equilibrated J-13 water (EJ-13) and deionized water. Methods used to characterize colloids produced during the tests include transmission electron microscopy (TEM) and filtration (analysis of filtrates with inductively coupled plasma-mass spectrometry or alpha spectroscopy; CRWMS M&O 2000a). Descriptions of the tests may be found in CRWMS M&O (2000a) and Ebert (1995).



NOTE: Schematic of colloid formation from waste form corrosion whereby several processes are represented: (1) spallation of radionuclide (RN) bearing alteration phases from the waste form that are within the colloidal size range, and (2) nucleation of colloids from ions dissolved from the waste form and sorption of ionic RN species or RN-bearing phases. Particle growth occurs by precipitation on nuclei and is controlled by factors such as ionic strength, temperature, pH, and solubility. When particle diameters exceed 1 micron or solution chemistry destabilizes the colloids, deposition, or coagulation and gravitational settling of RN-bearing alteration phases occur (modified Figure 2 from CRWMS M&O 2000a).

Figure 2. Schematic of Colloid Formation from Waste Form Corrosion

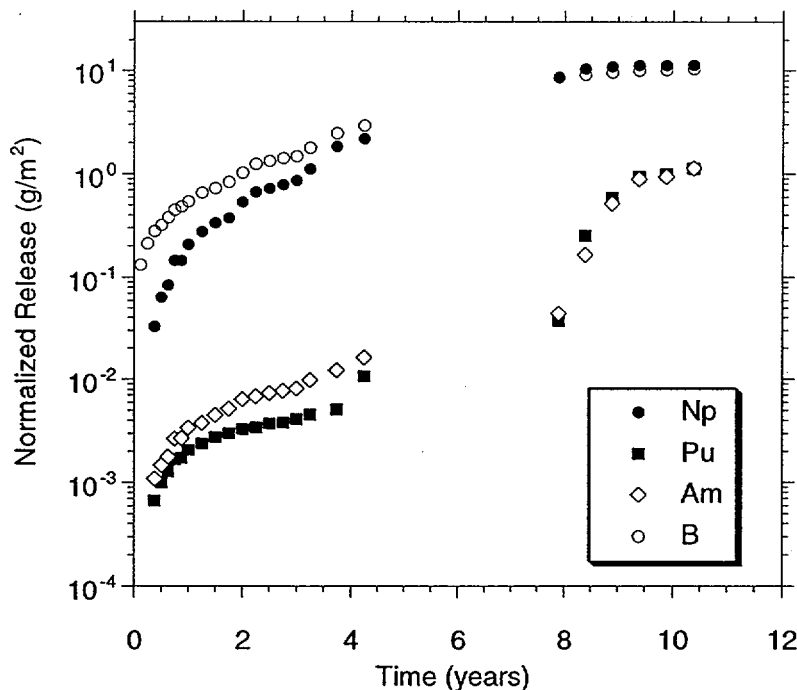
Colloids produced from both types of glass waste testing were primarily smectite clay containing discrete radionuclide-bearing phases which are incorporated (“entrained”) in the clay (CRWMS M&O 2000a). Iron silicate colloids were also observed. The entrained phases were identified as primarily brockite (thorium calcium orthophosphate) and an amorphous thorium-titanium-iron silicate, similar to thorutite. The phases also contained other actinides and REEs. Uranium was detected within the clays and iron silicates in some samples.

Currently, no data are available on the chemical and physical properties of the entrained phases, so that their solubility and disassociation/association properties with the clay cannot be derived and used in the model. The colloidal properties of the entrained radionuclide-bearing phases, therefore, are assumed to be governed by the properties of the smectite, and the stability (and therefore mobility) of smectite colloids will control the mobility of the entrained phases. (Testing is currently underway at LANL to determine the attachment/detachment properties of the entrained radionuclide-bearing phases in smectite colloids produced from the ANL glass tests.) Accordingly, the radionuclides are assumed to be “irreversibly attached” to the smectite colloids.

As the glass corrodes, the clay alteration product forms, grows, and evolves as a layer on the surface of the glass. The clay layer grows as the glass beneath the clay alters and as the clay-forming elements saturate in the solution and precipitate on the clay surface. Through these mechanisms colloid-sized clay that does not attach to the clay layer also precipitates from the solution (CRWMS M&O 2000a).

It was observed in the static tests that colloids developed and increased in concentration (population) with time, up to a point where the colloid concentration reached a maximum and then the dispersion became unstable. This was attributed by the investigators primarily to the concomitant increase in ionic strength to a threshold above which the colloids flocculated and settled by gravity (CRWMS M&O 2000a).

It was noticed that as the drip tests proceeded, whereas relatively soluble elements such as boron and neptunium increased smoothly with time, after about eight years the concentration in the leachate of the less soluble elements Pu and Am increased sharply (Figure 3). This was interpreted as evidence that colloid-sized fragments of the clay layer spalled from the clay layer on the surface of the corroding glass and were released into the fluid. This behavior was not observed in the static tests, in which the glass sample was not subjected to dripping water influx and remained submerged in the leachate.



NOTE: The cumulative normalized release of the elements B, Np, Pu, and Am from one of the tests in the N2 Series [Fortner-1999]. (Figure 10 from CRWMS M&O 2000a)

Figure 3. The Cumulative Normalized Release of the Elements B, Np, Pu, and Am

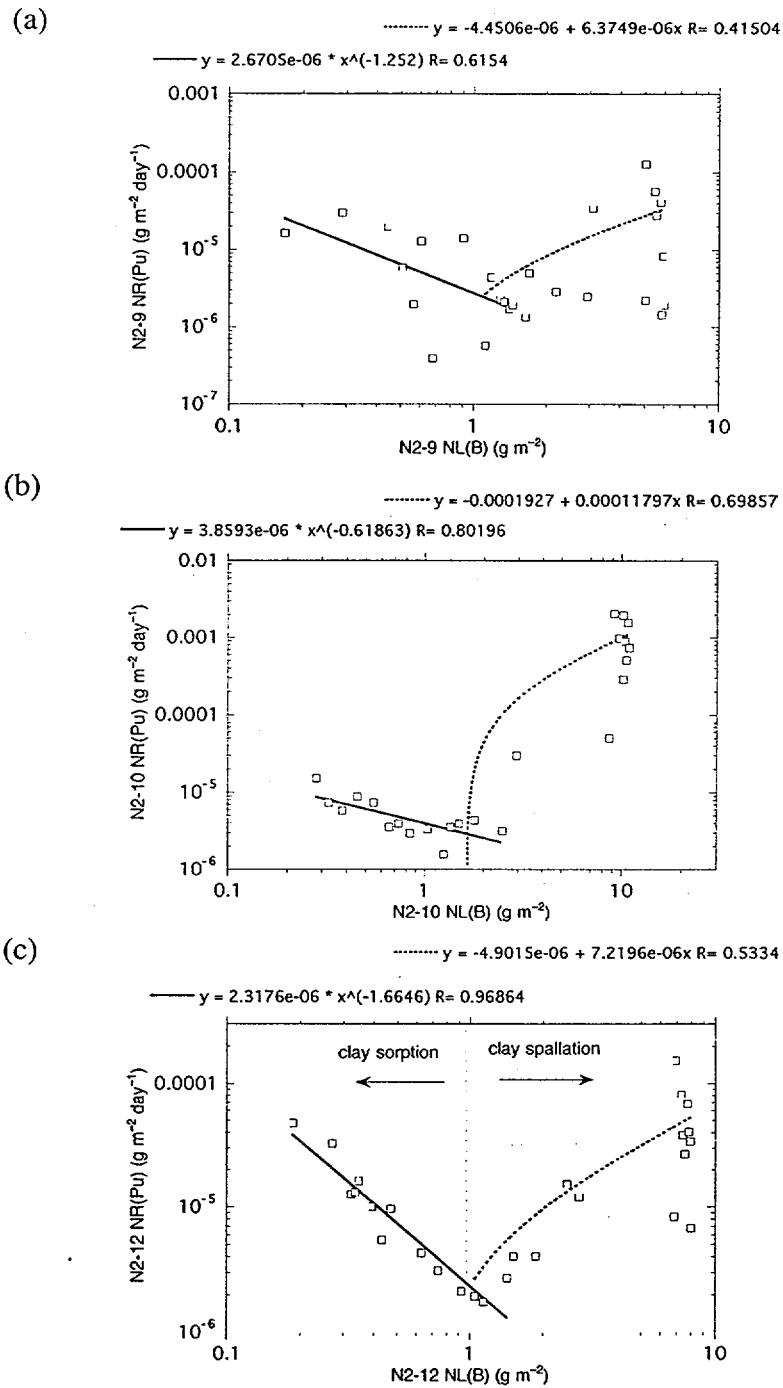
The experimental data on colloid generation resulting from HLW glass corrosion were used to develop a conceptual model for the "rate" and evolution of radionuclide release, described here, and an expression for use in predicting the rate of radionuclide release, described in Section 6.4.2, Alternative Models. The amount of boron released was used as a marker for the amount of glass corrosion as B was observed to increase smoothly in the leachate with glass corrosion, and it did not become incorporated in alteration phases. The normalized (to SA) mass loss of Pu, NL(Pu), from the glass was compared to the normalized mass loss of B, NL(B), as a function of reaction time; the ratio of the two indicates the quantity of Pu released relative to the quantity of glass corroded. In some of the tests, NL(Pu) was consistently lower than NL(B) by at least one order of magnitude. Marked decreases from this ratio can be attributed in specific tests to an increase in the glass corrosion rate due to secondary phase formation, as well as destabilization of the colloids (CRWMS M&O 2000a). NL(Pu)/NL(B) can be less than  $10^{-3}$  under solution conditions that inhibit colloid stability (see Section 6.4.2.1.2).

During the early stages of waste glass corrosion, the glass dissolves and releases components at a rate proportional to the rate of corrosion of the waste form. As this occurs, clay colloids nucleate in the solution and clay alteration layers form on the surface of the glass. These clay phases, which contain entrained radionuclide-bearing phases, also sorb ionic radionuclide species and/or colloidal radionuclide-bearing phases. If the ionic strength of the solution is low, the colloids are generally stable (see Section 6.1.2) and the rate of formation of the radionuclide-bearing colloids is proportional to the amount of altered glass (CRWMS M&O 2000a).

As the glass alters, the rate of radionuclide-bearing colloids production decreases; this is attributed by the investigators to colloid deposition (by sorption) on the fixed clay alteration layer. Once the cumulative normalized B release is greater than approximately  $1-3 \text{ g m}^{-2}$ , the radionuclide release is controlled by spallation of the clay layer. Figure 4 illustrates the observed increases in colloid production due to the onset of spallation.

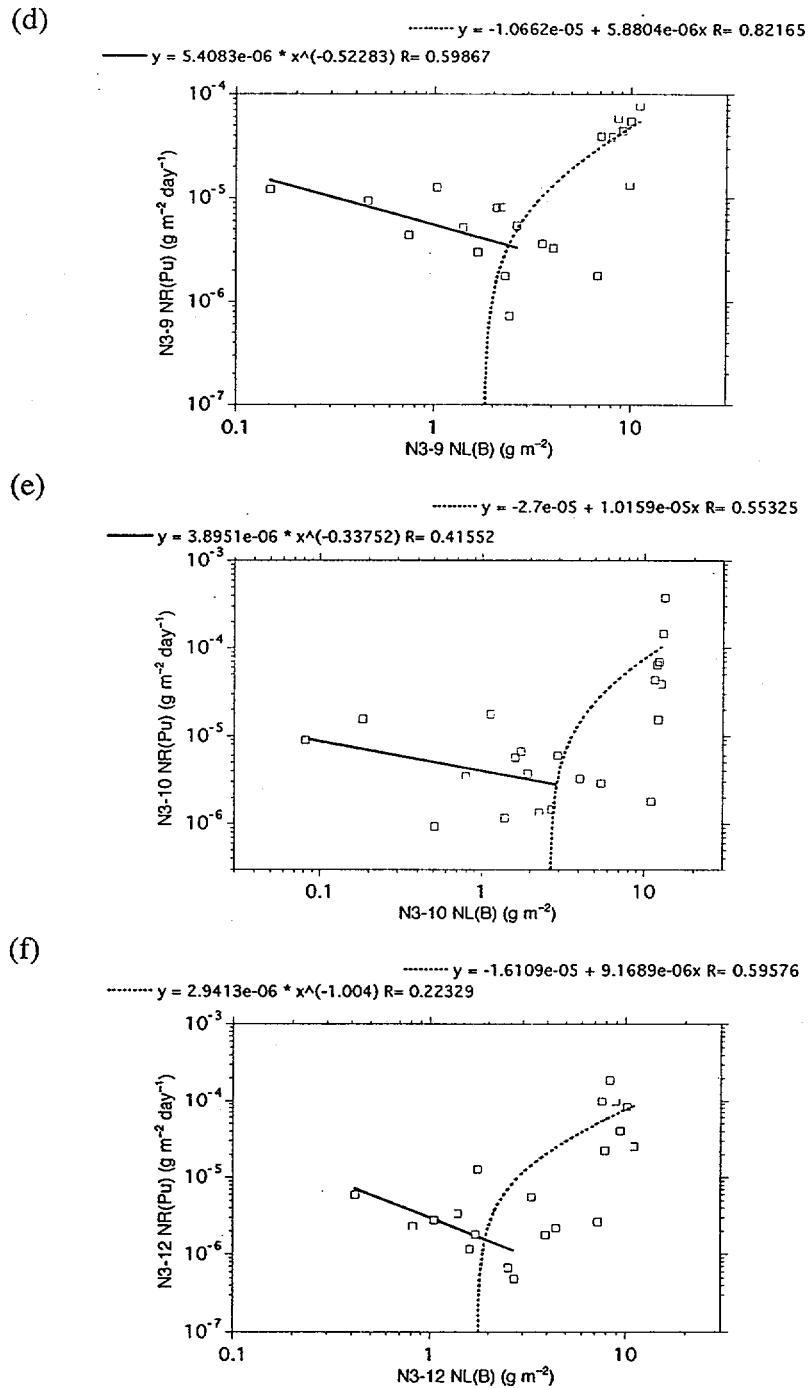
Thus, radionuclide release may be viewed as a two-step process: (1) alteration of the glass waste form and precipitation of colloids, and (2) erosion of colloid-sized fragments from the alteration products (CRWMS M&O 2000a). A preliminary quantitative version of this model is presented in Section 6.4.2, Alternative Models. The observed concentrations of HLW-derived colloids is discussed in Section 6.1.2, Colloid Stability and Concentration.

**Corrosion of Commercial SNF**—Testing on the corrosion of SNF has been conducted for over four years. Two types of spent fuel from pressurized water reactors with different burnups were used. EJ-13 water was introduced in two ways, at the bottom of the test vessel to maintain 100% relative humidity and onto the top of the spent fuel fragments. Generated colloids were characterized by using the same analytical techniques as were used in the glass testing. Descriptions of the SNF tests may be found in CRWMS M&O (2000a) and Finn et al. (1994).



NOTE: Plutonium release rate (calculated for each sampling interval) versus cumulative boron release: (a) N2-9, (b) N2-10, (c) N2-12. The total plutonium release is used, including vessel acid strip. (Figure 29 from CRWMS M&O 2000a)

Figure 4. Plutonium Release Rate versus Cumulative Boron Release



NOTE: Plutonium release rate (calculated for each sampling interval) versus cumulative boron release: (d) N3-9, (e) N3-10, (f) N3-12. The total plutonium release is used, including vessel acid strip. (Figure 29 from CRWMS M&O 2000a)

Figure 4. Plutonium Release Rate versus Cumulative Boron Release (continued)

In comparison to what was observed in the glass waste form tests, very little radionuclide-bearing colloidal material was detected in the fluid samples. (It is possible that this was partly a result of the test vessel configuration [CRWMS M&O 2000a].) In one sample, colloids

characterized were primarily a hydrous uranium oxide (schoepite) and a partially crystalline uranium silicate (soddyite). The colloids contained the rare earth elements (REEs) La, Ce, Pr, Nd, Sm, and Eu. Plutonium was not detected in these colloids; however, alteration on the corroded surface of the spent fuel contained significant concentrations of Pu, along with Zr, Ru, and REEs.

In another sample, smectite clay colloids were formed that were similar structurally and compositionally to the smectites produced in the glass tests, although they contained Mn, Ni, Fe, and Cr.

Elevated Pu concentrations in surficial corrosion mentioned above were found in several samples of both types of SNF. The Pu-bearing materials were overlain by a mat of cryptocrystalline U-bearing phase occurring as agglomerates of colloid-sized particles. The Pu layers were about 100 nm thick and may be colloidal aggregates within the alteration layer or may have accumulated as a result of filtering by the outer uranium silicate-aggregate mat (CRWMS M&O 2000a). It is the opinion of the investigators that the Pu layers were formed during dissolution of the fuel (CRWMS M&O 2000a), based largely on the fact that the Pu layer is "sandwiched" between the uranyl alteration phases and the fuel (CRWMS M&O 2000a).

Throughout the period of SNF testing, it was observed that most of the Pu was retained in the surficial corrosion concentration phase and little was released into the fluid. This may be due to the fact that the mat of uranium-bearing agglomerates, in effect, maintains the structural integrity of the alteration layer and prevents the Pu concentrations from spalling (CRWMS M&O 2000a). Based on experimental results, it is apparent that the Pu concentration phase is not released in a form in which it is irreversibly attached to colloids, and it is assumed in the abstraction that it will not be released in such form. (However, if these Pu regions became friable, e.g., due to humidity transients, Pu colloids might be released; another conservative approach would allow for the possibility of spallation of the Pu-concentration regions, although this process is not supported by the experimental data.) Further, filtered material with measurable associated Pu does not appear in TEM images to contain entrained radionuclide-bearing bases in the same manner as HLW glass corrosion colloids.

The experimental data on colloid generation resulting from SNF corrosion were used to develop a conceptual model for the "rate" and evolution of radionuclide release, described here, and an expression for use in predicting the rate of radionuclide release, described in Section 6.4.2. The amount of technetium released was used as a marker for the amount of SNF corrosion, as Tc was observed to increase smoothly in the leachate with glass corrosion, and it did not become incorporated in alteration phases. The normalized mass loss of Pu,  $NL(Pu)$ , from the glass was compared to the normalized mass loss of Tc,  $NL(Tc)$ ; the ratio of the two indicates the quantity of Pu released relative to the quantity of SNF corroded.

Dissolved Pu concentrations in the fluid were determined to be between  $10^{-10}$  and  $10^{-8}$ , less than to approximately the same as, the solubility of Pu in J-13 water determined by Efurd et al. (1998). Further, no correlation between the rate of Pu-bearing colloid formation and rate of SNF corrosion was observed. Consequently the Pu release as a function of Tc release was bounded by assuming that  $NL(Pu)/NL(Tc)$  is equal to  $10^{-5}$  (see Section 6.4.2.1.2).

In the conceptual model, most of the Pu and Am remain at the surface of the corroded fuel beneath and are protected by the mat of agglomerated uranium silicates. The Pu and Am concentrations associated with pseudocolloids are assumed to be similar to the Pu solubility as described above.

**Corrosion of DOE-SNF**—DOE-SNF consists of more than 250 distinct types of fuel. One type, an irradiated uranium metal fuel from the N-Reactor at Hanford, is being characterized as part of an ongoing program at ANL. In addition, drip tests and flowthrough tests are being performed on unirradiated uranium metal fuel. Preliminary results suggest that the metal degrades relatively rapidly, and there is evidence that colloid-size particulate material may form as a result of fuel degradation. It should be emphasized that the test data are preliminary and represent the initial results of an ongoing program. Clearly, however, the possible effects on repository performance of rapidly-formed colloid-size uranium particles must be considered.

A potentially mitigating factor is the small fraction of the DOE-SNF inventory represented by N-Reactor fuel. Out of almost 4000 co-disposal packages, only 160 are planned to contain N-Reactor fuel, or four percent of the co-disposal packages. On this basis, and because the data are preliminary and the ANL test program is ongoing, it is currently assumed that corroded N-reactor fuel will have little or no effect on repository performance. However, the assumption may be modified to reflect new information obtained during a verification process. It is proposed that verification be performed in three parts: (1) examine current data from the ongoing testing program at ANL; (2) perform sensitivity analyses using GoldSim; and (3) track the test program and its findings as the program proceeds.

#### **6.1.1.2 Iron-(Hydr)oxide Colloids from Internal Waste Package Corrosion**

As it is likely that some corrosion of the metallic components occurs and oxidizing conditions exist and that most of the metal is iron contained in several types of steel, it is assumed in the abstraction that iron will corrode and form iron-(hydr)oxides. It is further assumed that the iron-(hydr)oxides will occur in three forms: immobile scale, large particles that will settle out, and colloid-sized particles.

The proportions of these iron-(hydr)oxide occurrences may be represented by ranges or estimated from calculations of quantities of corrosion products based on known masses of metallic components. The iron-(hydr)oxide phases may be expected to provide abundant sorption sites for dissolved (aqueous) radionuclides in amounts determined by the appropriate effective  $K_{ds}$ . Stable iron-(hydr)oxide colloid suspensions may serve to increase the mobility of sorbed radionuclides (see Section 6.1.3). Their stability is controlled by fluid conditions including ionic strength and pH (see Section 6.1.2).

#### **6.1.1.3 Natural Colloids from Unsaturated Zone Groundwater**

Three types of groundwater colloids may be present at Yucca Mountain:

1. Mineral fragments are generally hydrophobic (see Section 6.1.2), hard particles that are kinetically stabilized or destabilized by electrostatic forces and may consist of crystalline or amorphous solids (Kim 1994). Steric coatings may enhance the stability of mineral

fragments by preventing close contact. Mineral fragments may act as substrates for sorption of radionuclides (they may also consist of precipitated or coprecipitated actinide solids).

2. Humic substances are generally hydrophilic particles that are stabilized by solvation forces. They can be powerful substrates for uptake of metal cations and are relatively small (less than 100,000 atomic mass units).
3. Microbes are relatively large colloidal particles that are stabilized by hydrophilic coatings on their surfaces, which behave as steric stabilizing compounds. They may act as substrates for extracellular actinide sorption, or they may actively bioaccumulate radionuclides intracellularly.

Clays, silica, hematite, and goethite colloids occur in groundwater in the vicinity of Yucca Mountain, and it is assumed that small quantities of these colloids will enter a failed waste package and be available to interact with released radionuclides. The presence and potential influence of natural colloids on formation of radionuclide-bearing colloids in the waste package are considered by assuming that groundwater colloids are smectite and iron (hydr)oxide.

An assessment of the concentration of humic substances in groundwaters collected near the Yucca Mountain was conducted by Minai et al. (1992). In that study, humic substances were extracted from several thousand gallons of J-13 well water through a series of steps including acidification, purifying with ion exchange columns, and freeze drying. The humic substances that were collected characterized with NMR and other spectroscopic techniques. Experiments were conducted to characterize site binding densities and complexation with Am. Results and supporting calculations indicated that the presence of humic substances in J-13 well water could affect oxidation speciation by reducing some radionuclide species. Considering the presence of calcium in J-13 well water, however, the authors estimated that the effective complexation capacity of humic substances is about  $2.3 \times 10^{-10}$  eq/L (equivalents per liter) at pH 6.9 and  $2.7 \times 10^{-11}$  eq/L at pH 8.2 (Minai et al. 1992, p. 199). Considering the very low complexation capacity of humic substances in this system, they are not considered as groundwater colloids.

Because of the relatively large sizes of microbes, they are very susceptible to filtration in geologic media. Consequently, microbe-facilitated contaminant transport is not considered in this abstraction. Refer to section 6.1.8 for more discussion on microbes.

Consequently, mineral colloids are considered in this abstraction and will, henceforth, be referred to generically as groundwater colloids.

### **6.1.2 Colloid Stability and Concentration**

In order for radionuclide-bearing colloids to affect repository performance, the colloidal dispersion must be stable for the time frame of transport and must carry significant amounts of radionuclides. Transport times can range from days/months/years for transport out of a failed waste package under a large seep, to hundreds of thousands of years for retarded transport to the accessible environment. Thus, some relatively unstable colloids generated at the waste form may persist long enough to be transported out of the waste package, increasing the radionuclide release from the waste package, but not traveling a significant distance away from the repository.

The more stable colloids, however, may remain suspended for years and travel a much greater distance. The clay colloids observed in the HLW and SNF corrosion tests are reasonably considered to have similar stability characteristics as natural clay colloids because the waste form-derived clays exhibit similar crystallographic and chemical properties as natural clays. The iron-(hydr)oxide colloids assumed to form from internal corrosion of the waste package are reasonably considered similar to natural iron-(hydr)oxide colloids for the same reasons. Following is a discussion of parameters affecting colloid stability.

**Background**—The stability and the coagulation, or agglomeration, of colloids is controlled by electrostatic and chemical processes at the colloid surfaces. In the 1940s and 1950s research on particle coagulation centered around the electrostatic properties of the particles in which the DLVO theory (independently developed by Derjaguin and Landau, and Verwey and Overbeek) of the particle electrical double layer was used to explain particle stability in terms of surface charges and potentials, the ionic strength of solutions, and the van der Waals forces between particles (Liang and Morgan 1990, p. 33). It was subsequently realized that the double-layer theory by itself was not complete, and that the origin of surface charges and the role of specific chemical interactions in the stabilization and destabilization of colloidal particles should be considered. At low surface potential and low surface charge density of particles, experiments to verify DLVO theory agreed with theoretical prediction. However, at high surface potential and charge density, due to the large repulsive forces of the particles, the theory predicted orders of magnitude higher stability ratios than were observed (Liang and Morgan 1990, p. 34). Beginning in the 1970s, surface complexation adsorption models were developed (Langmuir 1997b, p. 771); these models were used to analyze changes in particles' surface potential and charge brought about by complexation reactions (described by mass law equations) at the particle surface involving specific adsorbed chemical species (Dzombak and Morel 1987, p. 430; Liang and Morgan 1990, p. 34).

Hydrophobic colloidal particles are kinetically stabilized and destabilized by electrostatic forces. Mineral fragments, which are a hydrophobic colloid type, are affected by ionic strength in this way. Hydrophilic colloidal particles are stabilized by solvation forces, which are largely independent of the ionic strength of the dispersant. This type of colloidal particle is essentially a dissolved macromolecule. Humic materials are an example of the traditional hydrophilic colloid type.

**DLVO Theory and Surface Complexation**—The surfaces of dispersed, stable colloids have an electric charge sufficient to maintain the particles' separation by mutual repulsion. The surface charge of a particle can have two general causes: (1) specific characteristics of the crystal structure (see below), and preferential adsorption of specific ions onto the surface (van Olphen 1977, p. 18). The surface charges are compensated by the attraction of counter-ions, which have the opposite charge to the surface charges and to the vicinity of the particle surface. The charges at the particle surface and the oppositely charged, closely associated counter-ions make up the electric double layer (EDL) (van Olphen 1977, p. 18). The counter-ions are electrostatically attracted to the oppositely charged surface. However, they tend in water to diffuse away from the surface along a decreasing concentration gradient. As a result, counter-ions develop an "atmosphere" around the colloid that decreases in concentration away from the particle (van Olphen 1977, p. 30).

There are three causes of surface charge related to crystal structure (Langmuir 1997a, pp. 346-7): (1) isomorphous substitution in the crystal lattice (e.g.,  $\text{Al}^{3+}$  for  $\text{Si}^{4+}$  in the tetrahedral layer and  $\text{Mg}^{2+}$  for  $\text{Al}^{3+}$  in the octahedral layer resulting in an excess of  $\text{O}^{2-}$  bonds, the chief cause of negative surface charge in smectites); (2) lattice imperfections or defects (e.g., deficits in octahedral  $\text{Al}^{3+}$  or interlayer  $\text{K}^+$  causing a net negative surface charge, also important for smectites); and (3) broken or unsatisfied bonds (e.g., at crystal plate corners and edges usually resulting in a net negative surface charge due to exposed  $\text{O}^{2-}$  and  $\text{OH}^-$ , important for smectites). As clay particles decrease in size, the importance of broken bonds increases (Langmuir 1997a, p. 346).

The surface charge of oxides, hydroxides, phosphates, and carbonates originates chiefly from ionization of surface groups or surface chemical reactions (Langmuir 1997a, p. 349). Surface charge among this group is strongly dependent upon pH, being positive at lower pH and negative at higher pH. For example, in oxides and hydroxides, this is due largely to the adsorption of  $\text{H}^+$  at lower pH and  $\text{OH}^-$  at higher pH. The pH at which the net surface charge is neutral is called the zero point of charge (ZPC); if the change in charge is solely due to adsorption of  $\text{H}^+$  or  $\text{OH}^-$  ions, the pH at neutrality is called the point of zero net proton charge (PZNPC) (Langmuir 1997a, p. 350).

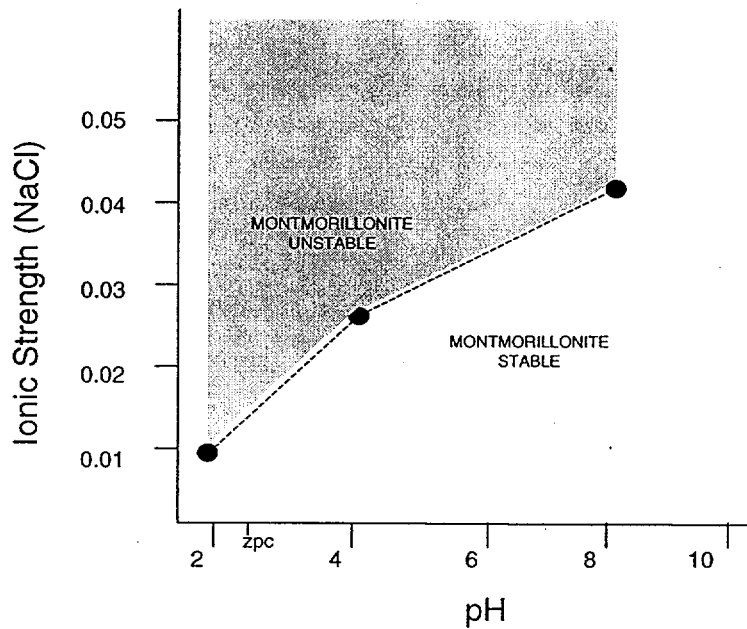
Far from the ZPC or PZNPC, the surface-charge density is relatively high; the particles are mutually repelled, and the suspension is stable. At or near the ZPC or PZNPC the repulsion force decreases to near zero, and the particles are more likely to agglomerate ("stick") when particle collisions occur.

**Stability of Smectite Colloids as a Function of pH**—The ZPC of smectite is approximately pH 2. Since a pH this low is not anticipated in the repository, it is a reasonable assumption that smectite colloids will remain in a stable pH range much of the time under anticipated repository conditions (unless ionic strength exceeds a certain threshold). However, it should be recognized that with decreasing pH, the charge density of smectite particle surfaces will decrease as more and more  $\text{H}^+$  sorb to the surface and offset negative charges, generally decreasing stability (Buck and Bates 1999; Tombacz et al. 1990). This decrease in stability has been taken into account in Section 6.2.2 and 6.3.

The HLW tests conducted at ANL resulted in measured pH ranging between approximately 9 and 11.5 (Buck and Bates 1999), which is part of the range at which smectite colloids exhibit the highest surface charge and, hence, are most stable. Tombacz et al. (1990) investigated the stability of montmorillonite (a smectite clay mineral) suspensions as a function of pH and ionic strength in a NaCl solution. It was found that suspensions became unstable and flocculated at pH 2, 4, and 8 in 0.01 M, 0.025 M, and 0.04 M NaCl solutions, respectively (Figure 5).

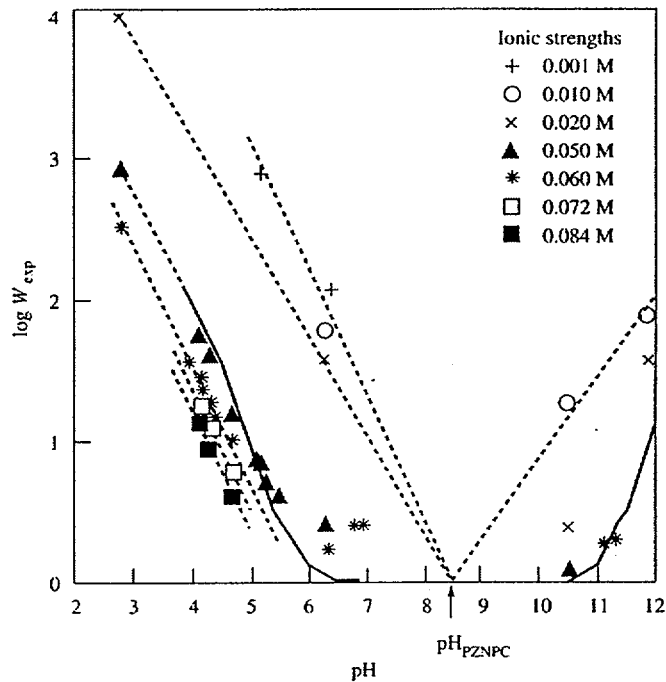
**Stability of Iron-(Hydr)oxide Colloids as a Function of pH**—The ZPC of iron-(hydr)oxide colloids is around pH 8.5, and at this pH they will be unstable and tend to agglomerate. At higher or lower pH, however, iron-(hydr)oxide colloids may be stable, depending upon ionic strength (see Sections 6.2.2 and 6.3.6). Liang and Morgan (1990) demonstrated that for a given ionic strength iron-(hydr)oxide stability increases as pH both increases and decreases away from the ZPC (Figure 6). In general the higher the ionic strength, the wider the pH range about the ZPC that iron-(hydr)oxide is unstable. For example, at an ionic strength of 0.05 M, iron-

(hydr)oxide is unstable between approximately pH 6 and 11. This relationship is incorporated in the abstraction and is discussed in Section 6.2.1.3.



NOTE: Data points represent combinations of ionic strength and pH at which montmorillonite stability is significantly decreased. Data from Tombacz et al. (1990).

Figure 5. Experimental Determination of Montmorillonite Stability as a Function of pH and Ionic Strength



NOTE: The pH of zero proton condition is indicated. Dashed lines are drawn through the experimental points as a guide. The solid line represents a DLVO model calculation for ionic strength 0.05 M. Note that  $W_{exp}$  represents the stability of the dispersion, in terms of the rate at which colloidal particles in the dispersion agglomerate. A high value represents a stable dispersion; a value of zero indicates rapid agglomeration. At ionic strengths of about 0.5 m or more, the stability ratio is very low between pH values of about 6 and 11. A relatively low  $\log W_{exp}$  of approximately 0.2 was selected for abstraction of pH and ionic strength data for use in Figure 11 (Figure 1 from Liang and Morgan 1990).

Figure 6. Experimentally Derived Stability Ratio,  $W_{exp}$ , of a Hematite Suspension Plotted as a Function of pH for Differing Ionic Strengths

**Ionic Strength**—In nearly pure water, dissolved ions are likely to contact only other water molecules. As the concentrations of the ions increase, the ions are likely to come in contact with one another. The interactions between and among the ions is proportional to their charge, as reflected in the definition of ionic strength:

$$I = \frac{1}{2} \sum (m_i z_i^2) \quad (\text{Eq. 1})$$

where  $I$  (and  $m$ ) is in molal units and  $z_i$  is the charge of ion  $i$  (e.g., Langmuir 1997a).

According to DLVO theory, colloids become unstable as ionic strength in a solution increases due to compression of the diffuse counter-ion atmosphere and decrease in surface potential, i.e., decrease in repulsive forces. Further, the degree of compression of the EDL is dependent on the concentration and valence of ions of opposite sign from that of the surface charge (van Olphen

1977, p. 34). The effect of valence is captured by the Schulze-Hardy rule, which incorporates the principle that for a given counter-ion concentration, the higher the valence of the counterions, the more unstable the colloids and the greater the tendency to flocculate (van Olphen 1977, p. 24).

In his treatise on clay colloidal dispersions, van Olphen (1977 p. 24) summarized empirically determined critical coagulation concentration (c.c.c.) values as follows:

<u>Counterion Valence</u>	<u>c.c.c. (μM)</u>
±1	25,000 to 150,000
±2	500 to 2000
±3	10 to 100

At pH values below the  $pH_{ZPC}$  for a mineral, the negatively charged counterions are important; above the  $pH_{ZPC}$ , positively charged counterions are important.

For comparison, concentrations of counterions in J-13 well water are as follows (CRWMS M&O 2000d):

<u>Ion</u>	<u>Valence</u>	<u>Concentration (μM)</u>
Na	+1	1990
K	+1	129
Ca	+2	324
Mg	+2	82.7
Al	+3	0.0255
Cl	-1	201
S (sulfate)	-2	192

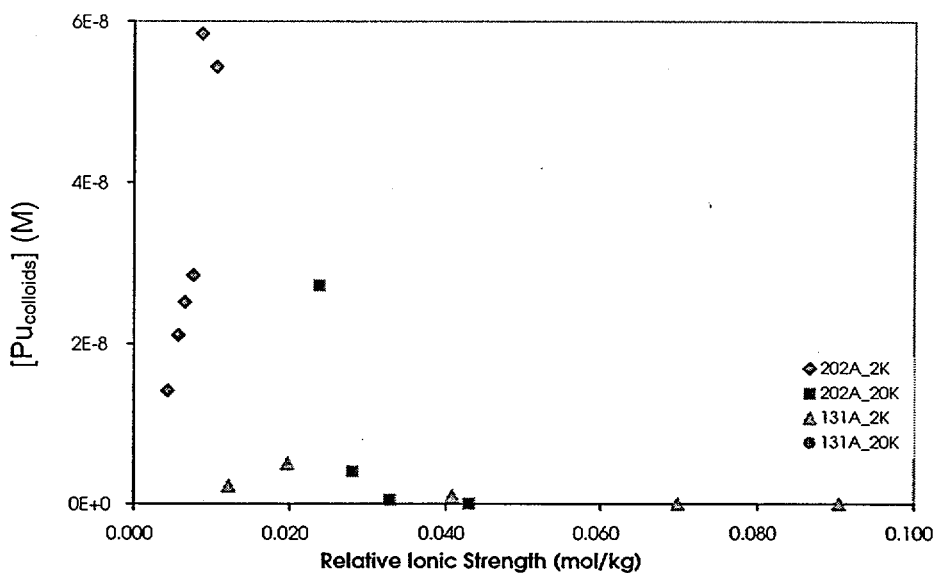
Note that none of the concentrations of individual ions in J-13 well water exceed van Olphen's empirical c.c.c. values, although  $Ca^{2+}$  is close.

**Stability and Concentration of Waste Form Colloids**—Colloids were formed in the course of static HLW tests on several of the glasses for different SA/V. It was observed that as the ionic strength increased, colloid concentration generally decreased, and ultimately a threshold value was reached above which the colloids were not observed or were observed in very low quantities (Figure 7) (CRWMS M&O 2000a). As this threshold was approached, it was also observed for one glass that the colloid size increased significantly due to aggregation of the colloids. The threshold at which flocculation occurred was approximately  $I = 0.05m$ . During the drip tests, ionic strength remained below this value, and colloids were stable throughout the tests.

**Stability and Concentration of Groundwater Colloids**—Colloids are thought to exist naturally in groundwater in all subsurface environments with the composition and concentration of colloids being site specific and determined by the geologic nature of the subsurface. Transport of radionuclides by iron-(hydr)oxides and clay colloids is a potentially important transport

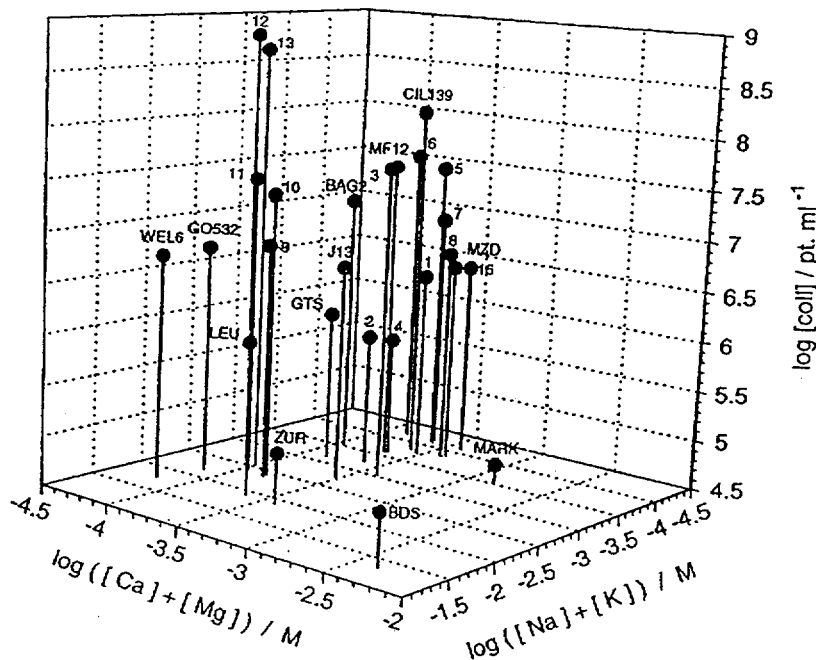
mechanism, and is thought to be generally more prevalent than transport by true colloids (McCarthy and Zachara 1989).

McCarthy and Degueudre (1993) conducted a significant effort to characterize the colloids of groundwaters from around the world from crystalline and sedimentary rocks in saturated and unsaturated hydrologic regimes. They showed that the colloid concentration and stability is dependent, among other things, upon pH, redox potential, ionic strength (including relative concentrations of the major cations Na, K, Ca, and Mg), counterion valence, and organic carbon; these factors were studied in the investigation. The results indicate that, in general, colloids tend to be stable if the concentration of alkalis (Na and K) is below approximately  $10^{-2}$  M and if alkali-earth elements (Ca and Mg) are below approximately  $10^{-4}$  M (Figure 8). This provides a guideline for assessing colloid stability and allows for very rough estimation of concentration. Whereas the DLVO calculations provide useful inferences on mechanisms of colloid destabilization, these empirical observations are more useful in developing approaches to PA calculations.



NOTE: Plutonium-bearing colloids as a function of ionic strength for corrosion tests on glass samples SRL 202A and SRL 131A at SA/V or 2,000 and 20,000/m (at 90°C) (Figure 8 in CRWMS M&O 2000a).

Figure 7. Plutonium-Bearing Colloids as a Function of Ionic Strength in Corrosion Tests



NOTE: Here, concentrations of colloids are compared on the basis of alkali and alkaline-earth element concentration for colloid size > 100 nm. (Figure 1 from CRWMS M&O 2000b)

Figure 8. Colloid Concentrations Versus Alkali and Alkaline-Earth Concentration for Groundwaters from Around the World

In Chapter 4 of *Total System Performance Assessment—Viability Assessment (TSPA-VA) Analyses Technical Basis Document* (CRWMS M&O 1998), data on colloid concentration and ionic strength for these groundwaters were plotted in an attempt to provide a predictive tool for estimation of colloid concentration, given the ionic strength. The plot illustrating the relationship is presented in Figure 9. Note that the uncertainty indicated by the error bars is quite high, approximately several orders of magnitude in both directions about the data points. Further, the shape of the curve is dominated by one groundwater with an ionic strength of approximately 0.07m. What the plot shows is that at higher ionic strengths there is a tendency toward lower colloid concentrations.

Colloid concentration is difficult to correlate precisely with ionic strength as there are other factors that can significantly affect concentration, such as pH. As described above, for example, at pH 8.5, hematite colloids would have a zero net surface charge (since their ZPC is approximately 8.5) resulting in elimination of mutual repulsive forces and the tendency to flocculate, even if the ionic strength were very low.

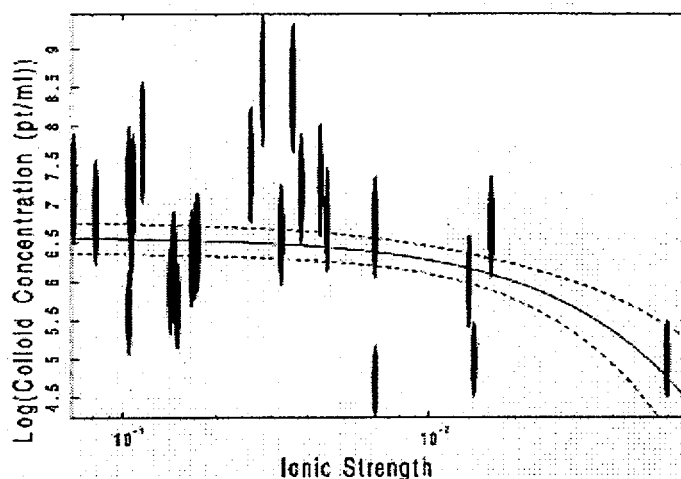


Figure 4-30. A Linear Fit to all of the Available Data for Colloid Concentrations in Various Groundwaters See Table 4-35 for Values.

DTN: MO0003SPAHL012.004

NOTE: Colloid concentration plotted as a function of ionic strength for the same groundwaters as those in Figure 8. Error bars denote uncertainty in concentration values. Note that this plot may illustrate that concentrations may be lower at higher ionic strengths. Ionic strength units: m (mol/kg).

Figure 9. Colloid Concentration Versus Ionic Strength for Groundwaters from Around the World

Further, site-specific studies of groundwater colloids (e.g., Kingston and Whitbeck 1991) suggest that when groundwater conditions favor colloid stability, there may be a very wide range of colloid concentrations observed for a narrow range of groundwater chemistry.

### 6.1.3 Radionuclide Attachment to Colloids

A brief description of radionuclide attachment to colloids is presented in this section. A more comprehensive treatment may be found in Attachment XVI.

Non-radioactive colloids are only important to repository performance insofar as radionuclides attach to them. Attachment as used here is a general term that implies no particular mechanism. Attachment may occur by a number of mechanisms and may be reversible or irreversible in the time frame of transport. Some of the mechanisms of attachment include coprecipitation (e.g., radionuclide phases entrained in smectite colloids), surface sorption (e.g., Pu sorbed onto smectite or iron-(hydr)oxide colloids), and ion exchange. The rate of attachment, detachment, and transport determine the effective reversibility of the attachment. When the attachment is fast and reversible, transport on colloids will be controlled by local equilibrium, and simple models, e.g., linear isotherm models, using effective distribution coefficients reasonably describe the radionuclide behavior. When attachment is irreversible or detachment is slow relative to transport times, then local equilibrium models may fail, resulting in over- or under-predictions of transport.

**Reversible Attachment**—Perhaps the most common approach used in assessment of contaminant-rock interactions in the subsurface is the linear isotherm, or  $K_d$ , approach, based on results of batch sorption experiments. The linear isotherm model relationship is defined as follows (Langmuir 1997a):

$$S = K_d C \quad (\text{Eq. 2})$$

where,

- $K_d$  distribution coefficient (mass-based)
- $S$  mass of a solute adsorbed on a unit mass of solid
- $C$  concentration of the adsorbing solute

The amount of solute adsorbed on a solid can also be defined on the basis of area as follows:

$$S = K_a C$$

where,

- $K_a$  distribution coefficient (area-based)
- $S$  amount of a solute adsorbed on a unit area of solid
- $C$  concentration of the adsorbing solute

For this relationship to be applicable, i.e., for the assumption of constant  $K_d$  to be valid, three critical assumptions must be met. First, the water-contaminant-rock system must be in thermodynamic equilibrium. In other words, sorption must be completely reversible. Second, contaminant uptake must scale linearly with contaminant concentration. Third, the presence of other solutes in the system cannot affect the sorption. Because of the nature of the formation of waste-form colloids and the interaction of some radionuclides, particularly some actinides, with mineral surfaces, critical assumptions of the linear isotherm model are not met, and special treatment must be made. Those approaches are described below.

Reversible radionuclide uptake chiefly occurs by ion exchange in clay minerals and adsorption in most other minerals. Because of the assumption of reversibility, coprecipitation of radionuclides along with other non-radionuclide ions is excluded. A large amount of data exists in published literature for sorption, and, in the past several decades, increasing attention has been given to understanding the mechanisms of sorption. In this section, the development of  $K_d$  values for uptake of strontium (Sr), cesium (Cs), thorium (Th), uranium (U), protactinium (Pa), neptunium (Np), plutonium (Pu), and americium (Am) on colloids is described, along with caveats. These radionuclide elements were chosen for analysis because, based on a screening exercise, they are considered by TSPA to be important to dose; high uncertainty surrounds their potential behavior as pseudocolloids; and daughter products of uranium may remain embedded in uranium-bearing colloids.

To a large extent, the effectiveness of colloids at facilitating contaminant transport is due to their very large mobile surface area available for sorption. Depending on the size distribution of

colloids in the dispersion, the impact of choosing a mass-based  $K_d$ , or a surface-area-based  $K_a$ , may be significant. The greatest deviation exists in situations in which an inordinately large number of very small colloids exist, which have a high surface-area-to-mass ratio. Based on experimental measurements and observations of colloids in Yucca Mountain Project (YMP) groundwaters, this situation does not exist at YMP, and the use of a mass-based  $K_d$  is satisfactory. That is fortuitous, since nearly all available sorption information is mass-based, and conversion to surface-area-based information is not always straightforward.

To develop colloid  $K_d$  information, information provided by an AMR (CRWMS M&O 2000b) and published literature were considered. Several significant compendia of sorption data have been assembled in the past decade. One useful example is the compendium developed by the National Cooperative for the Disposal of Radioactive Waste (NAGRA, Switzerland; Stenhouse, 1995). The objective of that work was to compile a set of  $K_d$  values useful for evaluation of waste-disposal in hypothetical sites in Switzerland. The sorbents considered were crystalline rock, marl, and bentonite, all with reducing groundwaters (or porewater, in the case of bentonite). Ionic strengths are similar to J-13 water or greater. Despite differences in those conditions, the information compiled in the NAGRA document is useful for YMP, in that it includes consideration of phenomena affecting sorption.

A second compendium that is particularly useful is a recent one developed for the U.S. Environmental Protection Agency (EPA 1999). In that work, information on radionuclides including Sr, Cs, Th, U, and Pu is compiled (no information for Pa, Np, or Am). The assembled data are interpreted to predict ranges of  $K_d$  values for soils in shallow subsurface environments. Redox conditions for that system are oxidizing, which makes it useful for the redox-sensitive radionuclides at YMP. Unfortunately, the group of radionuclides covered does not provide an analog element for trivalent or pentavalent elements, such as Am(III), Pa(V), or Np(V).

Several sources of YMP-specific sorption data exist from LANL research. Some specific experiments were conducted to evaluate sorption of Pu(IV) and Pu(V) on colloidal dispersions of hematite, goethite, montmorillonite, and silica. Information on Am(III) was also collected for all but goethite. Sorption was measured as a function of time up to 4 or 10 days. Desorption was measured after 150 days because desorption tends to be much slower in these mineral-sorbate systems. In Attachment XVI, Table XVI-5, available sorption data collected at 1 day and longer periods is compiled. To reduce these data, sorption measurements from tests conducted at 1, 2, and 4 days, or 1, 2, 4, and 10 days were averaged. The rationale is that sorption is typically quite fast, requiring less than one day to approach an asymptote. That hypothesis is supported by the LANL data, in that after one day, oscillation in values were observed, but  $K_d$  values did not increase appreciably. The sorption averages were used in a second averaging operation, by including the results of the desorption experiments. In general, desorption and the averaged sorption  $K_d$ s are very similar or within about a factor of 3 or 4, except in a few cases. It is clear, however, that desorption is significantly slower. A third averaging was conducted to consider the results of experiments conducted in synthetic J13 water and actual J13 water. The reason for the different results in the two waters is not clear. For plutonium, since both Pu(IV) and Pu(V) may be present in Yucca Mountain, results from the goethite experiments were averaged. Goethite was selected rather than the more sorptive hematite, because goethite, as a less crystalline material, should more closely resemble corrosion-product colloids produced from waste degradation. The developed values are listed in Attachment XVI, Table XVI-6.

A second source of sorption data is compiled in the AMR focusing on transport properties in the unsaturated and saturated zones (CRWMS M&O 2000b), which also considers previously done Yucca-Mountain reviews by Meijer (1992) and others. Values developed for devitrified tuff and iron-(hydr)oxides in the saturated zone are listed in Attachment XVI, Table XVI-6. These ranges are generally comparably to values extracted from the NAGRA report (Table XVI-3). For sorption on colloids, it is likely to be conservative to use the large  $K_d$  values in the ranges.

Table 4 summarizes recommended values, which have been extracted from the LANL data discussed above. Values for Sr, Cs, Pa, U, and Np were taken from the AMR discussing transport properties in the saturated and unsaturated zones (CRWMS M&O 2000b). The maximum  $K_d$  values from the ranges for devitrified tuff and iron-(hydr)oxides were used as an analog for colloids consisting of smectite and corrosion-product colloids, respectively. Values for Am were also used for Th, because of similar tendencies for sorption, not as an oxidation species analog. For Pu and Am, values were developed from Stenhouse (1995). Given the non-exact nature of developing these  $K_d$  values, a plus-or-minus one-order-of-magnitude uncertainty band can be assigned to each value.

Table 4. Sorption Data for Colloid Transport

Radionuclide Sorbate and Oxidation State(s) at YMP	Recommended $K_d$ (mL/g) Iron-(hydr)oxide Colloids Smectite Colloids	Source
Sr(II)	200 30	Maximum values developed in CRWMS M&O (2000b, Table 16), for devitrified tuff and iron-(hydr)oxides, respectively, for saturated zone units.
Cs(I)	1000 500	As above
Th(IV)	(use same values as developed for Am)	As above
Pa(V)	100 1000	As above
U(VI)	5 1000	As above
Np(V)	10 100	As above
Pu(IV, V, VI)	70,000 <sup>a</sup> 30,000 <sup>a</sup>	Average of results of each data set (~1 day tests) for Pu(IV) and Pu(V) sorption on goethite and Ca-montmorillonite (DTN: LA0003NL831352.002)
Am(III)	600,000 <sup>a</sup> 40,000 <sup>b</sup>	Average of results of each data set (~1 day tests) for Am sorption on hematite and Ca-montmorillonite (DTN: LA0003NL831352.003)

NOTES: <sup>a</sup> A value of 10,000 mL/g was provided to PA, based on preliminary data

<sup>b</sup> A value of 100,000 mL/g was provided to PA, based on preliminary data

**Irreversible Attachment**—The assumptions required for the linear sorption model described above are not met in HLW-glass degradation experiments, which show that plutonium is irreversibly attached to smectite colloids generated during the experiments (CRWMS M&O 2000a). Second, evidence on plutonium sorption experiments (Stenhouse 1995) with colloidal hematite and goethite show that the rate of desorption (backward rate) of Pu is significantly slower than the rate of sorption (forward rate). More importantly, over a significant time period (up to 150 days in some experiments), the extents of desorption is somewhat less than the extent of sorption. Special considerations must be made for these situations.

For the HLW-glass experiments, the conceptual model and abstraction developed below accounts for smectite colloids with “engulfed” plutonium and other radionuclides by treating them as a separate colloid subtype and assuming that the engulfed radionuclides are an intrinsic part of the colloid, not in equilibrium with the aqueous system. For the non-ideal sorption behavior of plutonium, a larger  $K_d$  was selected based on the desorption experiments, pending further results from LANL.

#### 6.1.4 Physical Filtration of Colloids

Colloid filtration as discussed here refers to the physical removal of colloids from a flow system by pore clogging, sieving, and straining. Filtration of colloids generally means the retention of

colloids moving with the suspending fluid in pores, channels, and fracture apertures that are too small or "dry" to allow passage of the colloids. Two types of physical filtration are recognized, conventional straining and film straining. Colloids are filtered by conventional straining if they are larger than a pore throat diameter or fracture aperture. Where water saturation is low, colloids may be filtered by film-straining if their size is greater than the thickness of the adsorbed water film coating the grains of the rock. The rate of colloid transport through thin water films depends upon the colloid size relative to the film thickness.

Filtration of colloids could conceivably occur within the waste package. Colloids may form within the waste form (e.g., corroded waste fuel pellets) and at its outer surfaces (e.g., corroded HLW glass). They could be filtered within fractures in fuel pellets or trapped at the boundaries of disaggregating grains. Colloids forming within fuel rods with breached cladding could be filtered at perforations in the cladding; colloids formed and spalled from the HLW glass could be filtered at perforations in the stainless steel HLW container. Colloids reaching the interior of the waste package (after escaping from fuel rod cladding and HLW containers) could be filtered at perforations in the skin of the waste package.

Existing colloid filtration models are empirically derived and to a considerable extent are specific to the system experimentally characterized. There have been no comprehensive studies of colloid filtration within spent fuel and HLW glass waste package environments. Therefore, meaningful analysis of colloid filtration within the waste package is currently not feasible.

The conservative assumption is therefore made that all colloids formed within the waste package (the calculated colloid source term) are assumed to exit the waste package and enter the drift; thus, consideration of colloid filtration processes is excluded from the TSPA-SR analysis.

### **6.1.5 Colloid Sorption at the Air-Water Interface**

Both hydrophilic and hydrophobic colloids (defined in Section 6.1.1.3) may be sorbed irreversibly at the gas-water interface under partially saturated conditions (Wan and Wilson 1994). Models of colloid transport in partially-saturated media have been developed in recent years, but there have been no experimental studies of transient flow in partially saturated porous media for model comparison and calibration.

As summarized, the concentration of colloids sorbed at the gas-water interface is a function of the following conditions:

- The interface surface area available for colloid uptake, which is a function of the total gas saturation
- The affinity of colloids for the gas-water interface (hydrophobic colloids have higher affinities than hydrophilic colloids)
- The electrostatic charge on the colloid—less negatively charged colloids exhibit a stronger affinity
- The salinity of the aqueous phase, with higher salinity promoting sorption.

Empirical evidence suggests that the sorption of colloids at the gas-water interface is irreversible and the affinity may be stronger than to the rock matrix (Wan and Wilson 1994).

Partially saturated conditions may be described or classified by considering degrees of saturation. At low water saturations the surface area of the gas-water interface approximates that of the rock matrix. Overall, colloid migration is retarded, although colloids may still move through the adsorbed water films. At intermediate water saturations there is still an interconnected gas phase, although gas flux may be lower. The interface may act as a static sorbing surface, but the estimating geometry and surface area is complicated, more so under changing saturation state. At high water saturations the majority of the gas is present at small gas bubbles that may migrate, transporting sorbed colloids. However, a proportion of the bubbles may become trapped in the rock and will effectively immobilize sorbed colloids.

Colloid migration rates depend more strongly on colloid size as lower saturation states are considered (CRWMS M&O 2000b; McGraw 1996). To examine the influence of colloid size on transport, McGraw (1996) investigated transport of monodisperse colloids (five different sizes, between 20 nm and 1900 nm) under both saturated and unsaturated conditions in a quartz sand. The results indicated that under saturated conditions the time required for breakthrough of each colloid at  $C/C_0 = 50\%$  was the same as that of the breakthrough of a non-reactive tracer, indicating no relationship of colloid size to migration under saturated conditions. However, the times required for breakthroughs of the colloids under highly unsaturated conditions exhibited a strong relationship between the colloid breakthrough and the colloid size with fairly complete breakthrough of the 20-nm colloid and little or no breakthrough of the 1900-nm colloid.

In another set of experiments, McGraw (1996) compared four sets of hydrophobic and hydrophilic colloids (functionalized latex microspheres). Her results indicated that transport of hydrophobic colloids depends on colloid size, water film thickness, and colloid charge density. In contrast, hydrophilic colloids were not affected by these variables and were rapidly transported through the system even under very low moisture contents. McGraw (1996) concluded that for hydrophobic colloids, the cumulative mass of colloids recovered relative to that input into the column was logarithmically dependent upon the ratio of the water film thickness to colloid diameter. In contrast, for hydrophilic colloids, the cumulative mass of colloids recovered relative to that input into the column was linearly dependent upon the ratio of the water film thickness to colloid diameter, similar but more pronounced than the effect with the non-reactive tracer. McGraw's findings suggest that the unsaturated zone is not necessarily an effective barrier to colloid migration even for relatively large colloids, although larger colloids will tend to be retarded more than smaller ones.

Although the potential effects of degree of saturation on colloid transport are varied and complex, on balance it appears that colloids would be at least somewhat retarded under low-saturation conditions. Therefore, neglect of colloid sorption onto the air-water interface in the TSPA calculations is believed to be conservative.

#### **6.1.6 Gravitational Settling of Colloids**

Over the relatively short transport distances within the waste package, larger colloidal particles may experience gravitational settling, thereby inhibiting transport. However, GoldSim does not

model settling; because of this and the fact that there are no conceptual models and data for gravitational settling within the waste package, this process is not incorporated into the abstraction. Instead, the conservative assumption is made that gravitational settling does not occur, but that all colloid-associated radionuclides leave a breached waste package.

### 6.1.7 Colloid Diffusion

Colloidal particles, together with any associated actinides, that are sufficiently small may diffuse into intercrystalline porosity and will be physically retarded.

Physical retardation of dissolved actinides is best evaluated using Fick's Law, in which the mass diffusion constant ( $D$ ; also referred to as diffusivity or the free-water diffusion constant) is a critical parameter. At a fundamental level, diffusivity is related to the physical characteristics of the diffusing molecule and the molecules of the host medium and the intermolecular forces acting between them. For example, the diffusivity of a gas molecule in another gas (the host gas) at low density is inversely proportional to the square root of the reduced mass of the diffusing and host gas molecules and the collision diameter. Whereas a rigorous theory of solute diffusion in liquids is apparently not available, order of magnitude estimates may be made on the basis of hydrodynamical theory. With that theory, the diffusivity of a solute in a liquid is inversely proportional to the radius of the diffusing particles (Bird et al. 1960, p. 513). Rates of diffusion of colloidal particles can be estimated by scaling those experimentally determined free water diffusion constants for dissolved actinides to dissolved colloidal materials on the basis of size (Stokes-Einstein relationship) as follows:

$$D_{\text{coll}} = D_{\text{ion}} \left( \frac{r_{\text{ion}}}{r_{\text{coll}}} \right)$$

where,

- $D_{\text{coll}}$  diffusion constant for a colloidal actinide of radius  $r_{\text{coll}}$
- $D_{\text{ion}}$  diffusion constant for a dissolved actinide of radius  $r_{\text{ion}}$
- $r_{\text{coll}}$  radius of the colloidal actinide
- $r_{\text{ion}}$  radius of the dissolved actinide

For example, given an ionic radius and a colloidal particle radius of 1 Å and 10 nm, respectively, the free-water diffusion constant for the colloidal particle would be that of the dissolved actinide reduced by a factor of 100. That approach is consistent with discussions in Hiemenz (1986, p. 81).

### 6.1.8 Microbes and Organic Components

The colloid source term from the repository may be sensitive to the presence of colloid-sized microbes, which could change aqueous chemical conditions, facilitate contaminant transport, affect the amount of colloidal material such as hematite, goethite, and silica that will be mobile, influence corrosion of the waste package, and effect agglomeration of colloids. The potential

effects of microbes in the repository on the colloidal source term concentration are described below.

Changes in near field chemistry in micro-environments in and around waste packages that can cause localized pH and Eh conditions to vary considerably from the measured or predicted bulk chemistry. For example, acidophilic microorganisms have been found in alkaline mine spoils actively creating acidic micro-environments. These localized changes in pH affect colloid stability. In the case of hematite, colloids are more stable at lower pH values (Langmuir 1997a).

Microbial influenced corrosion (MIC) can accelerate radionuclide release into the surrounding environment; microbial oxidation of metallic iron (Fe) can produce Fe oxide colloids and aggregates. Conversely, microorganisms can decrease the concentration of stable colloids by aggregating colloidal material that they use as a food source (electron acceptors) and can result in a decrease in colloid concentrations of up to 91% per ml (Hersman 1995).

It is unlikely that a significant concentration of radionuclide-associated microbes associated with radionuclides will be transported within the repository system due to the limited energy sources present near the repository. Although microbial transport in the SZ has been demonstrated in the literature, it is only significant for the YMP if microbial transport occurred from the repository through the UZ (e.g., Harvey and Garabedian 1991). The transport of microbes within the waste package, EBS, UZ, and SZ is not currently modeled in TSPA.

Considerable uncertainty surrounds the rate that microbes would affect the system around the repository. Thus, given our current knowledge, it is difficult to estimate their effects on the colloid source term, in particular the effect of microbes on colloid concentration and stability. However, it is understood that microbial action will tend to increase the sizes of inorganic colloids, which promotes gravitational settling and filtration. Thus, not including the effects of microbes in colloid source term and transport analysis is conservative.

### **6.1.9 Colloid Transport**

This section summarizes and integrates the preceding subsections of Section 6.1.

On the basis of the experiments conducted at ANL, it is anticipated that radionuclide-bearing colloids (primarily containing plutonium and americium) will form in the waste package from the degradation of the waste form. It is further anticipated that the majority of the colloids will be composed of clays with entrained radionuclide-bearing phases, with lesser amounts of pseudocolloids with reversibly attached radionuclides. The stability of the clay colloids will depend on ionic strength and to a certain extent on pH. In addition there are expected to be dissolved fractions of plutonium, americium, and other low-solubility, strongly sorbing radionuclides.

It is likely that some corrosion of the interior of the waste package and certain metal components will occur (although this process is not explicitly modeled in TSPA), producing primarily iron-(hydr)oxides as scale, large particles, and colloid-sized particles. Further, portions of the dissolved radionuclide fractions will likely sorb, probably reversibly, to these iron corrosion products; a fraction of the sorbed radionuclides would be onto the colloids, forming pseudocolloids.

The stability of the pseudo-colloids from metals corrosion will depend on such environmental factors as the concentration of colloids in the fluid and the fluid's ionic strength and pH. In general, colloids tend to agglomerate and settle out due to gravity (not explicitly analyzed) when ionic strength exceeds a certain value or the concentration of colloids exceeds a certain value that depends on the characteristics of the system. Further, iron-(hydr)oxide colloids would likely agglomerate at a fluid pH at around 8.

Because of the short transport distances within the waste package, it is assumed that all stable radionuclide-bearing colloids, including pseudocolloids, retain their radionuclides and exit the waste package.

## **6.2 PROCESS MODELS AND DATA**

### **6.2.1 Colloid Formation**

The conceptual models for the formation of colloids from HLW and SNF described in Section 6.1.1 are based primarily on testing performed at ANL over the past several years. The relatively long duration of the tests enabled a large amount of data to be collected which allowed useful and reasonable generalizations to be drawn.

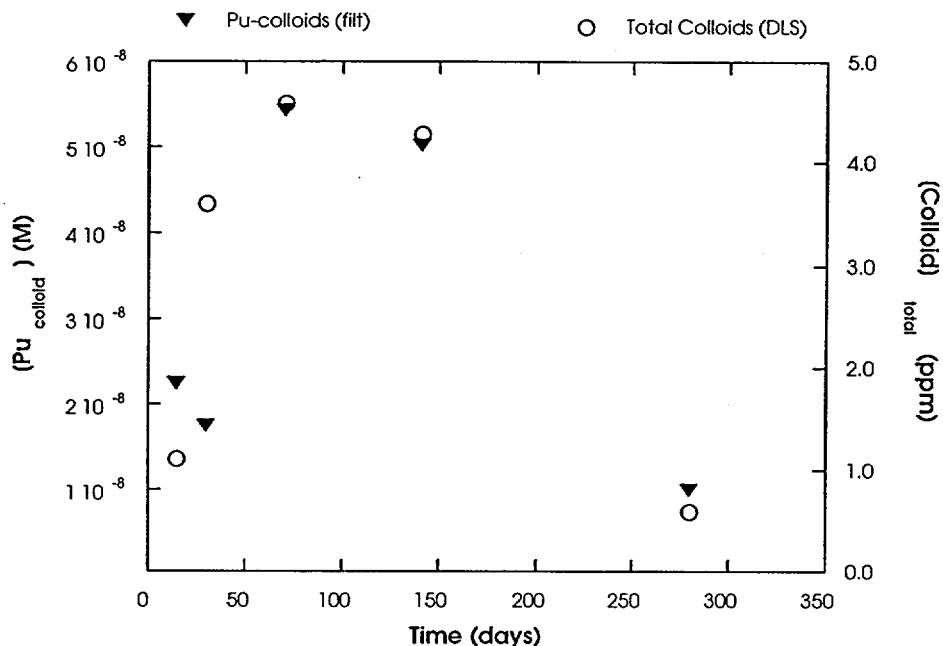
#### **6.2.1.1 Colloids Formed from HLW**

Colloids formed from HLW in the ANL tests were predominantly smectite containing discrete radionuclide-bearing phases entrained within the clay. For modeling purposes it is assumed that colloids derived from HLW are all radionuclide-bearing smectite. In addition, the radionuclides are assumed to be irreversibly attached to the smectite colloids, pending forthcoming data from LANL on radionuclide attachment and detachment to/from waste form colloids.

Based on ANL's experimental results (Figure 10) the following approximate relationship may be used to relate the Pu concentration to colloid concentration:

$$1 \text{ ppm colloids} \equiv 1 \times 10^{-8} \text{ M Pu}_{\text{coll}}$$

$\text{Pu}_{\text{coll}}$  is the concentration of Pu associated with colloids. This relationship is specific to the ANL experiments, but it provides a useful guideline for estimating colloid concentration from colloid-associated Pu concentration as defined by ionic strength and pH (see Section 6.2.2, Colloid Stability and Concentration). Since Pu and Am were observed to behave similarly, the colloid-associated Am concentration was calculated by multiplying the ratio of Am to Pu in the inventory by the Pu concentration.



NOTE: Concentration of Pu colloids (from filtration data, Ebert 1995) and total colloid concentration (from dynamic light scattering [DLS] measurements) as a function of test duration for the SRL 131A glass at 2,000/m (T = 90°C). The triangles, representing concentration of plutonium in filtered colloids, correspond to the left axis. The circles, representing the total colloid mass, correspond to the right axis. Note that, with the scales used in the graph, the triangles and circles coincide (Figure 24 from CRWMS M&O 2000b).

Figure 10. Concentration of Pu Colloids as a Function of HLW Corrosion Test Duration

### 6.2.1.2 Colloids Formed from SNF

Results from the ANL tests on corrosion of SNF indicate that very little colloidal material was detected. Colloids formed were smectites, some with apparently adsorbed Pu and uranium silicates. Further, for all leachate analyses but one, dissolved Pu was below the limit of detection; the one value obtained for dissolved Pu was  $4 \times 10^{-10}$  M. For modeling purposes it is assumed that colloid concentrations, and consequently, reversibly sorbed colloidal Pu and Am concentrations, are estimated based on consideration of ionic strength and pH. Further, the extent to which SNF corroded in GoldSim calculations contributes to the calculated I and pH will determine SNF contribution to the colloid source term.

### 6.2.1.3 Iron-(Hydr)oxide Colloids

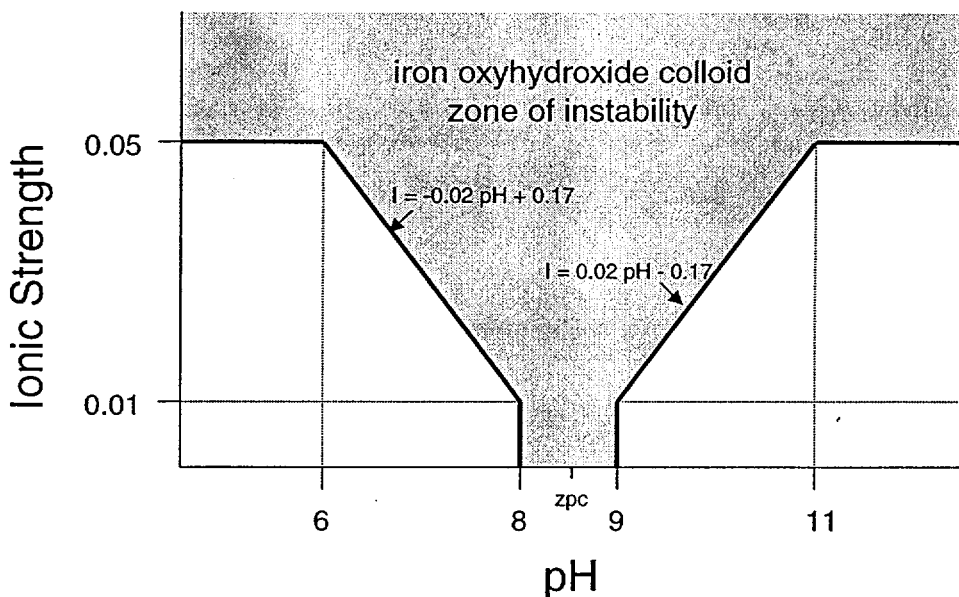
As described in Section 6.1.1.2, it is assumed for modeling purposes that iron will corrode and form iron-(hydr)oxides. It is further assumed that the iron-(hydr)oxides will occur as immobile scale, large particles that will settle out, and colloid-sized particles.

Because of the uncertainty in estimating the mass and surface area of iron-(hydr)oxide scale and the large particles that may be produced from corrosion of waste package components, they were

ignored for modeling purposes. This approach is conservative because it also ignores potential sorption sites on scale and large particles for dissolved radionuclides, which would tend to reduce the mobility of the dissolved radionuclides.

Concentrations of colloidal iron-(hydr)oxides are estimated by assuming that the maximum mass of colloids will occur for a given set of aqueous chemical conditions. This appears to be reasonable, as there is abundant source material for corrosion colloid formation. The stability and concentration of the colloids are determined by the fluid conditions including ionic strength and pH (see Section 6.1.2).

Dissolved (aqueous) radionuclides are assumed to sorb onto the iron-(hydr)oxide colloids (as well as onto waste form colloids) in amounts determined by the concentrations of both the colloids and dissolved radionuclides and by the respective  $K_d$ s for specific radionuclides onto the iron-(hydr)oxide colloids (see Section 6.1.3).

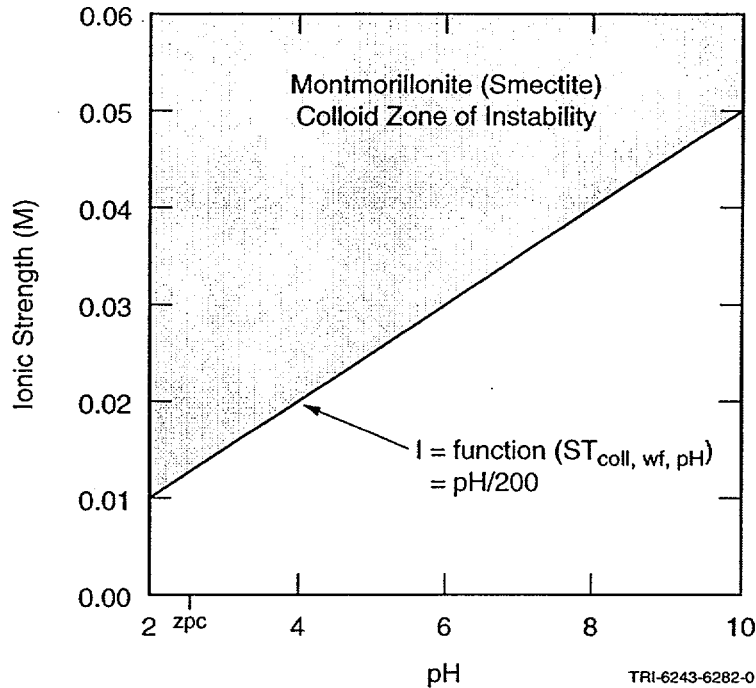


NOTE: Schematic representation (used in abstraction) of iron-(hydr)oxide colloid stability as a function of ionic strength and pH. At and near the ZPC colloids are unstable, even at low ionic strengths. At higher ionic strengths the pH range at which colloids are unstable is greater. Above ionic strength 0.05 colloids are assumed to be unstable for all pH (Abstracted from Liang and Morgan 1990, Figure 1).

Figure 11. Schematic Representation of Iron-(Hydr)oxide Colloid Stability as a Function of pH and Ionic Strength

### 6.2.2 Colloid Stability and Concentration

The stability of smectite colloids is determined primarily by ionic strength, but also to an extent by pH, as described in Section 6.1.2 and shown in Figure 5 and schematically for abstraction purposes) in Figure 12. The stability of iron-(hydr)oxide colloids is determined by both ionic strength and pH as described in Section 6.1.2 and shown schematically in Figure 11.



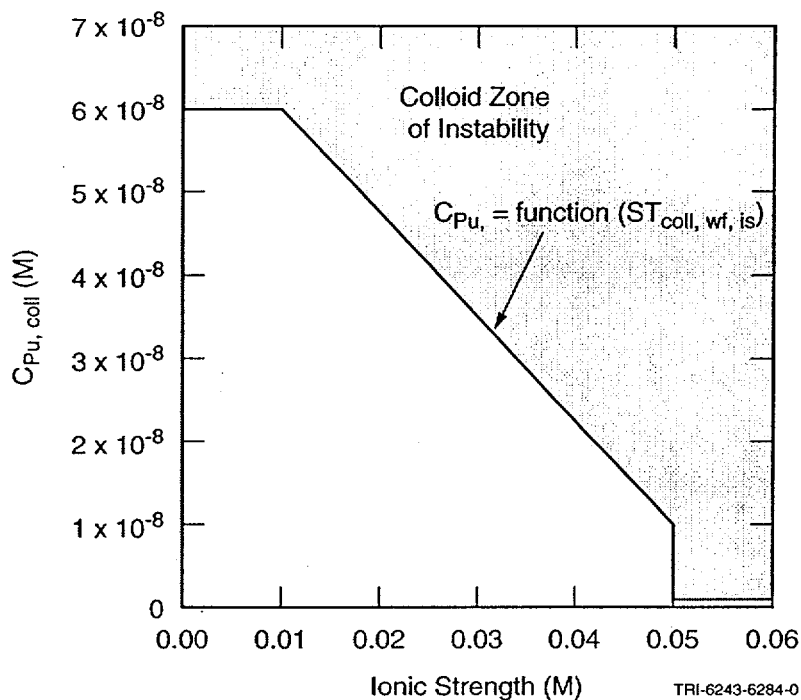
NOTE: Schematic representation (used in abstraction) of smectite stability as a function of pH and ionic strength, abstracted from data presented in Figure 5.

Figure 12. Schematic Representation of Smectite Stability as a Function of pH and Ionic Strength

The concentration of total colloid-associated radionuclides in the pH range 6 to 12 is calculated according to ionic strength as shown schematically in Figure 13. The derived relationship shown in Figure 13, which is based on bounding of the data shown in Figure 7, is:

$$[\text{Pu colloid}] = -1.25\text{E-}6 \times I + 7.25\text{E-}8 \quad (\text{Eq. 3})$$

valid for ionic strengths greater than 0.01 M and less than 0.05 M. Concentration at ionic strengths greater than 0.05 M is assumed to be  $1 \times 10^{-11}$  M/kg, approximately three orders of magnitude lower, based on experimental observations (CRWMS M&O 2000a). At ionic strengths less than 0.01 M, concentration is assumed to be constant at  $6 \times 10^{-8}$  M, based on experimental observations (CRWMS M&O 2000a; see Figure 13).

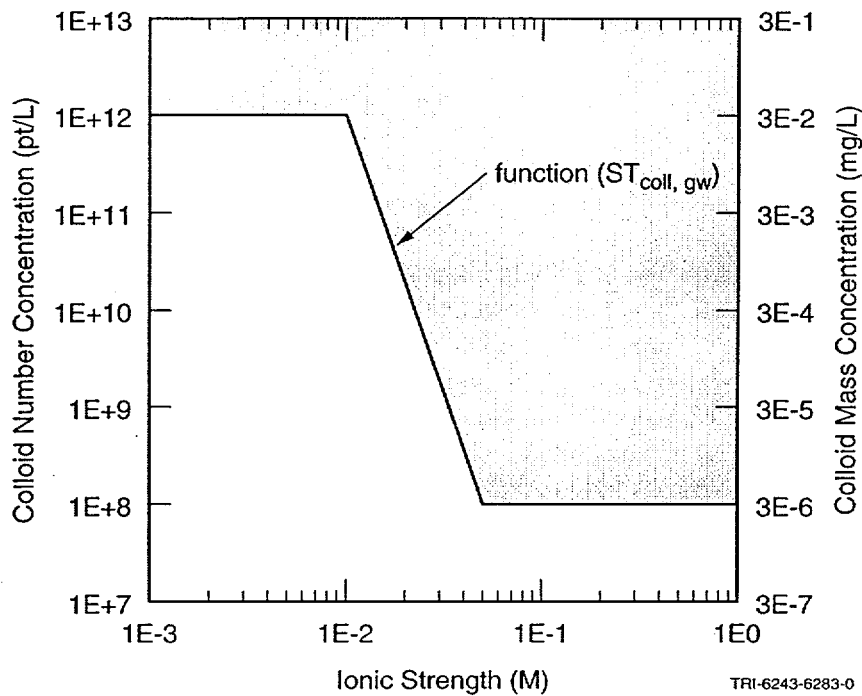


NOTE: Schematic relationship (used in abstraction) between RN-bearing colloid concentration and ionic strength. The function represents the bound of the HLW corrosion experimental data (see Figure 7); the maximum value represented,  $6 \times 10^{-8}$ , is the maximum concentration of colloids observed in the HLW experiments.

Figure 13. Schematic Relationship Between Radionuclide-Bearing Colloid Concentration and Ionic Strength

### 6.2.3 Treatment of Groundwater Colloids

Figure 9 illustrates the effect of ionic strength on stability, in terms of number population, of colloids from sites around the world. To be useful for calculations, these data must be converted to mass or surface area per unit volume. In general, the number of colloids increases by a factor of 1000 as colloid diameter decreases by a factor of 10 (assuming spherical colloids). Expressed mathematically, population = diameter<sup>-3</sup>. In natural systems, the power law exponent may be between about 2 and 5. By taking the first derivative of the cumulative distribution, combining it with masses of individual colloids assuming spherical geometry, and then integrating the function between a lower and upper size limit, the total colloidal mass is obtained. Figure 9 was constructed using populations of colloids greater than 100 nm (CRWMS M&O 1998). In Figure 14, colloid masses were calculated using number populations from Figure 9 extrapolated to include colloid sizes between 10 nm and 1 micrometer. A colloid mineral density of 2.5 g/cm<sup>3</sup> was assumed.



NOTE: Schematic relationship (used in abstraction) between groundwater colloid concentration and ionic strength. Colloid masses were calculated using number populations from Figure 9 extrapolated to include colloid sizes between 10 nm and 1 micrometer. A colloid mineral density of 2.5 g/cm<sup>3</sup> was assumed.

Figure 14. Schematic Relationship between Groundwater Colloid Concentration and Ionic Strength

In Figure 14, the upper and lower bounding lines capture the highest and lowest concentrations of colloids shown in Figure 9. Between ionic strengths of 0.01 and 0.05 M, number and mass concentrations decrease as groundwater colloids are destabilized. The decrease is a bounding approximation that is considered to be linear in log-log space, consequently derived as follows:

$$\text{function}(S_{\text{coll},\text{gw}}): 10^{[A \times \log(I) + B]}$$

where,

$$A = \frac{\log(M_{\text{coll},\text{gw},\text{max}}) - \log(M_{\text{coll},\text{gw},\text{min}})}{\log(I_{\text{lo - thresh, coll, gw}}) - \log(I_{\text{hi - thresh, coll, gw}})} \quad (\text{Eq. 4})$$

$$B = \frac{[\log(M_{\text{coll},\text{gw},\text{min}}) \times \log(I_{\text{lo - thresh, coll, gw}})] - [\log(M_{\text{coll},\text{gw},\text{max}}) \times \log(I_{\text{hi - thresh, coll, gw}})]}{\log(I_{\text{lo - thresh, coll, gw}}) - \log(I_{\text{hi - thresh, coll, gw}})} \quad (\text{Eq. 5})$$

The mineralogy of YMP groundwater colloids is assumed to be clays. Consequently, the effect of pH on groundwater colloid stability can be simulated using the same approach described above for waste-form colloids (Figures 5 and 12). Radionuclide sorption on groundwater colloids could be diminished due to sorption-site saturation by mono- and di-valent cations

during transport. Conversely, radionuclide sorption could be enhanced by the presence of thin coatings of organic materials or iron-(hydr)oxides. Because the surface chemistry of groundwater colloids is not known, it is assumed that sorption is similar to clay minerals, and the same  $K_d$  values used for waste-form colloids are used for groundwater colloids.

#### 6.2.4 Radionuclide Attachment to Colloids

According to the conceptual models, a large fraction of the radionuclide-bearing colloids will be smectite clay with entrained radionuclide-bearing phases; the radionuclides are effectively irreversibly attached. Clay and iron-(hydr)oxide pseudocolloids will be available for reversibly sorbing aqueous radionuclides or radionuclide-bearing colloids.

Effective  $k_d$ s for combined adsorption and desorption of Pu and Am on waste-form, iron-(hydr)oxides, and groundwater colloids are used to determine effective reversibility of the radionuclides on colloids according to the relationship:

$$RN_{\text{adsorbed/desorbed}} = RN_{\text{dissolved}} \times k_{d,RN} \times M_{\text{colloid}} \quad (\text{Eq. 6})$$

#### 6.2.5 Physical Filtration of Colloids

Physical filtration of colloids in the waste package is not analyzed in TSPA.

#### 6.2.6 Colloid Sorption at the Air-Water Interface

Colloid sorption at the air-water interface is not analyzed in TSPA.

#### 6.2.7 Gravitational Settling of Colloids

Gravitational settling of colloids is not analyzed in TSPA.

#### 6.2.8 Colloid Diffusion

The coefficient of diffusivity of colloids relative to dissolved solutes in water is assumed to be 0.01.

#### 6.2.9 Microbes and Organic Components

Microbes and organic components are not analyzed in TSPA.

#### 6.2.10 Colloid Transport

For modeling purposes, calculated colloid-associated radionuclide concentrations all leave the waste package. Further, desorption is assumed to be slow, relative to the transport time out of the waste package.

### 6.3 ABSTRACTION AND IMPLEMENTATION IN GOLDSIM

This section describes the method devised to incorporate the various process models described above into an abstraction of those process models, a simplified model intended to retain the

important principles and features of the process models. The following narrative describes the abstraction; Figure 15 shows the logic and flow of the abstraction approach.

### **6.3.1 Inputs to GoldSim**

The abstraction uses a set of input parameters for the TSPA code GoldSim; these parameters are listed and described in Table 1 in Section 4.1. Input parameters have been taken from the ANL colloid-related AMR (CRWMS M&O 2000a); others have been extracted from available project documents and the scientific literature.

### **6.3.2 Calculated GoldSim Parameters Needed for Abstraction**

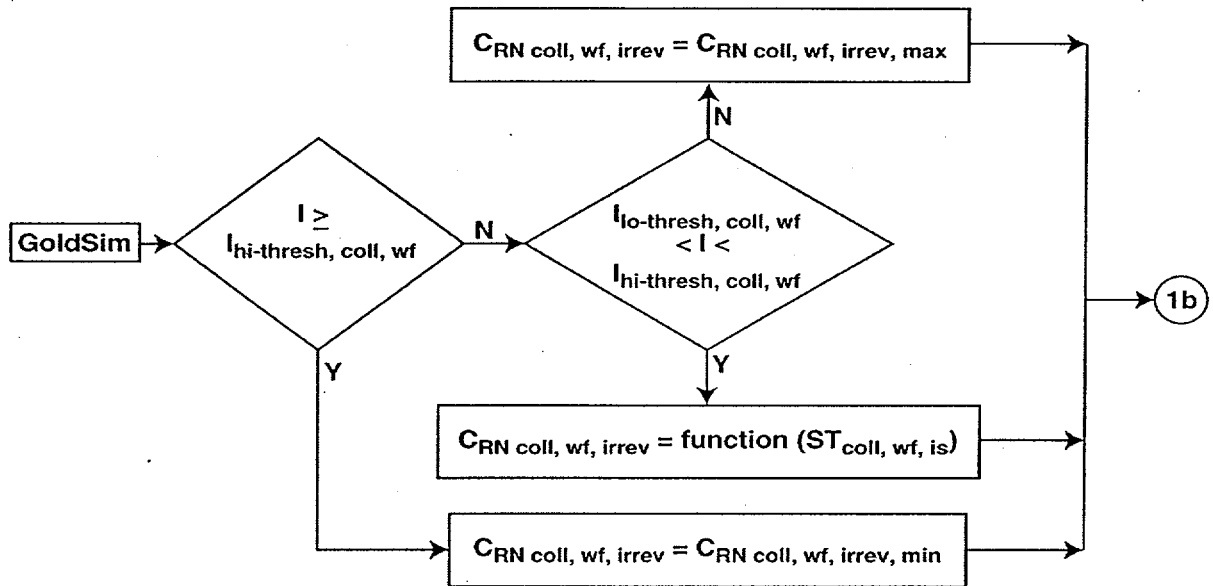
The abstraction requires three parameters to be calculated by GoldSim as output from in-package chemistry calculations:  $C_{RN,diss}$ ,  $I$ , and pH (see Table 1).

### **6.3.3 Calculation of Colloid and Colloid-Associated Radionuclide Concentrations**

The concentrations of colloids and colloid-associated radionuclides were calculated on the basis of abstractions of the experimental observations and chemical principles described above. A stepwise approach was taken in the abstraction, and each step is set out below with a flow diagram and logic statements that explicitly describe the abstraction step.

### 6.3.3.1 Waste-Form (Smectite) Colloids

The mass concentration of radionuclides irreversibly attached to waste form colloids, produced from corrosion of HLW glass, as a function of ionic strength is calculated in Step 1a (Figure 15a).

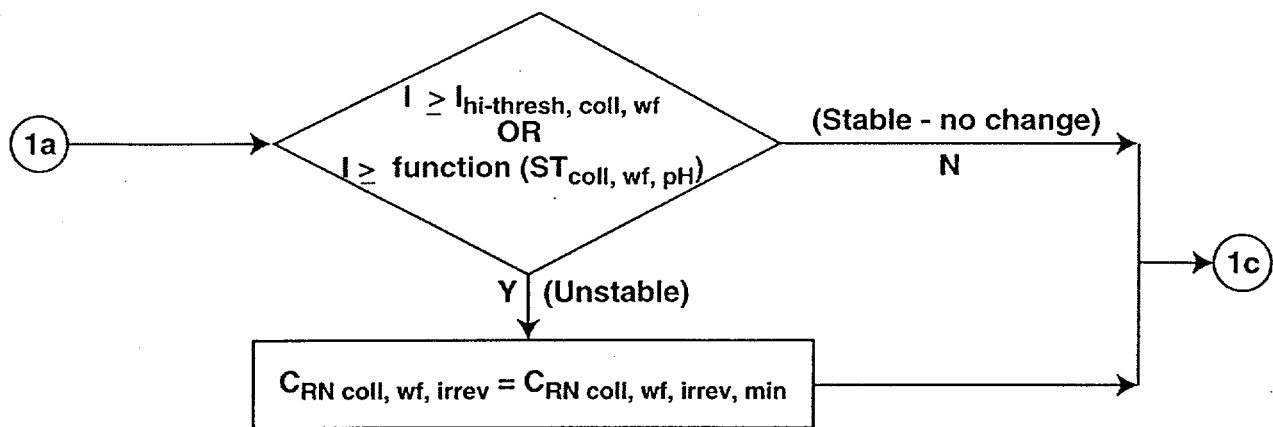


Step 1a Waste-Form Colloids - Generation from Degradation of HLW Glass

Input I  
 IF  $I \geq I_{hi-thresh, coll, wf}$   
 THEN  $C_{RNcoll, wf, irrev} = C_{RNcoll, wf, irrev, min}$   
 ELSE  
 IF  $(I > I_{lo-thresh, coll, wf})$  AND  $(I < I_{hi-thresh, coll, wf})$   
 THEN  $C_{RNcoll, wf, irrev} = function(ST_{coll, wf, is})$   
 ELSE  $C_{RNcoll, wf, irrev} = C_{RNcoll, wf, irrev, max}$   
 function( $ST_{coll, wf, is}$ ):  $-1.25E-6 \times I + 7.25E-8$

Figure 15a. Flow Chart and Logic Statements: Effect of Ionic Strength on the Concentration of Waste-form Colloids Generated during HLW Glass Degradation Based on Experiments Conducted at ANL (see Figure 13)

The stability of irreversibly attached waste form colloids from HLW glass is determined in Step 1b on the basis of the fluid ionic strength and pH (Figure 15b).



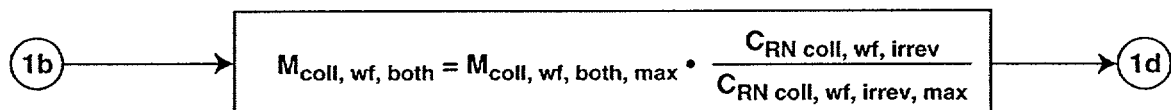
Step 1b Waste-Form Colloids - Effect of pH and Ionic Strength on Stability

IF  $(I \geq I_{hi-thresh, coll, wf})$  OR  $(I \geq \text{function}(ST_{coll, wf, pH}))$   
 THEN  $C_{RN coll, wf, irrev} = C_{RN coll, wf, irrev, min}$

function( $ST_{coll, wf, pH}$ ):  $pH/200$

Figure 15b. Flow Chart and Logic Statements: Effect of pH and Ionic Strength on Waste-form Colloid Stability Based on Stability Behavior of Montmorillonite Colloids (see Figure 12)

The mobile mass of waste form colloids from HLW glass is calculated in Step 1c (Figure 15c).

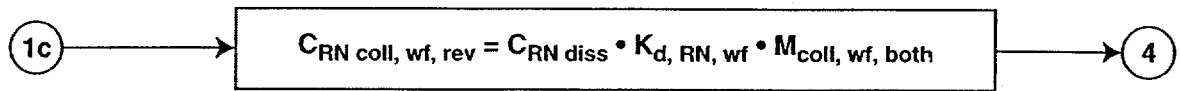


Step 1c Waste-Form Colloids - Mobile Colloid Mass

$$M_{coll, wf, both} = M_{coll, wf, both, max} \times C_{RN coll, wf, irrev} \div C_{RN coll, wf, irrev, max}$$

Figure 15c. Flow Chart and Logic Statements: Determination of Mobile Mass of Waste-form Colloids

The concentration of radionuclides reversibly sorbed on waste form colloids from HLW glass is calculated in Step 1d (Figure 15d), based on the mass of waste form colloids,  $k_d$ s describing the distribution of radionuclides between the fluid and montmorillonite clay, and the dissolved concentration of radionuclides as calculated by GoldSim.



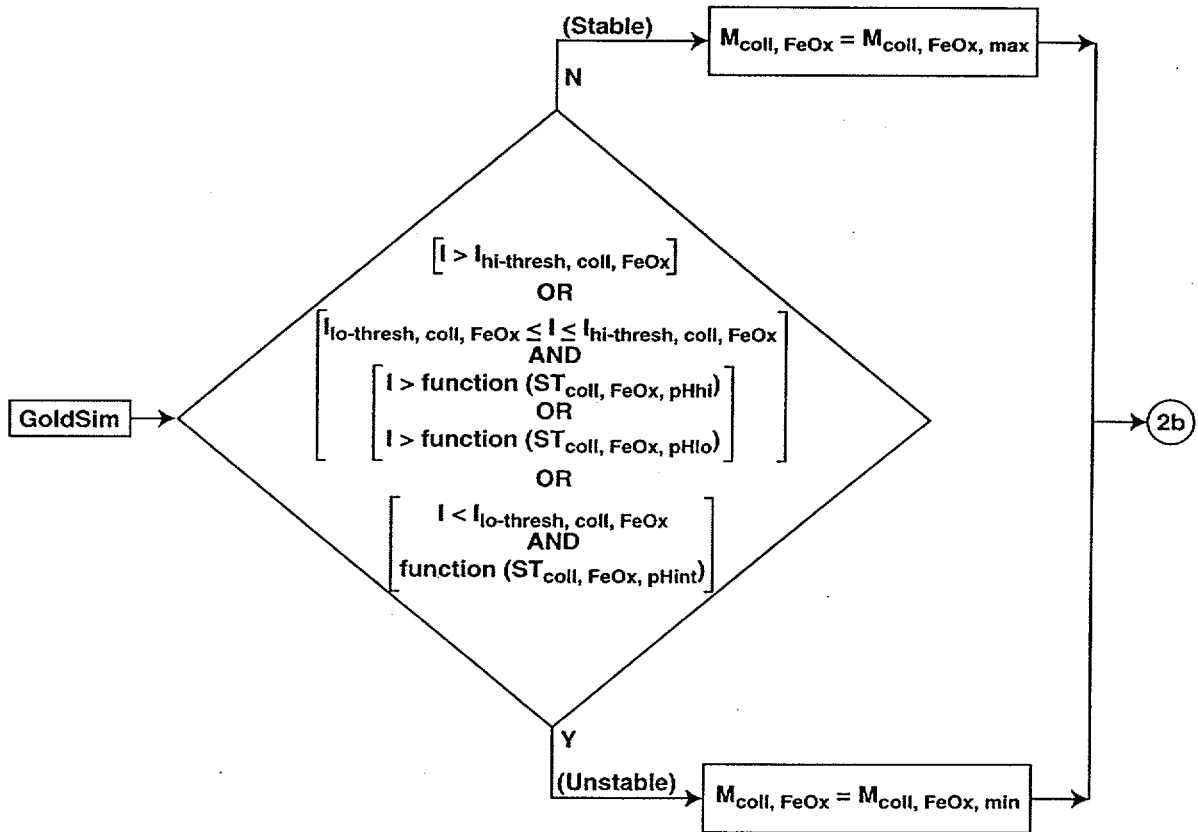
Step 1d Waste-Form Colloids - Sorption of Radionuclides

$$C_{RNcoll, wf, rev} = C_{RNdiss} \times K_{d, RN, wf} \times M_{coll, wf, both}$$

Figure 15d. Flow Chart and Logic Statements: Sorption of Radionuclides on Waste-form Colloids

### 6.3.3.2 Corrosion (Iron-[Hydr]oxide) Colloids

The stability of iron-(hydr)oxide colloids assumed to form as a result of the corrosion of waste package components is determined in Step 2a on the basis of the fluid ionic strength and pH (Figure 15e).



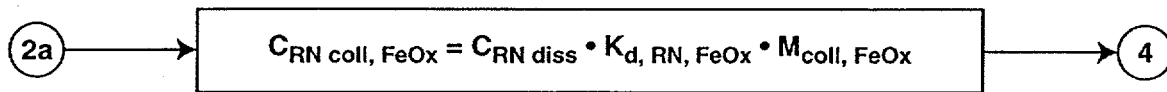
Step 2a Iron (Hydr)oxide Colloids - Effect of pH and Ionic Strength on Stability

```

IF
  BEGIN
    (I > Ihi-thresh, coll, FeOx)
    OR ((I ≥ Ilo-thresh, coll, FeOx)
      AND (I > function(STcoll, FeOx, pHhi)) OR (I > function(STcoll, FeOx, pHlo)))
    OR ((I < Ilo-thresh, coll, FeOx) AND (function(STcoll, FeOx, pHint)))
  END
  THEN
    Mcoll, FeOx = Mcoll, FeOx, min
  ELSE
    Mcoll, FeOx = Mcoll, FeOx, max
    function(STcoll, FeOx, pHhi): -0.02 × pH + 0.17
    function(STcoll, FeOx, pHlo): +0.02 × pH - 0.17
    function(STcoll, FeOx, pHint) (boolean): ((pH ≥ 8) AND (pH ≤ 9))
  
```

Figure 15e. Flow Chart and Logic Statements: Effect of Ionic Strength and pH on Stability of Iron-(Hydr)oxide Colloids (see Figure 11)

The concentration of radionuclides reversibly sorbed on iron-(hydr)oxide colloids is calculated in Step 2b (Figure 15f), based on the mass of iron-(hydr)oxide colloids,  $k_{ds}$  describing the distribution of radionuclides between the fluid and iron-(hydr)oxides and the dissolved concentration of radionuclides as calculated by GoldSim.



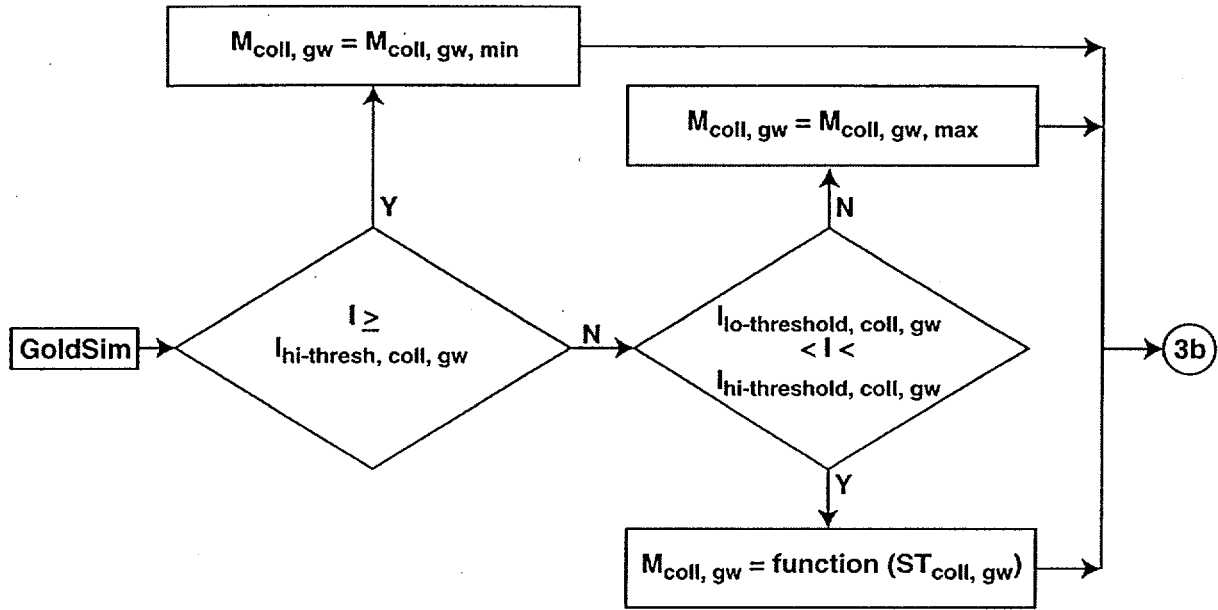
Step 2b Iron (Hydr)oxide Colloids - Sorption of Radionuclides

$$C_{RNcoll,FeOx} = C_{RNdiss} \times K_{d,RN,FeOx} \times M_{coll,FeOx}$$

Figure 15f. Flow Chart and Logic Statements: Sorption of Radionuclide RN on Iron-(Hydr)oxide Colloids.

### 6.3.3.3 Groundwater (Smectite) Colloids

The mobile mass of groundwater colloids is calculated on the basis of fluid ionic strength in Step 3a (Figure 15g).



Step 3a Groundwater Colloids - Effect of Ionic Strength on Mobile Mass (see Figure 14)

```

IF I ≥ Ihi-thresh, coll, gw
  THEN Mcoll, gw = Mcoll, gw, min
ELSE IF (I > Ilo-thresh, coll, gw) AND (I < Ihi-thresh, coll, gw)
  THEN Mcoll, gw = function(Scoll, gw)
ELSE Mcoll, gw = Mcoll, gw, max
  
```

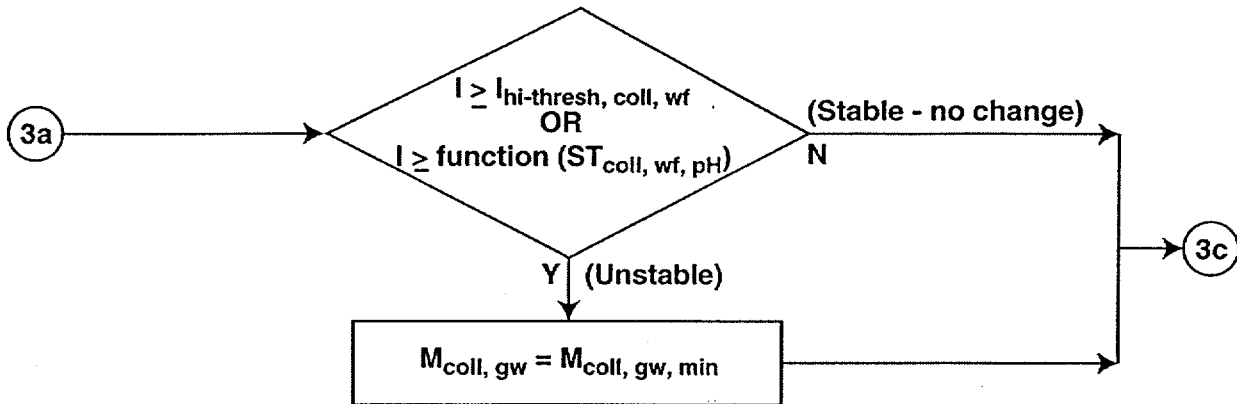
function(S<sub>coll, gw</sub>): 10<sup>[A × log(I) + B]</sup>  
 where:

$$A = \frac{\log(M_{\text{coll, gw, max}}) - \log(M_{\text{coll, gw, min}})}{\log(I_{\text{lo - thresh, coll, gw}}) - \log(I_{\text{hi - thresh, coll, gw}})}$$

$$B = \frac{[\log(M_{\text{coll, gw, min}}) \times \log(I_{\text{lo - thresh, coll, gw}})] - [\log(M_{\text{coll, gw, max}}) \times \log(I_{\text{hi - thresh, coll, gw}})]}{\log(I_{\text{lo - thresh, coll, gw}}) - \log(I_{\text{hi - thresh, coll, gw}})}$$

Figure 15g. Flow Chart and Logic Statements: Effect of Ionic Strength on Mobile Mass of Groundwater Colloids.

The stability of groundwater colloids is determined in Step 3b on the basis of the fluid ionic strength and pH (Figure 15h).



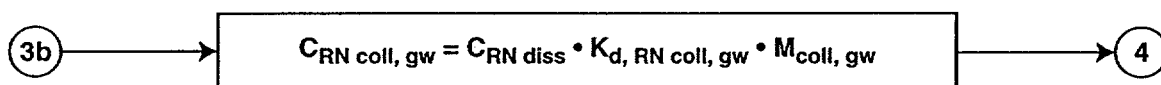
Step 3b Groundwater Colloids - Effect of pH on Stability (see Figure 12)

IF ( $I \geq I_{hi-thresh, coll, wf}$ ) OR ( $I \geq \text{function}(ST_{coll, wf, pH})$ )  
 THEN  $C_{RNcoll, wf, irrev} = C_{RNcoll, wf, irrev, min}$

function( $ST_{coll, wf, pH}$ ):  $pH/200$

Figure 15h. Flow Chart and Logic Statements: Effect of pH and Ionic Strength on Groundwater Colloids Stability Based on Stability Behavior of Montmorillonite Colloids

The concentration of radionuclides reversibly sorbed on groundwater colloids is calculated in Step 3c (Figure 15i), based on the mass of groundwater colloids,  $k_d$ s describing the distribution of radionuclides between the fluid and montmorillonite, and the dissolved concentration of radionuclides as calculated by GoldSim.



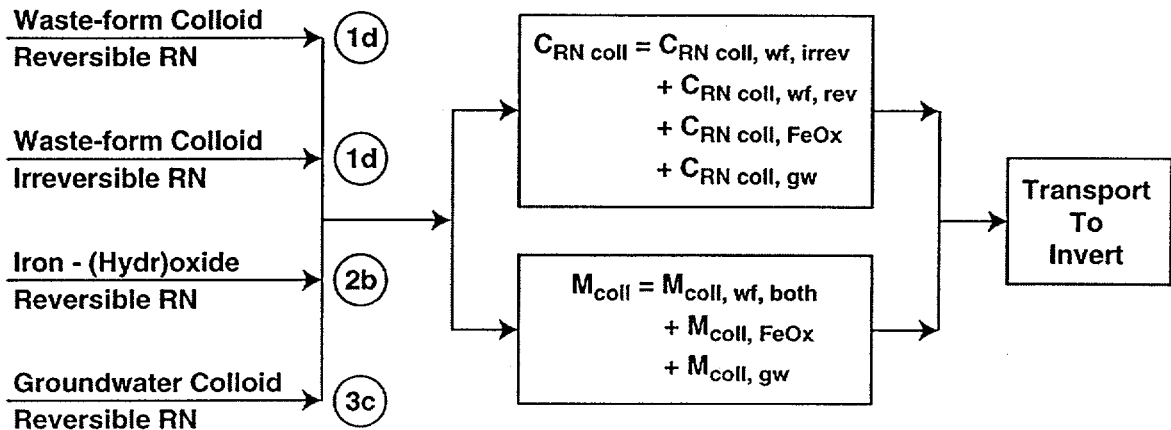
Step 3c Groundwater Colloids - Sorption of Radionuclides

$C_{RNcoll, gw} = C_{RNdiss} \times K_{d, RN, gw} \times M_{coll, gw}$

Figure 15i. Flow Chart and Logic Statements: Radionuclide Sorption on Groundwater Colloids

### 6.3.3.4 Colloid-Associated Radionuclide Source Term in Waste Package

The colloid-associated radionuclide source term is calculated in Step 4 by summing the contributions to the source term from Steps 1d, 2b, and 3c (Figure 15j).



Step 4 Colloidal Radionuclide Source-term in Waste Package  

$$C_{RNcoll} = C_{RNcoll, wf, irrev} + C_{RNcoll, wf, rev} + C_{RNcoll, FeOx} + C_{RNcoll, gw}$$

$$M_{coll} = M_{coll, wf, both} + M_{coll, FeOx} + M_{coll, gw}$$

Figure 15j. Flow Chart and Logic Statements: Calculation of Colloid-associated Radionuclide Source Term from Summation of Calculated Colloid and Radionuclide Masses

## 6.4 ASSESSMENT OF ABSTRACTION

### 6.4.1 Validity of Abstraction and Comparison to Data

Generally the model is considered valid for its intended purpose based on several considerations. The assumptions used are considered conservative and/or bounding, depending upon the assumption and the basis for the assumption. The exception is the assumption, described in Section 6.1.1.1, regarding the potential effects of colloids from corroded DOE-SNF on repository performance. This assumption is subject to update and revision, and a process for verification of the assumption is presented in Section 6.1.1.1.

The types and characteristics (including stability and concentration) of colloids formed from the degradation of the waste forms as used in the abstraction is based on extensive observations of colloids from testing programs and natural groundwaters. Because of the minute dimensions and unique properties of colloids, their study presents formidable difficulties; the body of work used for the abstraction developed in this AMR represents a significant fraction of the state-of-the-art colloid research performed to date.

Certain processes were not incorporated into the abstraction, including filtration of colloids in the waste package, sorption to the air-water interfaces in unsaturated environments, and gravitational settling. It was considered realistic to conservative to do so, as it was assumed that all of the

colloids generated within a breached waste package left the waste package and entered the invert in the drift. It may be argued that gravitational settling would facilitate the exit of colloids from a breach at the bottom of the waste package; the net effect, however, is the same.

Attachment mechanisms of radionuclides to colloids was also based on laboratory tests and field observations. The assumption that all radionuclides associated with colloids produced from corroded HLW glass were irreversibly attached is conservative and is based on numerous direct observations. An unknown quantity of radionuclides may be reversibly attached to the colloids, but measurements were not undertaken to determine this quantity, and so all were assumed to be irreversibly attached. The assumption that radionuclide attachment to colloids produced from degradation of CSNF is reversible is also based on numerous direct observations, in which no embedded phases of the sort observed in the HLW glass-derived colloids were detected. The data support the assumption; however, fewer data were obtained from the CSNF testing than from the HLW glass testing.

Test runs of the abstraction using GoldSim are planned in order to help assess code verification, model sensitivity, and confidence in model results. The test run results may be presented in a subsequent revision to this AMR or other vehicle.

## **6.4.2 Alternative Models**

The following sections describe a possible approach to estimating the rate of release of Pu from degraded waste, based on the rate of waste degradation. This modeling approach has not been developed to the same extent as the abstraction described in Section 6.3. It is preliminary and is provided here for information and as a basis for potential discussion and planning.

### **6.4.2.1 Rate-of-Colloid-Generation Model**

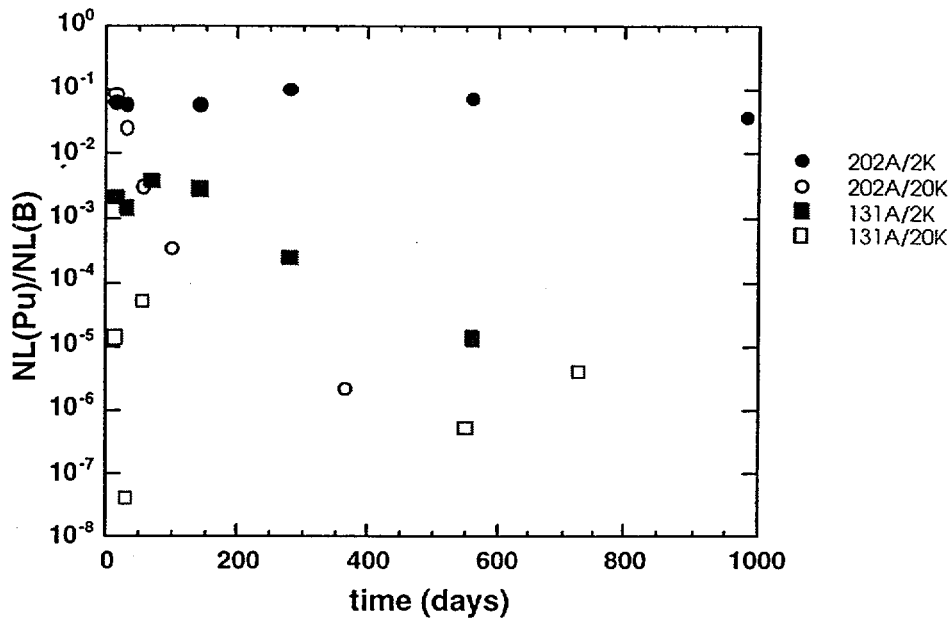
#### **6.4.2.1.1 Conceptual Model**

The conceptual models for the formation of colloids from HLW and SNF described in Section 6.1.1 are based on testing performed at ANL and are relevant to the rate-of-colloid-generation model. Section 6.1.1 describes the observed relationships between B release and extent of HLW corrosion, and between Tc release and SNF corrosion.

#### **6.4.2.1.2 Process Model**

The process models presented here were developed by ANL investigators and are based on observed relationships mentioned in Section 6.4.2.1.1 above and described in Section 6.1.1.

**Colloids Formed from HLW**—The normalized mass loss of Pu, NL(Pu), was compared to the normalized mass loss of boron, NL(B), to indicate the amount of Pu released relative to the amount of B released, which is assumed to represent the amount of HLW glass corroded. As indicated in Figure 16 the NL(Pu) is consistently lower than the NL(B) by at least one order of magnitude. NL(Pu)/NL(B) decreases for the longer duration tests at higher SA/V, up to about  $10^{-3}$  for conditions which inhibit stable colloids.



NOTE: Ratio of normalized mass loss of plutonium to normalized mass loss of boron, NL(Pu)/NL(B), as a function of test duration (in days) for static corrosion tests on the SRL 202A and SRL 131A glasses at 2,000 and 20,000/m (T = 90°C) [Ebert 1995] (Figure 27 from CRWMS M&O 2000a).

Figure 16. Ratio of Normalized Mass Loss of Plutonium to Normalized Mass Loss of Boron, NL(Pu)/NL(B)

Under low ionic strength conditions, the colloids are stable in the fluid and the rate of formation of Pu-bearing colloids,  $dm_{Pu-coll}/dt$ , is proportional to the amount of altered glass,  $M_{alt}$ . As the glass alters, the rate of radionuclide-bearing colloids production decreases, initially following a power-law, attributed to their sorption by the fixed clay alteration layer (CRWMS M&O 2000a). The rate of colloid formation can be described by the equation:

$$\frac{dm_{Pu-coll}}{dt} = a(M_{alt})^{-b} \quad (\text{Eq. 7})$$

The constants,  $a$  and  $b$ , derived for the various glasses may be a function of the SA/V, leachate composition (I, etc.), colloid composition, or other parameters. Table 5 summarizes the ranges and bounding values for  $a$  and  $b$ .

Table 5. Ranges and bounds for the constants,  $a$  and  $b$ , in Equation 7

Constant	Static Tests		Drip Tests		Bound
	Low	High	Low	High	
a	$9 \times 10^{-11}$	$3 \times 10^{-4}$	$2 \times 10^{-6}$	$5 \times 10^{-6}$	$10^{-4}$
b	2.5	11	0.3	1.7	1

At the high ionic strengths encountered in certain static tests, there was no correlation observed between Pu and B production rates since the quantity of colloids was very low. In the drip tests, ionic strength remained low because EJ-13 water was periodically injected.

Once the cumulative B release is greater than approximately 1 to 3 g m<sup>-2</sup>, the radionuclide release is controlled by spallation of the clay layer. Thus, radionuclide release is a two-step process: (1) alteration of the glass waste form and precipitation of colloids and (2) erosion of colloid-sized fragments from the alteration products. The first step may be represented by the following equation (CRWMS M&O 2000a):

$$M_{alt} = A \cdot \int_0^t (NR_i(\tau) - NR_{Pu}(\tau)) d\tau \quad (\text{Eq. 8})$$

where  $M_{alt}$  is the mass of altered waste form containing Pu,  $A$  is the surface area (geometric),  $\tau$  is the elapsed time, and  $NR_i(\tau)$  is the normalized release rate of marker element  $i$  (B for glass). (Note the term  $NR_{Pu}$ , which is the normalized release rate of Pu; this term is considered negligible by the investigators over the time scale of the experiments since  $NR_B$  is several orders of magnitude larger but could become significant over long periods.)

Release of colloids due to spallation is given by the derived relationship:

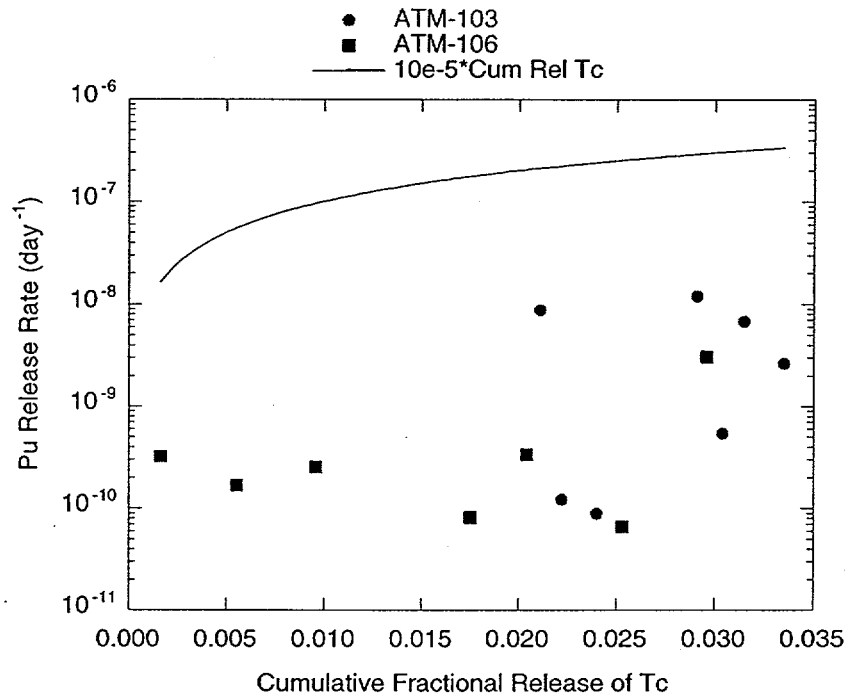
$$\frac{dm_{Pu-coll}}{dt} = \kappa M_{alt} \quad (\text{Eq. 9})$$

where  $m_{Pu-coll}$  is the mass release of Pu suspended as colloidal particulates and  $\kappa$  is a parameter that depends on, among other things, the mechanical condition of the altered waste form, the water flow rate over the waste form, and the water chemistry (CRWMS M&O 2000a). An empirical bound for  $\kappa$  is  $10^{-4} \text{ d}^{-1}$ .

These relationships have been incorporated into the abstraction in Section 6.4.2.1.2;  $\tau$  is represented in the abstraction by the time steps at which GoldSim performs iterative calculations.

**Colloids Formed from SNF**—The normalized mass loss of Pu,  $NL(\text{Pu})$ , was compared to the normalized mass loss of technetium,  $NL(\text{Tc})$ , to indicate the amount of Pu released relative to the amount of Tc released, which is assumed to represent the amount of SNF corroded. It was noted that the reaction of SNF under unsaturated drip test conditions does not exhibit a correlation

between the rate of Pu-bearing colloid formation and the corrosion of spent fuel (see Figure 17). The scattered data indicating Pu release rate versus Tc release rate (which are proportional to the NL(Pu) and NL(Tc), respectively) were bounded by assuming conservatively that NL(Pu)/NL(Tc) is equal to  $10^{-5} \text{ d}^{-1}$ .



NOTE: The fractional release rate of Pu as a function of cumulative fractional Tc release for the ATM-103 and ATM-106 high-drip-rate tests [SN 1644, p. 37]. The solid line is the conservative bound based upon a constant of  $10^{-5} \text{ d}^{-1}$  (Figure 30 from CRWMS M&O 2000a).

Figure 17. Fractional Release Rate of Pu as a Function of Cumulative Fractional Tc Release for the ATM-103 and ATM-106 High-drip-rate Tests

This relationship has been incorporated into the abstraction in Section 6.4.2.1.2.

### 6.4.2.1.3 Abstraction

This section describes the method devised to incorporate the process models described above into an abstraction of those process models, a simplified model intended to retain the important principles, and features of the process models. The following narrative describes the abstraction; Figure 18 shows the logic and flow of the abstraction approach.

**Inputs to GoldSim**—The abstraction uses a set of input parameters for the TSPA code GoldSim; these parameters are listed and described in Table 6 below. Input parameters have been taken from the ANL and LANL AMRs (CRWMS M&O 2000a; CRWMS M&O 2000b); certain others have been extracted from available project documents and the scientific literature.

**Calculation of Quantities of Radionuclides Mobilized at Each Time Step**—The masses of radionuclides “mobilized” by degradation of the waste at each time step is calculated directly by

GoldSim. Alternatively, the masses of the radionuclides may be determined by the product of mass of waste degraded and radionuclide inventory.

**Calculation of Quantity and Rate of Production of Irreversibly Attached Radionuclides—**

After the quantities of total mobilized radionuclides are calculated, they must be distributed between radionuclides irreversibly attached to colloids, dissolved (aqueous) radionuclides, and radionuclides precipitated in immobile secondary phases. Since the experimental evidence indicates that most waste form colloids are radionuclides and/or radionuclide-bearing phases irreversibly associated with smectite colloids, this fraction is given as the difference between the dissolved radionuclides and the total radionuclides mobilized by the waste degradation time step:

$$RN_{\text{coll,irrev}} + RN_{\text{layer,irrev}} = RN_{\text{mob}} - RN_{\text{diss}} - RN_{\text{secondaryphases}} \quad (\text{Eq. 10})$$

The irreversibly attached radionuclides are in turn distributed between the clay layers on altered HLW and clay colloids produced from both HLW and SNF; the aqueous radionuclides are available for reversible sorption onto colloids.

It was discussed in Sections 6.1.1 and 6.4.2.1.2 that boron was used as a marker to indicate the amount of HLW degraded at any point in time. If the cumulative release of boron,  $B_{\text{cum}}$ , is less than  $1 \text{ g m}^{-2}$ , then the following relationship (called Rate Model 1 in Figure 18) is invoked to calculate the quantity of radionuclides irreversibly attached to colloids produced for that time step. The equation for calculating the mass of radionuclides is:

$$\text{Mass of irreversibly attached RN} = a * (B_{\text{cum}})^{-b} \quad (\text{Eq. 11})$$

where  $B_{\text{cum}}$  represents the mass of HLW degraded and  $a$  and  $b$  are empirically-derived constants (see Section 6.4.2.1.2).

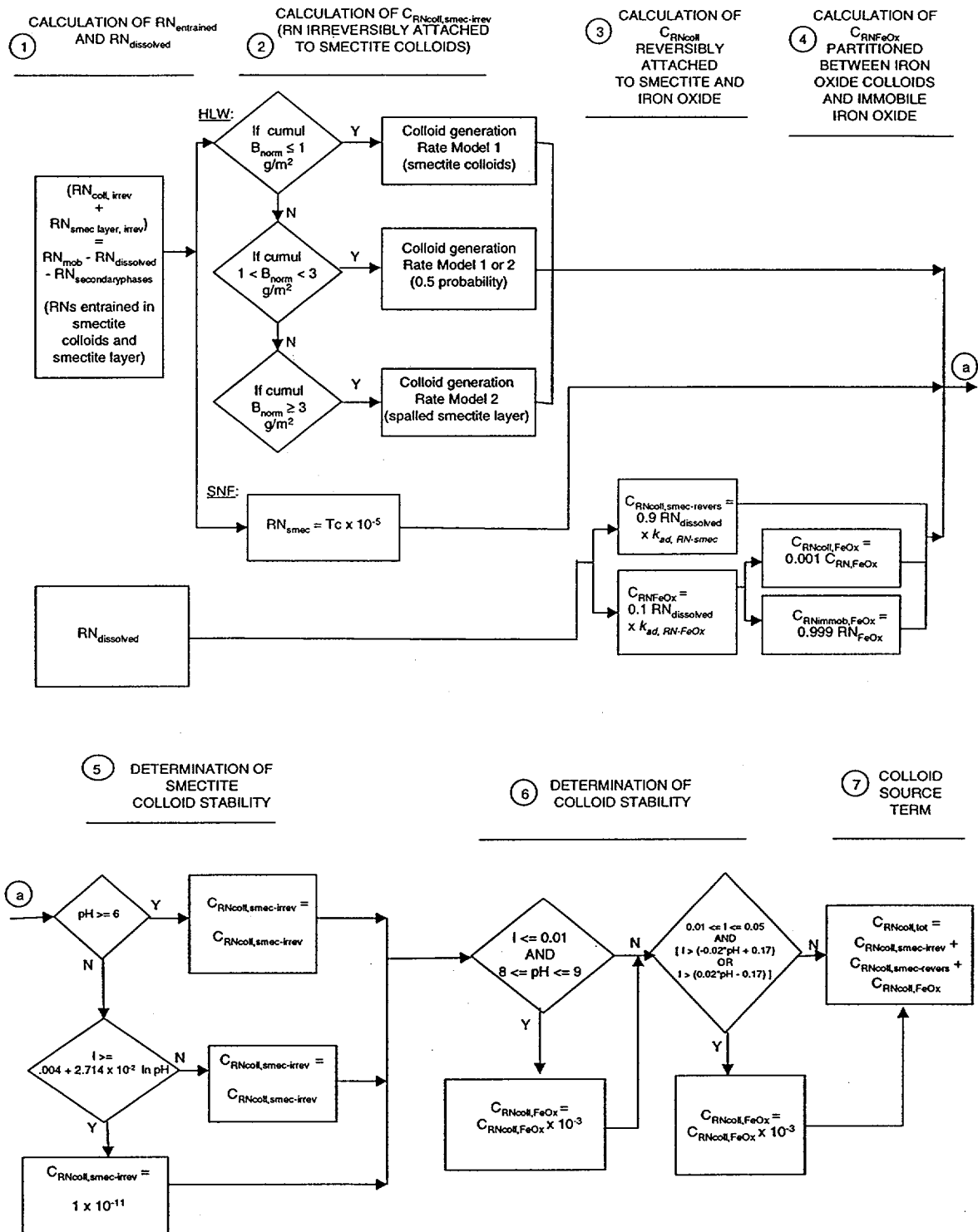


Figure 18. Flow Chart Illustrating Alternative Abstraction Logic

Table 6. Summary of Parameters for Prospective Alternative Abstraction

Parameter	Description	Value /Range/ Distribution	Source
WF <sub>deg</sub>	Fraction of waste degraded during time step	-----	Would be generated by GoldSim
WF <sub>SA</sub>	Surface area of waste form during time step	-----	Would be generated by GoldSim
B <sub>inv</sub> , T <sub>Cinv</sub> , P <sub>Uinv</sub> , A <sub>Minv</sub>	Masses of B, Tc, and RN's in unaltered waste form during time step	-----	Would be generated by GoldSim
B <sub>mob</sub> , T <sub>Cmob</sub> , P <sub>Umob</sub> , A <sub>Mmob</sub>	Masses of B and RN's "mobilized" in WF <sub>deg</sub> during time step	-----	Would be generated by GoldSim
B <sub>cum</sub>	Cumulative mass of B "mobilized" in WF <sub>deg</sub> for all previous time steps	-----	Would be generated by GoldSim
a	Empirically derived constant used in expression for precipitated smectite colloids	10 <sup>-4</sup> (bound)	CRWMS M&O (2000a)
b	Empirically derived constant used in expression for precipitated smectite colloids	1 (bound)	CRWMS M&O (2000a)
κ	Empirically derived constant used in expression for spalled smectite colloids	10 <sup>-4</sup> (bound)	CRWMS M&O (2000a)
I	Ionic strength of fluid during time step	-----	Would be generated by GoldSim
I <sub>thresh</sub>	Ionic strength at and above which all colloids are unstable	0.05 or (narrow) range	CRWMS M&O (2000a)
pH	pH of fluid during time step	-----	Would be generated by GoldSim
K <sub>ad, Pu-smec</sub> K <sub>ad, Am-smec</sub> K <sub>ad, Pu-FeOx</sub> K <sub>ad, Am-FeOx</sub>	Effective attachment-detachment K <sub>ads</sub> for Pu and Am on smectite and iron-(hydr)oxide colloids based on measured rates of adsorption and desorption	TBD	DTN pending
FRAC <sub>coll,min</sub>	Fraction of colloids remaining under conditions in which colloids agglomerate	0.001	Bounding from ANL results (CRWMS M&O 2000a)
FRAC <sub>smec</sub>	Fraction of smectite colloids versus (smectite + iron-[hydr]oxide) available for pseudocolloids	0.9 or range	To be derived
FRAC <sub>FeOx</sub>	Fraction of iron-(hydr)oxides (colloids plus immobile) versus (iron-[hydr]oxide + smectite colloids) available for pseudocolloids	0.1 or range	To be derived
FRAC <sub>FeOx, coll</sub>	Fraction of iron-(hydr)oxide colloids versus total iron-(hydr)oxides available for pseudocolloids	0.001 or range	To be derived

If B<sub>cum</sub> is greater than 3 g m<sup>-2</sup>, then Rate Model 2 is invoked to calculate the quantity of radionuclides irreversibly attached to colloids formed from spallation of the alteration clay layer. The equation for calculating radionuclide mass mobilized due to spallation is:

$$\text{Mass of irreversibly attached spalled RN} = \kappa * B_{cum} \quad (\text{Eq. 12})$$

where κ is an empirically-derived constant.

If B<sub>cum</sub> is between 1 and 3, then either Rate Model 1 or 2 is chosen randomly (0.5 probability).

In the case of SNF, the quantity of radionuclides irreversibly attached to colloids was bounded according to the expression:

$$\text{Mass of irreversibly attached RN} = (Tc_{\text{mob}} / Tc_{\text{inv}}) * 10^{-5} \quad (\text{Eq. 13})$$

at each time step.

**Calculation of Quantity and Rate of Production of Reversibly Attached Radionuclides**—Quantities of radionuclides reversibly attached to colloids are calculated by taking the mass of dissolved (aqueous) RN resulting from the waste degradation at each time step. This approach is similar to that described in Section 6.3.

Quantities of radionuclides reversibly attached to colloids are calculated by taking the mass of dissolved (aqueous) Pu and Am resulting from the waste degradation at each time step.

Dissolved Pu and Am are assumed to sorb onto smectite and iron-(hydr)oxide colloids as determined by the effective adsorption-desorption  $k_d$  (“ $k_{ad}$ ”) according to the following relationships:

$$RN_{\text{rev,smec}} = 0.9 * RN_{\text{diss}} * K_{\text{ad,RNsmec}} \quad (\text{Eq. 14})$$

$$RN_{\text{rev,FeOx}} = 0.1 * RN_{\text{diss}} * K_{\text{ad,RNFeOx}} \quad (\text{Eq. 15})$$

The values 0.9 and 0.1 are placeholders and are represented by a range.

Iron-(hydr)oxides are assumed to be 0.001 colloids and 0.999 immobile corrosion products (placeholders) and are represented by a range.

**Determination of Stability of Smectite and Iron-(Hydr)oxide Colloids**—This approach is identical to that described in Section 6.3.6. Figure 12 illustrates for purposes of the abstraction where smectite colloids are stable in I-pH space and was derived from experimental data (Figure 5). The upper limit of ionic strength is assumed to be 0.05 for the pH range 6 to 12. Below pH 6, stability is pH-dependent; at lower pH, smectite becomes unstable at lower ionic strength. Smectite stability is calculated as follows (see also Figure 13):

1. IF pH  $\geq$  6 AND I  $\geq$  0.05 THEN  $RN_{\text{smec, coll}} = 10^{-11}$  M
2. IF pH  $\geq$  6 AND  $0.01 < I < 0.05$  THEN  $RN_{\text{smec, coll}} = 4.327 \times 10^{-11} \times I^{-1.654}$
3. IF pH  $\geq$  6 AND I  $\leq$  0.01 THEN  $RN_{\text{smec, coll}} = 6 \times 10^{-8}$  M
4. IF pH  $<$  6 AND I  $\geq$   $(0.004 + 2.714 \times 10^{-2} \ln \text{pH})$  THEN  $RN_{\text{smec, coll}} = 10^{-11}$  M
5. IF pH  $<$  6 AND I  $<$   $(0.004 + 2.714 \times 10^{-2} \ln \text{pH})$  THEN  $RN_{\text{smec, coll}} = 4.327 \times 10^{-11} \times I^{-1.654}$

Figure 6 illustrates for purposes of the abstraction where iron-(hydr)oxide colloids are stable in I-pH space and was derived from a plot of stability ratio versus pH from Liang and Morgan (1990). Iron-(hydr)oxide stability is calculated as follows (see also Figure 13):

1. IF  $I \geq 0.05$  M, THEN  $RN_{FeOx, coll} = RN_{FeOx, coll} \times 10^{-3}$
2. IF  $(I \leq 0.01)$  AND  $(8 \leq pH \leq 9)$ , THEN  $RN_{FeOx, coll} = RN_{FeOx, coll} \times 10^{-3}$   
OTHERWISE  $RN_{FeOx, coll} = RN_{FeOx, coll}$
3. IF  $(0.01 < I < 0.05)$  AND  $I > (-0.02 * pH + 0.17)$  OR  $I > (0.02 * pH - 0.17)$  THEN  
 $RN_{FeOx, coll} = 0.01 RN_{FeOx, coll}$   
OTHERWISE  $RN_{FeOx, coll} = RN_{FeOx, coll}$

**Calculation of Colloid Source Term**—The colloid source term is the sum of radionuclides irreversibly attached to smectite colloids, radionuclides reversibly attached to smectite colloids, and radionuclides reversibly attached to oxyhydroxide colloids:

$$C_{RNcoll, sum} = C_{RNcoll, irrev} + C_{RNcoll, smec-revers} + C_{RNcoll, FeOx} \quad (\text{Eq. 16})$$

**Assessment**—This alternative abstraction takes into account many of the results from the ANL waste form corrosion experimental program as well as models derived from them. It incorporates an analytical approach that would couple the waste form degradation calculations by GoldSim more closely to the process model derived from the experiments.

While it takes advantage of the most complete information available on waste form corrosion, at the same time it is tailored very closely to the experimental conditions and configurations. There are aspects of the experiments which may make them inappropriate to apply to a more general case. A possible example is the rate of spallation of the clay layer from altered HLW, which is likely due to the impact of the drips falling on the sample in the HLW drip tests (recall that no spallation was observed in the static tests). If the corroded contents of a failed waste canister assumes a geometry that does not allow dripping of water onto the alteration products, spallation may not occur. If dripping does occur, of course, spallation may be a viable process, and an analysis of colloid production and transport would have to consider it.

Implementation of this abstraction requires parameters that, it is believed, are not available under the current TSPA approach, such as the surface area of the waste form at each time step, and the total masses and chemistries of secondary phases at each time step. In lieu of these parameters, assumptions would have to be made that may be difficult to defend and uncertainties incorporated to which the results may be overly sensitive. Should in-package chemistry calculations be developed along these lines, the applicability of this approach could improve.

### 6.4.3 Issues and Comments from the NRC IRSRs

Table 7. NRC IRSR Issues

Source	Issue	Resolution
NRC (1998b, p. 49)	DOE should specifically determine colloid contribution to actinide release from four types of colloid formation processes: condensation, detachment of secondary phases, sorption onto existing colloids, detachment of WF fragments.	This abstraction addresses the lack of condensation (true) colloids which may be expected in a failed waste canister, as well as sorption onto existing colloids. Detachment of secondary phases and waste form fragments is addressed in the alternative abstraction, which is impractical at this stage of TSPA development.
NRC (1998b, p. 50)	DOE should demonstrate the validity of its empirical correlation for colloid stability versus pH and ionic strength over a wide range of evolving environmental conditions on the bases of mechanistic interpretations.	This has been accomplished in the abstraction by taking existing data on smectite concentration and smectite and iron-(hydr)oxide stability as a function of ionic strength and pH, bounding the data, and developing simplified relationships useful in the abstraction.
NRC (1998b, p. 50)	The influence of corrosion products generated by steel components on the formation of colloids needs to be examined by DOE.	This has been incorporated as an assumption. Quantitative estimates of corrosion products and colloids are not currently available.
NRC (1998b, p. 53)	DOE should develop appropriate scenarios and estimations of colloid transport through package perforations.	In this abstraction all colloids are assumed to exit the failed canister by whatever perforation is present.
NRC (1998b, p. 54)	DOE should consider higher RN releases from glass due to colloids and pulse-release of colloidal RN's from hydrated glass.	Detachment of secondary phases and waste form fragments is addressed in the alternative abstraction, which is impractical at this stage of TSPA development.
NRC (1998b, p. 56)	DOE should account for large excursions in glass corrosion behavior due to spallation of colloids.	Detachment of secondary phases and waste form fragments is addressed in the alternative abstraction, which is impractical at this stage of TSPA development.
NRC (1999b, p. 23)	DOE has identified and considered likely processes for SNF degradation... [including] dissolution of the irradiated UO <sub>2</sub> matrix, with...formation of secondary minerals and colloids.	Colloid formation from degradation of SNF was considered by evaluating the test data from Argonne National Laboratory and incorporating the results into the abstraction.
NRC (1999b, p. 25)	DOE has identified and considered likely processes for degradation of HLW glass... [including] dissolution of the primary phase [and] formation of secondary minerals and colloids.	Colloid formation from degradation of HLW glass was considered by evaluating the test data from Argonne National Laboratory and incorporating the results into the abstraction.
NRC (1999b, p. 46)	...resolution [of Subissue 3]...is achieved through examination of [among other things] the consistency of the information with evidence generated by studies in other countries.	A comprehensive review of the programs of other countries was not performed for this AMR.
NRC (1999b, p. 55)	...it has been recommended that DOE determine colloid contribution to actinide release [from SNF]...in PA calculations.	Colloid contribution to actinide release was considered by evaluating the test data from Argonne National Laboratory and incorporating the results in the abstraction.
NRC (1999b, p. 59)	DOE has not conducted any relevant scale-down test to evaluate the location, morphology, and characteristics of corrosion penetrations.	Corrosion penetrations were not addressed in the abstraction.

Source	Issue	Resolution
NRC (1999b, p. 60)	DOE should provide confirmation that...radionuclides are not released [from HLW glass] at rates greater than SNF. Otherwise, DOE should consider the effects of [release from the hydrated layer] and...radionuclide release from HLW glass in PA	Release of colloid-associated radionuclides from HLW glass was incorporated into the abstraction, based on test results from Argonne National Laboratory.
NRC (1999b, p. 62)	It is important that the long-term radionuclide release rate in the corrosion models used by DOE include the influence of stage III behavior [in which reprecipitation of secondary phases occurs, as well as cracking and exfoliation of the altered surface layer].	Release of colloid-associated radionuclides from HLW glass due to such processes was incorporated into the abstraction, based on test results from Argonne National Laboratory.
NRC (1999b, p. 63)	Recent research...ha[s] shown formation of colloids in the alteration phases...[and] transport of 100 percent of the actinides as colloids to the environment.	Transport of actinides has been treated in the abstraction by considering colloids with irreversibly attached actinides and dissolved actinides available for reversible attachment.

## 7. CONCLUSIONS

The following conclusions may be drawn regarding this development of an abstraction for the calculation of the waste form colloid source term in TSPA:

- A useful model has been developed for GoldSim to calculate colloid concentration as a function of ionic strength, assuming that colloids are stable, as well as for determining the stability of smectite and iron-(hydr)oxide colloids as a function of both ionic strength and pH.
- The abstraction employs bounding relationships that are closely tied to the colloid generation and characterization experimental programs conducted at ANL and LANL.
- The abstraction is conservative, relies on bounding estimates, and incorporates as much realism as is considered defensible.
- The abstraction addresses many of the comments and concerns presented in the NRC IRSRs.
- Regarding spallation of altered waste form, this observation in the experiments may be due in part to the vessel configuration and may or may not apply to the interior of a failed and corroded waste canister. The alternative abstraction does begin to address spallation-related colloid release by incorporating the colloid rate generation developed by ANL investigators.

There are several significant sources of uncertainty attached to this abstraction. The potential formation of colloids from degradation of N-Reactor fuel, and its potential contribution to repository performance, must be investigated. At this time the data are preliminary; however, the program is ongoing, and more data are anticipated. For now, it is assumed in the abstraction that, due to the small quantity of N-reactor fuel, any colloids generated from degradation of the fuel will have little or no effect on repository performance. A plan for verifying this assumption and concomitantly reducing the associated uncertainty, is described in Section 6.1.1.1. If this assumption, after examination, proves untrue, use of the assumption could result in underestimation of the contribution of colloids derived from degradation of N-reactor fuel to repository performance.

Another, but less significant, uncertainty is the assumed nature of radionuclide attachment to colloids produced as a result of CSNF degradation. The assumption, that radionuclides may only be reversibly attached to smectite colloids produced from degradation of CSNF, is based on observations, i.e., that no embedded radionuclide phases were seen to occur in the few clay colloids that were produced during the degradation testing. This is described in Section 6.4.1. If any of the colloids contain embedded (irreversibly attached) radionuclides, the consequences for waste package releases would be minimal since it is assumed that all colloid-associated radionuclides leave a breached waste package. However, this could result in underestimation of mobile colloids in the drift and unsaturated and saturated zones and, possibly, underestimation of their impact on repository performance.

The abstraction is considered valid and usable in TSPA calculations for any time after the temperature in the repository has decreased to below boiling after the thermal pulse. Many of the waste degradation tests were performed at 90°C but mostly sampled at near room temperature. Therefore the test results may be applied to this post-thermal period. The range of ionic strength and pH for which colloid masses and stability are calculated in the abstraction are within the ranges anticipated from in-package chemistry calculations and abstraction.

In general, the bounding relationships employed in the abstraction incorporate uncertainty present in the data used. Additional uncertainty may result from GoldSim and the ways in which GoldSim performs calculations. For example, the choices of distributions and the method of sampling a particular distribution may result in uncertainties in determination of colloid concentrations, ionic strength, pH, and radionuclide concentrations.

Data used directly as input were taken from Liang and Morgan (1990) and Tombacz et al. (1990) and are currently TBV, awaiting approval as accepted data. The data form a part of the basis for this abstraction, and accordingly this approval is necessary for the abstraction in its current form. The data are from frequently cited peer-reviewed journal articles in highly respected journals, so approval is anticipated.

This document may be affected by technical product input information that requires confirmation. Any changes to the document that may occur as a result of completing the confirmation activities will be reflected in subsequent revisions. The status of the input information quality may be confirmed by review of the Document Input Reference System database.

## 8. INPUTS AND REFERENCES

### 8.1 DOCUMENTS CITED

Bird, R.B; Stewart, W.E.; and Lightfoot, E.N. 1960. *Transport Phenomena*. New York, New York: John Wiley & Sons. TIC: 208957.

Buck, E.C. and Bates, J.K. 1999. "Microanalysis of Colloids and Suspended Particles from Nuclear Waste Glass Alteration." *Applied Geochemistry*, 14, 635-653. New York, New York: Elsevier Science Ltd. TIC: 245946.

CRWMS M&O 1998. *Total System Performance Assessment-Viability Assessment (TSPA-VA) Analyses Technical Basis Document*. Las Vegas, Nevada: CRWMS M&O. ACC: MOL.19981008.0001; MOL.19981008.0002; MOL.19981008.0003; MOL.19981008.0004; MOL.19981008.0005; MOL.19981008.0006; MOL.19981008.0007; MOL.19981008.0008; MOL.19981008.0009; MOL.19981008.0010; MOL.19981008.0011.

CRWMS M&O 1999a. *Classification of the MGR Uncanistered Spent Nuclear Fuel Disposal Container System*. ANL-UDC-SE-000001 REV 00. Las Vegas, Nevada: CRWMS M&O. ACC: MOL.19990928.0216.

CRWMS M&O 1999b. *Conduct of Performance Assessment*. Activity Evaluation, September 30, 1999. Las Vegas, Nevada: CRWMS M&O. ACC: MOL.19991028.0092.

CRWMS M&O 2000a. *Colloid-Associated Radionuclide Concentration Limits: ANL*. ANL-EBS-MD-000020 REV 00. Las Vegas, Nevada: CRWMS M&O. ACC: MOL.20000329.1187.

CRWMS M&O 2000b. *Unsaturated Zone and Saturated Zone Transport Properties*. ANL-NBS-HS-000019 REV 00. Las Vegas, Nevada: CRWMS M&O Submit to RPC URN-0038.

CRWMS M&O 2000c. *Colloid-Associated Concentration Limits - Abstraction and Summary*. Development Plan TDP-WIS-MD-000011 REV 00. Las Vegas, Nevada: CRWMS M&O. ACC: MOL.20000207.0693.

CRWMS M&O 2000d. *Summary of In-Package Chemistry for Waste Forms*. ANL-EBS-MD-000050 REV 00. Las Vegas, Nevada: CRWMS M&O. ACC: MOL.20000217.0217.

Dyer, J.R. 1999. "Revised Interim Guidance Pending Issuance of New U.S. Nuclear Regulatory Commission (NRC) Regulations (Revision 01, July 22, 1999), for Yucca Mountain, Nevada." Letter from Dr. J.R. Dyer (DOE/YMSCO) to Dr. D.R. Wilkins (CRWMS M&O), September 3, 1999, OL&RC:SB-1714, with enclosure, "Interim Guidance Pending Issuance of New NRC Regulations for Yucca Mountain (Revision 01)." ACC: MOL.19990910.0079.

Dzombak, D.A. and Morel, F.M.M. 1990. *Surface Complexation Modeling, Hydrous Ferric Oxide*. New York, New York: John Wiley & Sons. TIC: 224089.

Ebert, W.L. 1995. *The Effects of the Glass Surface Area/Solution Volume Ratio on Glass Corrosion: A Critical Review*. ANL-94/34. Argonne, Illinois: Argonne National Laboratory. TIC: 215400.

Efurd, D.W.; Runde, W.; Banar, J.C.; Janecky, D.R.; Kaszuba, J.P.; Palmer, P.D.; Roensch, F.R.; and Tait, D. 1998. "Neptunium and Plutonium Solubilities in a Yucca Mountain Groundwater." *Environmental Science & Technology*, 32, (24), 3893-3900. Easton, Pennsylvania: Environmental Science & Technology. TIC: 243857.

EPA (Environmental Protection Agency) 1999. *Understanding Variation in Partition Coefficient,  $K_d$ , Values*. EPA 402-R-99-004A&B Two volumes. Washington, D.C.: U.S. Environmental Protection Agency.

Finn, P.A.; Buck, E.C.; Gong, M.; Hoh, J.C.; Emery, J.W.; Hafenrichter, L.D.; and Bates, J.K. 1994. "Colloidal Products and Actinide Species in Leachate from Spent Nuclear Fuel." *Radiochimica Acta*, 66/67, 197-203. Munchen, Germany: R. Oldenbourg Verlag. TIC: 238493.

Fontes, D.E.; Mills, A.L.; Hornberger, G.M.; and Herman, J.S. 1991. "Physical and Chemical Factors Influencing Transport of Microorganisms Through Porous Media." *Applied and Environmental Microbiology*, 57, (9), 2473-2481. Washington, D.C.: American Society of Microbiology. TIC: 247563.

Harvey, R.W. and Garabedian, S.P. 1991. "Use of Colloid Filtration Theory in Modeling Movement of Bacteria Through a Contaminated Sandy Aquifer." *Environmental Science and Technology*, 25, 175-185. Washington, D.C.: American Chemical Society. TIC: 245733.

Harvey, R.W.; George, L.H.; Smith, R.L.; and LeBlanc, D.R. 1989. "Transport of Microspheres and Indigenous Bacteria Through a Sandy Aquifer: Results of Natural- and Forced-Gradient Tracer Experiments." *Environmental Science and Technology*, 23, (1), 51-56. Washington, D.C.: American Chemical Society. TIC: 224869.

Hersman, L. 1995. *Microbial Effects on Colloidal Agglomeration*. LA-12972-MS. Los Alamos, New Mexico: Los Alamos National Laboratory. ACC: MOL.19971210.0253.

Hiemenz, P.C. 1986. *Principles of Colloid and Surface Chemistry*. 2nd edition, Revised and Expanded. New York, New York: Marcel Dekker. TIC: 246392.

Kim, J.I. 1994. "Actinide Colloids in Natural Aquifer Systems." *MRS Bulletin*, 19, (12), 47-53. Pittsburgh, Pennsylvania: Materials Research Society. TIC: 246128.

Kim, S. and Corapcioglu, M.Y. 1996. "Kinetic Approach to Modeling Mobile Bacteria-Facilitated Groundwater Contaminant Transport." *Water Resources Research*, 32, (2), 321-331. Washington, D.C.: American Geophysical Union. TIC: 247566.

Kingston, W.L. and Whitbeck, M. 1991. *Characterization of Colloids Found in Various Groundwater Environments in Central and Southern Nevada*. DOE/NV/10384-36. Las Vegas, Nevada: U.S. Department of Energy. ACC: NNA.19930607.0073.

Langmuir, D. 1997a. *Aqueous Environmental Geochemistry*. Upper Saddle River, New Jersey: Prentice Hall. TIC: 237107.

Langmuir, D. 1997b. "The Use of Laboratory Adsorption Data and Models to Predict Radionuclide Releases from a Geological Repository: A Brief History." *Scientific Basis for Nuclear Waste Management XX, Symposium held December 2-6, 1996, Boston, Massachusetts*. Gray, W.J. and Triay, I.R., eds. 465, 769-780. Pittsburgh, Pennsylvania: Materials Research Society. TIC: 238884.

Liang, L. and Morgan, J.J. 1990. "Chemical Aspects of Iron Oxide Coagulation in Water: Laboratory Studies and Implications for Natural Systems." *Aquatic Sciences*, 32, (1), 32-55. Basel, Switzerland: Birkhauser Verlag. TIC: 246125.

McCarthy, J.F. and Degueudre, C. 1993. "Sampling and Characterization of Colloids and Particles in Groundwater for Studying Their Role in Contaminant Transport." Chapter 6 of *Environmental Particles*. Buffle, J. and van Leeuwen, H.P., eds. Volume 2. Boca Raton, Florida: Lewis Publishers. TIC: 245905.

McCarthy, J.F. and Zachara, J.M. 1989. "Subsurface Transport of Contaminants." *Environmental Science & Technology*, 23, (5), 496-502. Easton, Pennsylvania: American Chemical Society. TIC: 224876.

McGraw, M.A. 1996. *The Effect of Colloid Size, Colloid Hydrophobicity, and Volumetric Water Content on the Transport of Colloids Through Porous Media*. Ph.D. dissertation. Berkeley, California: University of California. TIC: 245722.

Meijer, A. 1992. "A Strategy for the Derivation and Use of Sorption Coefficients in Performance Assessment Calculations for the Yucca Mountain Site." *Proceedings of the DOE/Yucca Mountain Site Characterization Project Radionuclide Adsorption Workshop at Los Alamos National Laboratory, September 11-12, 1990*. Canepa, J.A., ed. LA-12325-C. Pages 9-40. Los Alamos, New Mexico: Los Alamos National Laboratory. ACC: NNA.19920421.0117.

Minai, Y.; Choppin, G.R.; and Sisson, D.H. 1992. "Humic Material in Well Water from the Nevada Test Site." *Radiochimica Acta*, 56, 195-199. Munchen, Germany: R. Oldenbourg Verlag. TIC: 238763.

Stenhouse, M.J. 1995. *Sorption Databases for Crystalline, Marl and Bentonite*. NAGRA Technical Report 93-06. Wetingen, Switzerland: National Cooperative for the Disposal of Radioactive Waste. On Order Library Tracking Number-1527.

Tombacz, E.; Abraham, I.; Gilde, M.; and Szanto, F. 1990. "The pH-Dependent Colloidal Stability of Aqueous Montmorillonite Suspensions." *Colloids and Surfaces*, 49, 71-80. Amsterdam, The Netherlands: Elsevier Science. TIC: 246046.

van Olphen, H. 1977. *An Introduction to Clay Colloid Chemistry for Clay Technologists, Geologists, and Soil Scientists*. 2nd Edition. New York, New York: John Wiley & Sons. TIC: 208918.

Wan, J. and Tokunaga, T.K. 1997. "Film Straining on Colloids in Unsaturated Porous Media: Conceptual Model and Experimental Testing." *Environmental Science and Technology*, 31, (8), 2413-2420. Washington, D.C.: American Chemical Society. TIC: 234804.

Wan, J. and Wilson, J.L. 1994. "Colloid Transport in Unsaturated Porous Media." *Water Resources Research*, 30, (4), 857-864. Washington, D.C.: American Geophysical Union. TIC: 222359.

Weiss, T.H.; Mills, A.L.; Hornberger, G.M.; and Herman, J.S. 1995. "Effect of Bacterial Cell Shape on Transport of Bacteria in Porous Media." *Environmental Science Technology*, 29, (7), 1737-1740. Washington, D.C.: American Chemical Society. TIC: 247490.

Yates, M.V. and Yates, S.R. 1988. "Modeling Microbial Fate in the Subsurface Environment." *Critical Reviews in Environmental Control*, 17, (4), 307-345. Boca Raton, Florida: CRC Press. On Order Library Tracking Number-1530

## 8.2 CODES, STANDARDS, REGULATIONS, AND PROCEDURES

10 CFR 960. 1988. Energy: General Guidelines for the Recommendation of Sites for Nuclear Waste Repositories. Readily Available

64 FR 8640. Disposal of High-Level Radioactive Wastes in a Proposed Geologic Repository at Yucca Mountain, Nevada. Proposed rule 10 CFR 63. Readily Available

AP-3.10Q, Rev. 02, ICN 0. *Analyses and Models*. Washington D.C., Washington D.C.: Office of Civilian Radioactive Waste Management. ACC: MOL.20000217.0246.

DOE (U.S. Department of Energy) 2000. *Quality Assurance Requirements and Description*. DOE/RW-0333P, Rev. 9. Washington, D.C.: U.S. Department of Energy, Office of Civilian Radioactive Waste Management. ACC: MOL.19991028.0012.

NLP-2-0, Rev. 5. *Determination of Importance Evaluations*. Las Vegas, Nevada: CRWMS M&O. ACC: MOL.19981116.0120.

NRC (U.S. Nuclear Regulatory Commission) 1998a. *Issue Resolution Status Report Key Technical Issue: Total System Performance Assessment and Integration*. Rev. 1. Washington, D.C.: U.S. Nuclear Regulatory Commission. ACC: MOL.19990105.0083.

NRC (U.S. Nuclear Regulatory Commission) 1998b. *Issue Resolution Status Report Key Technical Issue: Container Life and Source Term*. Rev. 1. Washington, D.C.: U.S. Nuclear Regulatory Commission. ACC: MOL.19990105.0081

NRC (U.S. Nuclear Regulatory Commission) 1999a. *Issue Resolution Status Report Key Technical Issue: Evolution of the Near-Field Environment*. Rev. 2. Washington, D.C.: U.S. Nuclear Regulatory Commission. ACC: MOL.19990810.0640.

NRC (U.S. Nuclear Regulatory Commission) 1999b. *Issue Resolution Status Report Key Technical Issue: Container Life and Source Term*. Rev. 2. Washington, D.C.: U.S. Nuclear Regulatory Commission. TIC: 245538.

QAP-2-3, Rev. 10. *Classification of Permanent Items*. Las Vegas, Nevada: CRWMS M&O. ACC: MOL.19990316.0006.

QAP-2-0, Rev. 5, ICN 1. *Conduct of Activities*. Las Vegas, Nevada: CRWMS M&O. ACC: MOL.19991109.0221.

### 8.3 SOURCE DATA

LL991109851021.095. Colloid Size and Concentration Investigations in Scientific Notebook SN 1381. Submittal date: 01/10/2000.

MO0003SPALOW12.001. Lowest Observed Or Expected Concentration Of Radionuclide Element Rn Associated With Waste-Form Colloids. Submittal date: 03/02/2000.

MO0003SPAHIGH12.002. Highest and Lowest Observed or Expected Masses of Iron-(hydr)Oxide Colloids Per Unit Volume or Mass of Water. Submittal date: 03/02/2000.

MO0003SPAION02.003. Values Of Ionic Strength That Define The Stability Limits Of Iron-(Hydr)Oxide Colloids. Submittal date: 03/03/2000.

MO0003SPAHL012.004. Highest and Lowest Observed or Expected Groundwater Colloid Masses Per Unit Volume or Mass of Water; Values of Ionic Strength Above Which Groundwater Colloid Dispersions Are Unstable Concentration and Stability of Groundwater Colloids as Defined by Ionic Strength of Groundwater. Submittal date: 03/16/2000.

MO0004SPAKDS42.005. K<sub>d</sub>s for Pu and Am on Waste Form, Iron (hydr)Oxide, and Groundwater Colloids. Submittal date: 04/10/2000.

LA0003NL831352.002. The K<sub>d</sub> Values of <sup>239</sup>Pu on Colloids of Hematite, Ca-Montmorillonite and Silica in Natural and Synthetic Groundwater. Submittal date: 03/29/2000.

LA0003NL831352.003. The K<sub>d</sub> Values of <sup>243</sup>Am on Colloids of Hematite, Montmorillonite and Silica in Natural and Synthetic Groundwater. Submittal date: 03/29/2000.

**ATTACHMENT I -  
YMP NO. 2.1.09.14.00  
NEA NO. 2.1.09AO-COLLOID FORMATION IN WASTE AND EBS**

**I.1 YMP PRIMARY FEP DESCRIPTION**

Colloids in the waste and EBS may affect radionuclide transport. Several types of colloids may occur naturally and may form during the evolution of the system by a variety of mechanisms. This FEP is broad in scope, general in its descriptions, and groups the several types of colloids into a single category. Discussions of colloids for the Yucca Mountain repository are presented elsewhere for true colloids (YMP No. 2.1.09.15.00), colloids formed by co-precipitation of waste alteration phases (YMP No. 2.1.09.16.01), natural pseudo-colloids (YMP No. 2.1.09.16.00), pseudo-colloids formed from corrosion products (YMP No. 2.1.09.17.00), and microbial colloids (YMP No. 2.1.09.18.00).

**I.2 SCREENING DECISION**

Include

**I.3 SCREENING ARGUMENT**

Colloids are particles and large molecules ranging from approximately 1 nanometer to 1 micrometer in size. Several types of colloids may form in the waste form/waste package and EBS environment. Radionuclides may become associated with colloids in several possible ways: (1) radionuclides may form "true" colloids through hydrolysis and polymerization; (2) dissolved (aqueous) radionuclides may sorb to existing colloids (e.g., clay, iron-(hydr)oxides, silica), forming pseudocolloids; (3) radionuclide-bearing phases may coprecipitate with waste form alteration phases, such as clay, forming multiphase colloids in which the radionuclide-bearing phases are entrained in (embedded in, or occluded by) the alteration-phase colloid; and (4) colloid-sized microbe fragments or large organic molecules may associate with radionuclides.

Colloids thus formed in the waste and EBS may influence radionuclide transport. Depending on their size and on their surface and chemical characteristics, colloids may travel at velocities greater than the average groundwater velocity or may travel more slowly due to retardation processes. Analyses and field studies show that certain radionuclides attached to colloids may be transported long distances relative to the aqueous species.

YMP No. 2.1.09.14.00 (this FEP) groups the several modes of colloid formation as a set of processes. Specific colloid processes relevant to the Yucca Mountain repository are discussed in separate FEPs: True colloids (YMP No. 2.1.09.15.00), colloids from co-precipitation of waste alteration phases (YMP No. 2.1.09.16.01), natural-colloid-based pseudocolloids (YMP No. 2.1.09.16.00), pseudocolloids formed from corrosion of introduced materials in the EBS and the WP (YMP No. 2.1.09.17.00) and microbial colloids (YMP No. 2.1.09.18.00). Retardation is discussed in YMP No. 2.1.09.19.00 and filtration in YMP No. 2.1.09.20.00.

DOE-SNF and DHLW are being evaluated for the purpose of improving our understanding of colloid formation and stability and colloids' effect on radionuclide transport. Issues recently resolved or under investigation include:

- Mechanisms of waste-derived colloid formation (ANL)
- Stability and concentration of waste-derived and intrinsic colloids (ANL, LANL)
- Stability and concentration of pseudo-colloids (LANL)
- Attachment/detachment rates and effective  $K_{ds}$  of pseudo-colloids (LANL)
- Fraction of effectively "irreversibly attached" colloids and pseudo-colloids (LANL).

A model abstraction that defines the waste form colloid source term for TSPA calculations has been developed from the data and models that result from these investigations.

#### **I.4 TSPA DISPOSITION**

A waste-form colloid source term will be abstracted from the data and models produced from several investigations (see section 3 above, "Screening Argument").

#### **I.5 BASIS FOR SCREENING DECISION**

Plutonium and several other radionuclides of concern have low solubilities under the geochemical conditions anticipated in the repository, and as dissolved metal ions, they tend to sorb readily to the mineral phases present in the host rock. However, there have been several cases at the Nevada Test Site and DOE weapons complex sites where radionuclides were observed to have traveled distances greater than expected or predicted from models. Upon investigation it was determined that the radionuclides formed or were associated with colloidal particles.

As described in section 3 above, "Screening Argument," radionuclides may become attached to colloid-sized mineral fragments, waste form alteration phases, or organically derived colloids and as a result may travel greater distances than would be predicted for the aqueous radionuclide.

True, or primary, colloids (formed from hydrolysis or polymerization of dissolved radionuclides) and colloid particles formed by coprecipitation of phases that include a radioactive component may result from corrosion of SNF and HLW glass within the waste package. Radioactive pseudocolloids may form where dissolved or colloidal radionuclides sorb onto colloid-sized clay, silica, or iron-(hydr)oxides. These minerals occur naturally in the groundwater; they may also form from the degradation of introduced repository materials such as steel and concrete and be introduced into a failed waste package. They may also be formed within the waste package from degradation of the waste form (e.g., clays) and the waste package itself (e.g., iron-(hydr)oxides).

Microbes and microbe fragments may occur in groundwater as colloid-sized particles to which radionuclides can sorb. They may affect the repository environment in several ways and are a potential cause of localized changes in groundwater chemistry in and around the waste package, oxidation of metallic iron, and aggregation of colloidal materials used as a food source (resulting in decreased concentration). Colloid-sized organic (e.g., humic) materials may sorb radionuclides as well.

The occurrence and stability of colloids, including radioactive colloids, depends on such environmental factors as the concentration of colloids in the fluid, the fluid's ionic strength, and the fluid's pH. In general, colloids tend to agglomerate (clump together to form larger particles) and settle out due to gravity when ionic strength exceeds a certain value or the concentration of colloids exceeds a certain value that depends on the characteristics of the system. Agitation and high groundwater velocities are additional (but low probability) processes that may facilitate colloid formation and promote stability. These are not analyzed in TSPA.

**ATTACHMENT II -  
YMP NO. 2.1.09.15.00  
NEA NO. 2.1.09C-FORMATION OF TRUE COLLOIDS  
IN WASTE AND EBS**

## **II.1 YMP PRIMARY FEP DESCRIPTION**

True colloids are colloidal-sized assemblages (between approximately 1 nanometer and 1 micrometer in diameter) of hydrolyzed and polymerized dissolved radionuclides. They may form in the waste package and EBS during waste-form degradation and radionuclide transport. True colloids are also called radionuclide intrinsic colloids (or actinide intrinsic colloids, for those including actinide elements).

## **II.2 SCREENING DECISION**

Exclude (Note: this FEP addresses waste forms only.)

## **II.3 SCREENING ARGUMENT**

The formation of true colloids involves the release of radionuclide ions from the waste form into solution and the subsequent hydrolysis and polymerization of the radionuclide ions to form colloid-sized species. However, based on the results of investigations of SNF and DHLW, in the course of which no true colloids were observed, it is considered unlikely that true colloids will form during the corrosion of waste forms.

DOE-SNF and DHLW are being evaluated with regard to their effect or contribution to the technical issues discussed in this FEP.

## **II.4 TSPA DISPOSITION**

Not applicable.

## **II.5 BASIS FOR SCREENING DECISION**

For the past several years tests have been conducted at ANL to characterize the modes of degradation of SNF and DHLW under anticipated repository groundwater and geochemical conditions. As a part of these tests, colloids produced as a result of degradation have been sampled and characterized. The results of the colloid characterization may be summarized as follows: (1) true (intrinsic) colloids have not been observed from corrosion tests in glass or spent fuel, and (2) the colloids which form from waste-form corrosion are associated with waste-form corrosion phases (largely clays).

These results are consistent with the argument that true colloids are unlikely to form under anticipated repository conditions. The formation of true colloids requires supersaturation or near-supersaturation conditions with respect to the radionuclide. The test results indicate that the concentration of dissolved plutonium, for example, was below its concentration limit. Since (1)

the test conditions were intended to approximate anticipated repository conditions, (2) the test conditions were not conducive to true colloid formation, and (3) true colloids were not observed, it was concluded that true colloids are not likely to form as a result of waste degradation. It is, therefore, recommended that this FEP be excluded.

**ATTACHMENT III -  
YMP NO. 2.1.09.16.00  
NEA NO. 2.1.09D-FORMATION OF PSEUDO-COLLOIDS (NATURAL)  
IN WASTE AND EBS**

**III.1 YMP PRIMARY FEP DESCRIPTION**

Pseudocolloids are colloidal-sized particles (between approximately 1 nanometer and 1 micrometer in diameter), usually (but not necessarily) nonradioactive, that have radionuclides sorbed to them. Natural pseudocolloid particles may include mineral fragments formed from the host rock and present in the groundwater, microbes and microbe fragments, and humic and fulvic acids. This FEP addresses radionuclide-bearing colloids formed from host-rock materials and interactions of the waste and EBS with the host rock environment. Pseudocolloids formed from corrosion of the waste form and EBS are discussed in YMP No. 2.1.09.17.00. The occurrence, stability, and transport of bacteria and organic colloids is addressed in YMP No. 2.1.09.18.00.

**III.2 SCREENING DECISION**

Include

**III.3 SCREENING ARGUMENT**

Natural colloids (clay, silica, and iron-(hydr)oxides) may be transported in groundwater into the repository from the vadose zone above it or may be formed from the erosion of natural backfill and inert materials (e.g., crushed tuff). Pseudo-colloids may form due to the sorption onto these natural colloids of radionuclides mobilized from degradation of the waste form.

Pseudocolloids thus formed in the waste and EBS may influence radionuclide transport. Analyses and field studies show that radionuclides attached to colloids may be transported long distances relative to the aqueous radionuclide.

DOE-SNF and DHLW are being evaluated with regard to their effect or contribution to the technical issues discussed in this FEP.

**III.4 TSPA DISPOSITION**

This will be incorporated into the waste form colloid-associated radionuclide concentration limits.

**III.5 BASIS FOR SCREENING DECISION**

Plutonium and several other radionuclides of concern have low solubilities under the geochemical conditions anticipated in the repository, and as dissolved metal ions they tend to sorb readily to the mineral phases present in the host rock. However, there have been several cases at the Nevada Test Site and DOE weapons complex sites where radionuclides were observed to have traveled distances greater than expected or predicted from models. Upon

investigation it was determined that the radionuclides formed or were associated with colloidal particles.

As described in section 3, "Screening Argument," radionuclides may become attached to colloid-sized mineral fragments (clay, silica, iron-[hydr]oxides), forming radioactive pseudocolloids, and as a result may travel greater distances than would be predicted for the aqueous radionuclide.

Radionuclides tend to sorb reversibly to the mineral colloids, i.e., after they sorb, they eventually desorb. As observed in tests conducted at LANL, the radionuclides tend to desorb more slowly than they sorb. Sorption and desorption rates of plutonium and americium on several types of mineral colloids have been and are currently being determined. The results of these determinations will indicate whether desorption should be considered fast or slow within transport times of interest in different parts of the repository system and, therefore, whether the sorption should be considered effectively reversible or effectively irreversible in the TSPA analysis.

Microbes and microbe fragments may occur in groundwater as colloid-sized particles to which radionuclides can sorb or be actively bioaccumulated across the cell membrane. They may effect localized changes in groundwater chemistry in and around the waste package, oxidation of metallic iron, and aggregation of colloidal materials used a food source (resulting in decreased concentration). Colloid-sized organic (e.g., humic) materials may sorb radionuclides as well.

The occurrence and stability of pseudo-colloids, as any colloids, depend on such environmental factors as the concentration of colloids in the fluid, the fluid's ionic strength, and in some cases the fluid's pH. In general, colloids tend to agglomerate (clump together to form larger particles) and settle out due to gravity when ionic strength exceeds a certain value or the concentration of colloids exceeds a certain value that depends on the characteristics of the system. Agitation and high groundwater velocities are additional (but low probability) processes that may facilitate colloid formation and promote stability. These are not analyzed in TSPA.

**ATTACHMENT IV -  
YMP NO. 2.1.09.16.01  
NEA NO. 2.1.09A-COLLOID PHASES PRODUCED BY CO-PRECIPIATION  
(IN WASTE AND EBS)  
(SECONDARY TO YMP 2.1.09.16.00 [NEA 2.1.09D])**

**IV.1 YMP PRIMARY FEP DESCRIPTION**

Colloidal phases of minerals containing radionuclides are formed by co-precipitation that occurs at the waste form. (YMP)

**IV.2 SCREENING DECISION**

Include (Note: only production of colloid phases by co-precipitation in the WP is considered here)

**IV.3 SCREENING ARGUMENT**

The most important processes contributing to the formation of waste form colloids, as observed in investigations of the degradation of SNF and DHLW, are: (1) co-precipitation of radionuclide-bearing phases with colloid-sized clay phases formed homogeneously in the solution contacting the waste, and (2) under conditions in which water drops onto the waste, spallation of colloid-sized fragments of co-precipitated clay (primarily) and radionuclide-bearing phases from the alteration layers formed on the waste form surfaces. Through these mechanisms, radionuclide-bearing phases can become entrained in alteration phases, primarily clays.

Colloids thus formed from the waste may have a large influence on radionuclide transport because of the apparently stable attachment of the radionuclides. Depending on their size and on their surface and chemical characteristics, colloids may travel at velocities greater than the average groundwater velocity or may travel more slowly due to retardation processes. Analyses and field studies show that radionuclides attached to colloids may be transported long distances relative to the aqueous radionuclide.

DOE-SNF and DHLW are being evaluated with regard to their effect or contribution to the technical issues discussed in this FEP.

**IV.4 TSPA DISPOSITION**

This will be incorporated into the waste form colloid-associated radionuclide concentration limits abstraction.

**IV.5 BASIS FOR SCREENING DECISION**

Plutonium and several other radionuclides of concern have low solubilities under the geochemical conditions anticipated in the repository, and as dissolved metal ions they tend to sorb readily to mineral phases present in the host rock. Further, there have been several cases at

the Nevada Test Site and DOE weapons complex sites where radionuclides were observed to have traveled distances greater than expected or predicted from models. Upon investigation it was determined that the radionuclides formed or were associated with colloidal particles.

As described in section 3, "Screening Argument," radionuclides may become entrained in colloid-sized fragments of waste form alteration phases, clay colloids in particular, and as a result may travel greater distances than would be predicted for the aqueous radionuclide.

It is considered that radionuclide-bearing phases coprecipitating with clay from alteration of the waste form will form colloids that may be stable under anticipated repository conditions. The occurrence and stability of colloids, including coprecipitated radioactive colloids, depend on such environmental factors as the concentration of colloids in the fluid, the fluid's ionic strength, and the fluid's pH (although clay colloid stability is relatively pH-independent). In general, colloids tend to agglomerate (clump together to form larger particles) and settle out due to gravity when ionic strength exceeds a certain value or the concentration of colloids exceeds a certain value that depends on the characteristics of the system. Agitation and high groundwater velocities are additional (but low probability) processes that may facilitate colloid formation and promote stability (these are not analyzed in TSPA).

DOE-SNF and DHLW are being evaluated with regard to their effect or contribution to the technical issues discussed in this FEP.

**ATTACHMENT V -  
YMP NO. 2.1.09.17.00  
NEA NO. 2.1.09E-FORMATION OF PSEUDO-COLLOIDS  
(DEPENDENT ON CORROSION PRODUCTS) (IN WASTE AND EBS)**

**V.1 YMP PRIMARY FEP DESCRIPTION**

Pseudocolloids are colloid-sized particles (between approximately 1 nanometer and 1 micrometer in diameter), usually (but not necessarily) nonradioactive, that have radionuclides sorbed to them. Possible pseudocolloid particle types formed from corrosion of materials introduced into the repository during construction and waste emplacement include iron-(hydr)oxides from corrosion of waste package and EBS components; silica from degradation of cementitious materials; and construction materials including diesel fuel, rockbolt resin, extruded polystyrene, bentonite clay, and cable lubricant. This FEP addresses pseudocolloids formed from corrosion of the metals in the waste package and EBS. Radionuclide-bearing colloids formed from natural materials are discussed in YMP No. 2.1.09.16.00. The formation, stability, and transport of bacteria and organic colloids are addressed in YMP No. 2.1.09.18.00.

**V.2 SCREENING DECISION**

Include

**V.3 SCREENING ARGUMENT**

Artificial materials (e.g., cement grout, carbon steel, stainless steel, aluminum, titanium-7, and Alloy-22) will be introduced during construction of the repository. The corrosion of these materials may produce significant quantities of colloids, primarily metal oxyhydroxides. Radionuclides will tend to sorb onto the colloids, forming pseudo-colloids as well as onto larger particles and scale. In addition, the degradation of waste glass and spent nuclear fuel will likely produce clays (with and possibly without entrained radionuclide-bearing phases), another "substrate" for pseudocolloids in the drift.

Pseudocolloids thus formed in the waste and EBS may influence radionuclide transport. Analyses and field studies show that radionuclides attached to colloids may be transported long distances relative to the aqueous radionuclide.

DOE-SNF and DHLW are being evaluated with regard to their effect or contribution to the technical issues discussed in this FEP.

**V.4 TSPA DISPOSITION**

This will be incorporated into the waste form colloid source term model abstraction.

## V.5 BASIS FOR SCREENING DECISION

Plutonium and several other radionuclides of concern have low solubilities under the geochemical conditions anticipated in the repository, and as dissolved metal ions they tend to sorb readily to the mineral phases present in the host rock. However, there have been several cases at the Nevada Test Site and DOE weapons complex sites where radionuclides were observed to have traveled distances greater than expected or predicted from models. Upon investigation it was determined that the radionuclides formed or were associated with colloidal particles.

As described in section 3 above, "Screening Argument," radionuclides may become attached to colloid-sized particles resulting from the corrosion of metals in the waste package and EBS, forming radioactive pseudocolloids, and as a result may travel greater distances than would be predicted for the aqueous radionuclide.

Radionuclides tend to sorb reversibly to the metal oxyhydroxide colloids, i.e., after they sorb they eventually desorb if the dissolved radionuclide concentration decreases. As observed in tests conducted at LANL, the radionuclides tend to desorb more slowly than they sorb. Sorption and desorption rates of plutonium and americium on several types of mineral colloids have been and are being determined. The results of these determinations will indicate whether desorption should be considered fast or slow within transport times of interest in different parts of the repository system and, therefore, whether the sorption should be considered effectively reversible or effectively irreversible in the TSPA analysis.

The occurrence and stability of pseudocolloids from metals corrosion depend on such environmental factors as the concentration of colloids in the fluid, the fluid's ionic strength, and in some cases the fluid's pH. In general, colloids tend to agglomerate (clump together to form larger particles) and settle out due to gravity when ionic strength exceeds a certain value or the concentration of colloids exceeds a certain value that depends on the characteristics of the system. Agitation and high groundwater velocities are additional (but low probability) processes that may facilitate colloid formation and promote stability. These are not analyzed in TSPA.

**ATTACHMENT VI -  
YMP NO. 2.1.09.18.00  
NEA NO. 3.2.04AA-MICROBIAL COLLOID TRANSPORT  
IN THE WASTE AND EBS**

**VI.1 YMP PRIMARY FEP DESCRIPTION**

This FEP addresses the formation and transport of microbial colloids in the waste and EBS. Pseudocolloids formed from corrosion and degradation of the metals in the waste package and EBS are discussed in YMP No. 2.1.09.17.00. Pseudocolloids formed from host-rock materials and interactions of the waste and EBS with the host rock environment are discussed in YMP No. 2.1.09.16.00.

**VI.2 SCREENING DECISION**

Exclude

**VI.3 SCREENING ARGUMENT**

Microbes can affect the amount of mobile colloidal material such as clay, hematite, goethite, and silica by influencing the rate of waste package corrosion. Given the present state of knowledge, estimates of the effects of microbes on corrosion processes are highly uncertain. However, it is unlikely that sufficient quantities of microbes will be available to accelerate corrosion rates significantly. Also, microbial action tends to increase colloid size, which would result in increased gravitational settling and filtration. Therefore, exclusion of microbial effects from TSPA may be considered conservative.

**VI.4 TSPA DISPOSITION**

N/A

**VI.5 BASIS FOR SCREENING DECISION**

The colloid source term from the repository may be sensitive to the presence of microbes, which could affect the amount of colloidal material such as clay, hematite, goethite, and silica that will be mobile. The effects of microbes in the repository on the colloidal source term concentration can include:

- Changes in near-field in micro-environments in and around waste packages that can cause localized pH and Eh conditions to vary considerably from the measured or predicted bulk chemistry. For example, acidophilic microorganisms in alkaline mine spoils may actively create acidic micro-environments. These localized changes in pH affect colloid stability. For example, hematite colloids are more stable at lower (acidic) pH values (Langmuir 1997a).
- Microbial oxidation of metallic iron (Fe) can produce Fe oxide colloids and aggregates.

- Microbially influenced corrosion can accelerate radionuclide release into the surrounding environment.
- Microorganisms can decrease the concentration of stable colloids by aggregating colloidal material that they use as a food source and can result in a decrease in colloid concentrations of up to 91% under certain conditions (Hersman 1995).

The transport of microbes, which are colloidal in size, through the vadose zone is not considered in the current unsaturated zone (UZ) or saturated zone (SZ) colloid model. Microbes could be included in the model if data were available on concentration, size, shape, sorption properties, the effect of microbial activity on mobility, biofilm formation, rock-microbe interaction, plume characteristics, nutrient availability, longevity, etc. Nevertheless, it is unlikely that a significant concentration of microbes associated with radionuclides will be transported through the UZ due to the availability of energy sources near the repository. Although microbial transport in the SZ has been demonstrated in the literature, it is only significant when microbial transport occurs from the repository through the UZ (Fontes et al. 1991; Harvey et al. 1989; Kim and Corapcioglu 1996; Weiss et al. 1995; Yates and Yates 1988).

Considerable uncertainty surrounds the rate that microbes would affect the system around the repository. Thus, given our current knowledge, it is difficult to approximate a colloid source term from the repository and even more difficult to determine the effect of microbes on colloid concentration and stability.

However, the effect of overriding interest here is the fact that microbial action will tend to increase the colloid size, which will increase gravitational settling and filtration. Conservatism thus indicates that microbial transport may be excluded from the TSPA analyses.

DOE-SNF and DHLW were evaluated with regard to their effect or contribution to the technical issue(s) discussed in this FEP.

**ATTACHMENT VII -  
YMP NO. 2.1.09.19.00  
NEA NO. 3.2.04Z-COLLOID TRANSPORT AND SORPTION**

**VII.1 YMP PRIMARY FEP DESCRIPTION**

Interactions between radionuclide-bearing colloids and the waste and EBS may result in retardation of the colloids during transport by sorption mechanisms.

**VII.2 SCREENING DECISION**

Exclude in waste form and waste package.

**VII.3 SCREENING ARGUMENT**

It is assumed in TSPA that all radionuclide-bearing colloids generated from waste form degradation within a failed waste package will leave the waste package and enter the drift and EBS, and that a relatively small fraction of dissolved radionuclides may be retarded under certain chemical conditions. Currently, it is planned that retardation of colloids within the EBS and drift will not be analyzed in TSPA, although retardation of colloids in the unsaturated zone (UZ) and saturated zone (SZ) may be considered in UZ and SZ transport analyses.

DOE-SNF and DHLW were evaluated with regard to their effect or contribution to the technical issue(s) discussed in this FEP. There was not any unique or significant effect not already accounted for by CSNF.

**VII.4 TSPA DISPOSITION**

Waste form/waste package: will not be analyzed.

**VII.5 BASIS FOR SCREENING DECISION**

On the basis of experiments conducted at ANL, it is anticipated that radionuclide-bearing colloids (primarily containing plutonium and americium) will form in the waste package from the degradation of the waste form. It is further anticipated that the majority of the colloids will be composed of coprecipitated clays and radionuclide-bearing phases (see YMP No. 2.1.09.16.01). In addition there are expected to be dissolved fractions of plutonium, americium, and other relatively insoluble and strongly sorbing radionuclides, at concentration levels below their solubility limits.

It is likely that some corrosion of the interior of the waste package and certain metal components will occur, producing primarily iron-(hydr)oxides as scale, large particles, and colloid-sized particles. Further, portions of the dissolved radionuclide fractions will likely sorb, probably reversibly, to these iron corrosion products; a fraction of the sorbed radionuclides would be onto the colloids, forming pseudo-colloids.

The stability of the pseudo-colloids from metals corrosion will depend on such environmental factors as the concentration of colloids in the fluid and the fluid's ionic strength and pH. In general, colloids tend to agglomerate (clump together to form larger particles) and settle out due to gravity when ionic strength exceeds a certain value or the concentration of colloids exceeds a certain value that depends on the characteristics of the system. Further, iron-(hydr)oxide colloids would likely agglomerate at a fluid pH of around 8.5.

**ATTACHMENT VIII -  
YMP NO. 2.1.09.20.00  
NEA NO. 3.2.04Y-COLLOID FILTRATION**

**VIII.1 YMP PRIMARY FEP DESCRIPTION**

Filtration processes may affect transport of radionuclide-bearing colloids in the waste and engineered barrier system (EBS).

**VIII.2 SCREENING DECISION**

Exclude

**VIII.3 SCREENING ARGUMENT**

Filtration processes may affect transport of radionuclide-bearing colloids in the waste and EBS.

Physical colloid filtration within the waste package will not be analyzed in the TSPA, and it is anticipated that it will not be analyzed in the EBS. Instead the conservative assumption is made that all colloids produced within the waste package (the calculated colloid source term) exit the waste package through a perforation in the waste package and enter the drift/EBS.

DOE-SNF and DHLW were evaluated with regard to their effect or contribution to the technical issue(s) discussed in this FEP.

**VIII.4 TSPA DISPOSITION**

N/A

**VIII.5 BASIS FOR SCREENING DECISION**

Colloid filtration as discussed herein refers to the physical removal of colloids from a flow system by pore clogging, sieving, and straining. Filtration of colloids generally means the retention of colloids moving with the suspending fluid in pores, channels, and fracture apertures that are too small or "dry" to allow passage of the colloids. Two types of physical filtration are recognized (e.g., Wan and Tokunaga 1997), conventional straining and film straining. Colloids are filtered by conventional straining if they are larger than a pore throat diameter or fracture aperture. Where water saturation is low, colloids may be filtered by film-straining if their size is greater than the thickness of the adsorbed water film coating the grains of the rock. The rate of colloid transport through thin water films depends upon the colloid size relative to the film thickness.

These processes could conceivably occur within the waste package, the EBS, and the host rock. Colloid filtration within the waste package is not analyzed in TSPA, primarily because the requisite research has not been performed and because a conservative assumption can be made which incorporates its potential effects. Chemical and electrostatic processes affecting colloid

flow (e.g., sorption), included as processes of filtration in much of the literature, are treated separately in YMP No. 2.1.09.19.00.

Within the waste package, colloids may form within the waste form (e.g., corroded waste fuel pellets) and at its outer surfaces (e.g., corroded HLW glass). They could be filtered within fractures in fuel pellets or trapped at the boundaries of disaggregating grains. Colloids forming within fuel rods whose cladding has been breached could be filtered at perforations in the cladding; colloids formed and spalled from the HLW glass could be filtered at perforations in the stainless steel HLW container. Colloids reaching the interior of the waste package (after escaping from fuel rod cladding and HLW containers) could be filtered at perforations in the skin of the waste package.

Existing colloid filtration models are empirically derived and to a considerable extent are specific to the system experimentally characterized. There have been no comprehensive studies of colloid filtration within the spent fuel and HLW glass waste package environments. Therefore, meaningful analysis of colloid filtration within the waste package is currently not feasible.

Therefore, a conservative assumption is made: all colloids formed within the waste package (the calculated colloid source term) are assumed to exit the waste package and enter the drift. This is the justification for excluding colloid filtration processes from the TSPA-SR analysis.

DOE-SNF and DHLW are being evaluated with regard to their effect or contribution to the technical issues discussed in this FEP.

**ATTACHMENT IX -  
YMP NO. 2.1.09.21.00  
NEA NO. 3.2.08C—SUSPENSIONS OF PARTICLES LARGER THAN COLLOIDS**

**IX.1 YMP PRIMARY FEP DESCRIPTION**

Groundwater flow through the waste could remove radionuclide-bearing particles by a rinse mechanism. Particles of radionuclide-bearing material larger than colloids could then be transported in water flowing through the waste and EBS by suspension.

**IX.2 SCREENING DECISION**

Exclude.

**IX.3 SCREENING ARGUMENT**

Although it is conceivable that some particles larger than colloids could get “rinsed” out of the waste package, depending on the flow-through scenario under consideration, particles leaving the waste package is a process considered to have low consequence. The following discussion focuses on the possible fate of particles “downstream” of the waste package.

The particles may flow through the EBS, or may be trapped. Beyond that, suspension of particles in groundwater flowing downward through discrete fractures in the UZ is possible. It is unlikely, however, that larger-than-colloid particles will have access to a sufficient number of vertical or subvertical fractures whose apertures permit their passage to be transported in significant quantities. The relatively small quantity of particles that may make it through the UZ would encounter low groundwater velocities in the SZ, which would likely result in the particles settling and becoming immobile.

**IX.4 TSPA DISPOSITION**

Suspension of particles larger than colloids is not analyzed in the TSPA.

**IX.5 BASIS FOR SCREENING DECISION**

Suspensions of particles having sizes above the colloid range are by definition not stable. (Colloids by definition may form stable suspensions under certain conditions; their properties derive from their high surface area and surface charge relative to their mass.) Unlike stable suspended colloids, they are subject to gravitational settling. They do not have the requisite surface properties to effect mutual repulsion and stability in suspension.

Small particles could be entrained by high groundwater flow velocities. It is conceivable that vertical or subvertical fractures in the UZ could, under relatively high-flow conditions, pass larger-than-colloid particles. It is unlikely, however, that significant quantities of radionuclide-bearing particles would be transported to the SZ in this fashion.

This would require numerous *continuous* vertical fractures through the geologic sequence between the floor of the repository and the SZ, which is highly unlikely. During fracture transport, particles would be physically removed along the length of the fracture in surface irregularities, dead ends, and possibly by water films of insufficient thickness to transmit them. In the event that particles did reach the SZ, it is unlikely that sufficiently high velocities will be encountered in the SZ to enable further transport. The particles would instead become immobile due to gravitational settling.

**ATTACHMENT X -  
YMP NO. 2.1.10.01.00  
NEA NO. 2.1.10D-BIOLOGICAL ACTIVITY IN WASTE AND EBS**

**X.1 YMP PRIMARY FEP DESCRIPTION**

Biological activity in the waste and EBS may affect disposal-system performance by altering degradation processes such as corrosion of the waste packages and waste form (including cladding) by affecting radionuclide transport through the formation of colloids and biofilms and by generating gases.

Identified as "biological activity" by originator.

**X.2 SCREENING DECISION**

Exclude

**X.3 SCREENING ARGUMENT**

Microbes can affect the mobility of colloidal material as well as influence the rate of waste package corrosion. Given the present state of knowledge, estimates of the effects of microbes on corrosion processes are highly uncertain. However, it is unlikely that sufficient quantities of microbes will be available to generate the biological activity needed to affect colloid mobility or accelerate corrosion rates significantly. Exclusion of effects of biological activity in the waste and EBS from TSPA may be considered inconsequential.

**X.4 TSPA DISPOSITION**

Not considered in TSPA.

**X.5 BASIS FOR SCREENING DECISION**

The colloid source term from the repository may be sensitive to the presence of colloid-sized microbes, which could change chemistry, affect the amount of colloidal material such as clay, hematite, goethite, and silica that will be mobile, influence corrosion of the waste package, and effect agglomeration of colloids. The potential effects of biological activity from microbes in the repository on the colloidal source term concentration are described below.

Changes in near field chemistry in micro-environments in and around waste packages that can cause localized pH and Eh conditions to vary considerably from the measured or predicted bulk chemistry. For example, acidophilic microorganisms in alkaline mine spoils may actively create acidic micro-environments. These localized changes in pH affect colloid stability. In the case of hematite, colloids are more stable at lower pH values (Langmuir 1997a).

MIC can accelerate radionuclide release into the surrounding environment; microbial oxidation of metallic iron (Fe) can produce Fe oxide colloids and aggregates. Conversely, microorganisms

can decrease the concentration of stable colloids by aggregating colloidal material that they use as a food source and can result in a decrease in colloid concentrations of up to 91% per ml (Hersman 1995).

The transport of microbes within the waste package and EBS is not currently modeled in TSPA. This is due to the lack of data on concentration, size, shape, sorption properties, and the effects of microbial activity on mobility. Nevertheless, it is unlikely that a significant concentration of microbes associated with radionuclides will be transported within the repository system due to the lack of energy sources near the repository. Although microbial transport in the SZ has been demonstrated in the literature, it is only significant when microbial transport occurs from the repository through the UZ (Fontes et al. 1991; Harvey et al. 1989; Kim and Corapcioglu 1996; Weiss et al. 1995; Yates and Yates 1988).

Considerable uncertainty surrounds the rate that microbes would affect the system around the repository. Thus, given our current knowledge, it is difficult to estimate their effects on the colloid source term, in particular the effect of microbes on colloid concentration and stability. However, it is understood that microbial action will tend to increase the colloid size, which would increase gravitational settling and filtration. Thus, excluding the effects of biological activity from microbes in the colloid source term and transport analysis is conservative.

DOE-SNF and DHLW were evaluated with regard to their effect or contribution to the technical issue(s) discussed in this FEP.

**ATTACHMENT XI -  
YMP NO. 2.1.13.03.00  
NEA NO. 2.1.13A-MUTATION**

**XI.1 YMP PRIMARY FEP DESCRIPTION**

Radiation fields could cause mutation of microorganisms, leading to unexpected chemical reactions and impacts.

**XI.2 SCREENING DECISION**

Exclude

**XI.3 SCREENING ARGUMENT**

Microbes can affect the mobility of colloidal material as well as influence the rate of waste package corrosion. Given present knowledge, estimates of the effects of microbes on corrosion processes are highly uncertain; the potential effects of mutated microbes are more uncertain. No analyses or experimental research have been performed to investigate this problem specifically. However, general principles of population genetics indicate that most mutations are either neutral or deleterious to the fitness of an organism and, in the absence of strong natural selection, are unlikely to produce any definite change in the phenotypes of the organisms. Thus, exclusion of effects of mutated microbes from TSPA is probably conservative.

**XI.4 TSPA DISPOSITION**

Not considered.

**XI.5 BASIS FOR SCREENING DECISION**

The colloid-associated radionuclide concentration from the repository may be sensitive to the presence of microbes, which could affect the amount of mobile colloidal material. The effects of microbes in the repository on the colloid-associated radionuclide concentration can include: (1) changes in near field chemistry in micro-environments in and around waste packages, (2) microbial oxidation of metallic iron (Fe) to produce Fe oxide colloids and aggregates, (3) MIC, accelerating radionuclide release into the surrounding environment, and (4) decrease in the concentration of stable colloids by aggregating colloidal material used as a food source.

Considerable uncertainty surrounds the degree to which small, isolated populations of microbes affect chemical systems around the repository. In the absence of much organic material, microbial effects are believed to be small in comparison to changes induced in chemistry by global variables such as heat and radiation.

Regarding the process of mutation: Populations of microorganisms not destroyed by heat and radiation in the post-closure repository could in time *evolve* phenotypic traits very different from traits of the pre-closure populations; and it is possible that these altered phenotypes could be

associated with unusual manifestations of effects (items 1-4 noted above). The process of mutation, however, is not sufficient to drive evolution in a definite direction; most mutations are either neutral or deleterious with regard to an organism's phenotype. Thus, mutational processes alone are highly unlikely to produce the aforementioned effects. The process dominating directional evolution of isolated populations of prokaryotes is *natural selection* which acts over successive generations to maintain the fitness of an organism for life in its environment; but the manner and direction in which selective forces "move" an organism's phenotype is not predictable except under the most closely controlled conditions (*artificial selection*).

In any case, if mutated microbes were to occur, it is unlikely that sufficient quantities will be available to accelerate corrosion rates significantly or have unpredictable effects. Also, as mentioned above, microbial action tends to increase colloid size, which would result in decreased colloid stability. Therefore, the potential effects of mutated microbes are excluded from TSPA.

**ATTACHMENT XII -  
YMP NO. 2.1.09.22.00  
COLLOID SORPTION AT THE AIR-WATER INTERFACE**

**XII.1 YMP PRIMARY FEP DESCRIPTION**

Both hydrophilic and hydrophobic colloids may be sorbed irreversibly at the gas-water interface under partially saturated conditions.

**XII.2 SCREENING DECISION**

Exclude

**XII.3 SCREENING ARGUMENT**

Models of colloid transport in partially-saturated media have been developed in recent years, but there have been no experimental studies of transient flow in partially saturated porous media for model comparison and calibration. Although the potential effects of degree of saturation on colloid transport are varied and complex, it appears that colloids would be at least somewhat retarded under low-saturation conditions. Therefore, neglect of colloid sorption onto the air-water interface in the TSPA calculations is believed to be conservative.

**XII.4 TSPA DISPOSITION**

Not included in TSPA.

**XII.5 BASIS FOR SCREENING DECISION**

The concentration of colloids sorbed at the gas-water interface is a function of the following conditions:

- The interface surface area available for colloid uptake, which is a function of the total gas saturation
- The affinity of colloids for the gas-water interface (hydrophobic colloids have higher affinities than hydrophilic colloids)
- The electrostatic charge on the colloid—less negatively charged colloids exhibit a stronger affinity
- The salinity of the aqueous phase, with higher salinity promoting sorption.

Empirical evidence suggests that the sorption of colloids at the gas-water interface is irreversible and the affinity may be stronger than to the rock matrix (Wan and Wilson 1994).

Partially saturated conditions may be described or “classified” by considering degrees of saturation. At low water saturations the surface area of the gas-water interface approximates that

of the rock matrix. Overall, colloid migration is retarded, although colloids may still move through the adsorbed water films. At intermediate water saturations there is still an interconnected gas phase, although gas flux may be lower. The interface may act as a static sorbing surface, but the estimating geometry and surface area is complicated, more so under changing saturation state. At high water saturations the majority of the gas is present at small gas bubbles that may migrate, transporting sorbed colloids. However, a proportion of the bubbles may become trapped in the rock and will effectively immobilize sorbed colloids.

McGraw (1996) concluded that for hydrophobic colloids, the cumulative mass of colloids recovered relative to the mass input into the column was logarithmically dependent upon the ratio of the water film thickness to colloid diameter. In contrast, for hydrophilic colloids, the cumulative mass of colloids recovered relative to that input into the column was linearly dependent upon the ratio of the water film thickness to colloid diameter, similar but more pronounced than the effect with the non-reactive tracer. McGraw's findings suggest that the unsaturated zone is not necessarily an effective barrier to colloid migration even for relatively large colloids, although larger colloids will tend to be retarded more than smaller ones.

**ATTACHMENT XIII -  
YMP NO. 2.1.09.23.00  
COLLOID STABILITY AND CONCENTRATION DEPENDENCE ON AQUEOUS  
CHEMISTRY**

**XIII.1 YMP PRIMARY FEP DESCRIPTION**

In order for radionuclide-bearing colloids to affect repository performance, the colloidal dispersion must be stable for the time frame of transport and must carry significant amounts of radionuclides. The stability of smectite colloids is determined primarily by ionic strength but also to an extent by pH. The stability of iron-(hydr)oxide colloids is determined by both ionic strength and pH as well as the concentrations of polyvalent cations.

**XIII.2 SCREENING DECISION**

Include.

**XIII.3 SCREENING ARGUMENT**

In order for radionuclide-bearing colloids to affect repository performance, the colloidal dispersion must be stable for the time frame of transport and must carry significant amounts of radionuclides. Transport times can range from days/months/years for transport out of a failed waste package under a large seep to hundreds of thousands of years for retarded transport to the accessible environment. Thus, some relatively unstable colloids generated at the waste form may persist long enough to be transported out of the waste package, increasing the radionuclide release from the waste package, but not traveling a significant distance away from the repository. The more stable colloids, however, may remain suspended for years and travel a much greater distance.

**XIII.4 TSPA DISPOSITION**

Considered in waste form colloid source term abstraction.

**XIII.5 BASIS FOR SCREENING DECISION**

The ZPC of smectite is approximately pH 2. Since a pH this low is not anticipated in the repository, it is a reasonable assumption that smectite colloids will remain in a stable pH range much of the time under anticipated repository conditions (unless ionic strength exceeds a certain threshold). However, with decreasing pH, the charge density of smectite particle surfaces will decrease as more and more H<sup>+</sup> sorb to the surface and offset negative charges, generally decreasing stability (Buck and Bates 1999; Tombacz et al. 1990). This decrease in stability should be taken into account.

The HLW tests conducted at ANL resulted in measured pH ranging between approximately 9 and 11.5 (Buck and Bates 1999), which is part of the range at which smectite colloids exhibit the highest surface charge and hence are most stable.

The ZPC of iron-(hydr)oxide colloids is around pH 8.5, and at this pH they will be unstable and tend to agglomerate. At higher or lower pH, however, iron-(hydr)oxide colloids may be stable, depending upon ionic strength. Liang and Morgan (1990) demonstrated that for a given ionic strength iron-(hydr)oxide stability increases as pH both increases and decreases away from the ZPC. In general the higher the ionic strength, the wider the pH range about the ZPC that iron-(hydr)oxide is unstable. For example, at an ionic strength of 0.05 M, iron-(hydr)oxide is unstable between approximately pH 6 and 11

Colloids were formed in the course of certain HLW glass corrosion tests on several glass samples. It was observed that as the ionic strength increased, colloid concentration generally decreased, and ultimately a threshold value was reached above which the colloids were not observed, or were observed in very low quantities. The threshold at which flocculation occurred was approximately  $I = 0.05m$ .

Colloid concentration and stability is also dependent upon the concentrations of the major cations Na, K, Ca, and Mg. In an investigation of natural groundwaters, it appeared that in general colloids tend to be stable if the concentration of alkalis (Na and K) is below approximately  $10^{-2} M$  and if alkali-earth elements (Ca and Mg) are below approximately  $10^{-4} M$ .

**ATTACHMENT XIV -  
YMP NO. 2.1.09.24.00  
COLLOID DIFFUSION**

**XIV.1 YMP PRIMARY FEP DESCRIPTION**

The diffusivity of a solute in a liquid is inversely proportional to the radius of the diffusing particles. Colloidal particles, together with any associated actinides, that are sufficiently small may diffuse into intercrystalline porosity and will be physically retarded.

**XIV.2 SCREENING DECISION**

Include.

**XIV.3 SCREENING ARGUMENT**

Physical retardation of dissolved actinides should be evaluated; it is best evaluated using Fick's Law, in which the mass diffusion constant (D; also referred to as diffusivity or the free-water diffusion constant) is a critical parameter.

**XIV.4 TSPA DISPOSITION**

TSPA uses a diffusion coefficient of  $10^{-2}$ , i.e., the free-water diffusion constant for a colloidal particle is that of a dissolved actinide reduced by a factor of 100.

**XIV.5 BASIS FOR SCREENING DECISION**

At a fundamental level, diffusivity is related to the physical characteristics of the diffusing molecule and the molecules of the host medium and the intermolecular forces acting between them. For example, the diffusivity of a gas molecule in another gas (the host gas) at low density is inversely proportional to the square root of the reduced mass of the diffusing and host gas molecules and the collision diameter. Whereas a rigorous theory of solute diffusion in liquids is apparently not available, order of magnitude estimates may be made on the basis of hydrodynamical theory. With that theory, the diffusivity of a solute in a liquid is inversely proportional to the radius of the diffusing particles (Bird et al. 1960, p. 513). Rates of diffusion of colloidal particles can be estimated by scaling those experimentally determined free water diffusion constants for dissolved actinides to dissolved colloidal materials on the basis of size (Stokes-Einstein relationship) as follows:

$$D_{\text{coll}} = D_{\text{ion}} \left( \frac{r_{\text{ion}}}{r_{\text{coll}}} \right)$$

where:

$D_{\text{coll}}$  diffusion constant for a colloidal actinide of radius  $r_{\text{coll}}$

$D_{\text{ion}}$  diffusion constant for a dissolved actinide of radius  $r_{\text{ion}}$

$r_{\text{coll}}$  radius of the colloidal actinide  
 $r_{\text{ion}}$  radius of the dissolved actinide

For example, given an ionic radius and a colloidal particle radius of 1 Å and 10 nm, respectively, the free-water diffusion constant for the colloidal particle would be that of the dissolved actinide reduced by a factor of 100. That approach is consistent with discussions in Hiemenz (1986, p. 81).

**ATTACHMENT XV -  
YMP NO. 2.1.09.24.00  
COLLOID GRAVITATIONAL SETTLING**

**XV.1 YMP PRIMARY FEP DESCRIPTION**

Over the relatively short transport distances within the waste package, larger colloidal particles may experience gravitational settling, thereby inhibiting transport.

**XV.2 SCREENING DECISION**

Exclude.

**XV.3 SCREENING ARGUMENT**

The conservative assumption is made that gravitational settling of radionuclide-bearing colloids does not occur, but instead all of the colloids (if stable) leave a breached waste package.

**XV.4 TSPA DISPOSITION**

Not included in TSPA.

**XV.5 BASIS FOR SCREENING DECISION**

GoldSim does not model settling; because of this and the fact that there are no conceptual models and data for gravitational settling within the waste package, this process is not incorporated into the abstraction. Instead, the conservative assumption is made that gravitational settling does not occur, but instead all of the colloids (if stable) leave a breached waste package.

## ATTACHMENT XVI – RADIONUCLIDE UPTAKE MECHANISMS

### XVI.1 RADIONUCLIDE UPTAKE MECHANISMS

Perhaps the most common approach used in assessment of contaminant-rock interactions in the subsurface is the linear isotherm, or  $K_d$ , approach, based on results of batch sorption experiments. The linear isotherm model relationship is defined as follows:

$$S = K_d \times C \quad (\text{Eq. XVI-1})$$

where  $K_d$  is the distribution coefficient (mass or surface-area based),  $S$  is the mass of a solute sorbed on a unit mass (or surface area) of solid, and  $C$  is the concentration of the sorbing solute. For this relationship to be applicable (i.e., for the  $K_d$  to be constant), three critical assumptions must be met. First, the water-contaminant-rock system must be in thermodynamic equilibrium. In other words, sorption must be completely reversible. Second, contaminant uptake must scale linearly with contaminant concentration (i.e.,  $K_d$  must be a constant value). Third, the presence of other solutes in the system cannot affect the sorption. Because of the nature of the formation of waste-form colloids, and the interaction of some radionuclides, particularly some actinides, with mineral surfaces, critical assumptions of the linear isotherm model are not met, and special treatment must be made. Those approaches are described in the next two sections.

#### XVI.1.1 REVERSIBLE UPTAKE

Because of the assumption of reversibility, coprecipitation of radionuclides along with other non-radionuclide ions is excluded. A large amount of data exists in published literature for sorption, and, in the past several decades, increasing attention has been given to understanding the mechanisms of sorption. In this section, the development of  $K_d$  values for uptake of strontium (Sr), cesium (Cs), thorium (Th), protactinium (Pa), uranium (U), neptunium (Np), plutonium (Pu), and americium (Am) on colloids is described, along with caveats.

To a large extent, the effectiveness of colloids at facilitating contaminant transport is due to their very large mobile surface area available for sorption. Depending on the size distribution of colloids in the groundwater, the impact of choosing a mass-based  $K_d$ , or a surface-area-based  $K_a$ , may be significant. The greatest variability exists in situations in which an inordinately large number of very small colloids exist, which have a high surface-area-to-mass ratio. Based on experimental measurements and observations of colloid characteristics in Yucca Mountain groundwaters, this situation does not exist at Yucca Mountain, and the use of a mass-based  $K_d$  is satisfactory.

For Yucca Mountain colloid transport calculations,  $K_d$  values are in units of volume of sorbate per mass solid sorbent (e.g., mL/g). To calculate the concentration of a radionuclide associated with colloids in a colloidal dispersion, the following expression is used (RN = radionuclide):

$$C_{\text{RNcoll}} = C_{\text{RNdiss}} \times K_{d,\text{RN}} \times M_{\text{coll}} \times 10^{-6} \quad (\text{Eq. XVI-2})$$

where:

$C_{\text{Rncoll}}$  = concentration of radionuclide RN associated with the colloidal dispersion (e.g., moles RN/L dispersion)

$C_{\text{Rndiss}}$  = concentration of dissolved RN (moles RN/L)

$K_{\text{d,RN}}$  = distribution coefficient (ML/g)

$M_{\text{coll}}$  = mass of colloids in dispersion (mg/L)

To develop colloid  $K_{\text{d}}$  information, information provided by project-related data (CRWMS M&O 2000b) and published literature was considered. Several significant compendia of sorption data have been assembled in the past decade. One useful example is the compendium developed by the National Cooperative for the Disposal of Radioactive Waste (NAGRA, Switzerland; Stenhouse, 1995). The objective of that work was to compile a set of  $K_{\text{d}}$  values useful for evaluation of waste-disposal in hypothetical sites in Switzerland. The sorbents considered were crystalline rock, marl, and bentonite, all with reducing groundwaters (or porewater, in the case of bentonite). Ionic strengths are similar to J-13 well water, or greater. Despite differences in those conditions, the information compiled in the NAGRA document is useful for YMP, in that it includes consideration of phenomena affecting sorption. A second compendium that is particularly useful is a recent one developed for the U.S. EPA (EPA, 1999). In that work, information on radionuclides including Sr, Cs, Th, U, and Pu is compiled (no information for Pa, Np, or Am). The assembled data are interpreted to predict ranges of  $K_{\text{d}}$  values for soils in shallow subsurface environments. Redox conditions for that system are oxidizing, which makes it useful for the redox-sensitive radionuclides at YMP. Unfortunately, the group of radionuclides covered does not provide an analog element for trivalent or pentavalent elements, such as Am(III), Pa(V), or Np(V).

By considering the effect of aqueous chemical conditions on sorption, the selection of relevant  $K_{\text{d}}$  values is simplified. The behavior of the mineral surface is primarily controlled by pH and ionic strength (particularly concentrations of sodium, calcium, and potassium). The behavior of the sorbate is primarily controlled by its oxidation state, pH, and the partial pressure of carbon dioxide ( $P_{\text{CO}_2}$ ). In Table XVI-1, the effect of key phenomena affecting sorption are summarized for each radionuclide, for clay and metal-(hydr)oxide minerals. For minerals in which the sorption mechanism is primarily by ion exchange (e.g., clay minerals), ionic strength impacts sorption of Sr and Cs on clay minerals (especially at their edges), because cations compete with radionuclides for exchange sites. Ionic strength is less important for actinides, in that some anions and cations contributing to ionic strength affect sorption by forming complexes with the actinides. Under the oxidizing redox condition at Yucca Mountain, radionuclides occur in oxidized forms, which, in general results in decreased sorption. Plutonium will disproportionate and be simultaneously present in multiple valence states (IV, V, and VI at YMP). The actinide elements discussed exhibit strong hydrolysis behavior and a tendency to form strong carbonate complexes. The actinides tend to be completely hydrolyzed at pH values above about 6, where they are present as neutral hydroxo complexes. At slightly alkaline pH values and above, they will exist as negatively charged anionic hydroxo complexes. Consequently, sorption is greatest in the near neutral pH range. The  $P_{\text{CO}_2}$  of the system has minor or negligible effect on sorption of Sr and Cs, but a strong effect on sorption of the actinides. Carbonate is a strong complexant, and at alkaline pH values, the actinides may form mono-, di-, and tri-carbonato complexes,

depending on the actinide (and valence). The presence of these complexes tends to decrease sorption.

#### **XVI.1.1.1 NAGRA Results**

In the NAGRA study, the mineralogic compositions of three relevant rock and engineered barrier types were compiled, and used to weight relevant sorption values from their compendium. The rock or barriers selected were crystalline rock, marl, and bentonite. The chemical compositions of relevant groundwaters or porewaters, all at least somewhat reducing, were also compiled. For Yucca Mountain colloid calculations, the sorption values for crystalline rock were selected for two reasons. First, the mineral phase dominating sorption is similar in mineralogy to Yucca Mountain waste-form and groundwater colloids. A significant observation made in the NAGRA report, is that sorption by a rock is typically dominated by one mineral constituent, usually a phyllosilicate mineral. Second, the groundwater is closest to Yucca Mountain groundwater in terms of pH, ionic strength, and redox conditions (Table XVI-2). NAGRA proposed "realistic values" and "conservative values." The conservative values for the actinides were developed by NAGRA to account for uncertainty in oxidation states (composite  $K_d$  values were reduced by an order-of-magnitude). With respect to the oxidation state, the conservative values would be more relevant to Yucca Mountain. However, to compensate for the use of a mass-based  $K_d$  approach on colloids, the realistic values are useful. In Table XVI-3, the rock composite  $K_d$ s and individual  $K_d$ s for smectite and oxides/quartz are compiled. The latter are probably more suitable to consider for Yucca Mountain colloid  $K_d$ s.

#### **XVI.1.1.2 EPA Results**

In the EPA (1999) study, published literature was reviewed to determine the predominant aqueous chemical conditions affecting sorption in soils for each contaminant. For Sr, soil clay content and groundwater pH were used as criteria to recommend  $K_d$ s. For Cs, clay content was also used, but pH is less important because Cs exists as an aquo ion and does not complex, and it sorbs by ion exchange, a process that is not affected by pH-dependent surface charge. For Th, pH and sorbate concentration are important. At concentrations close to its solubility limit,  $K_d$ s tend to increase. For U, pH was crucial. For Pu carbonate complexation has a strong influence on sorption, and so carbonate concentration, as well as clay content, was used as criteria to select a relevant  $K_d$ . In Table XVI-4,  $K_d$  values are compiled based on aqueous chemical conditions closest to those expected in ambient groundwater at Yucca Mountain. Unfortunately, the  $K_d$  values are expressed in a minimum to maximum format, with no indication of distribution. Some ranges, for example U, span almost six orders of magnitude. To narrow the range, the geometric means were calculated in this AMR, and reported in Table XVI-5. It would be useful to examine the data in the EPA (1999) report, and extract a subset that is particularly applicable to Yucca Mountain, and decrease the ranges of  $K_d$  values.

#### **XVI.1.1.3 LANL Results**

Several sources of YMP-specific sorption data exist from LANL research. Stenhouse (1995) provides useful information on the sorption of Pu(IV) and Pu(V) on colloidal dispersions of hematite, goethite, montmorillonite, and silica. Information on Am(III) is provided for all but goethite. Sorption was measured as a function of time up to 4 or 10 days. Desorption was

measured after 150 days, because desorption tends to be much slower in these mineral-sorbate systems. In Table XVI-5, available sorption data collected at 1 day and longer periods is compiled. To reduce these data, sorption measurements from tests conducted at 1, 2, and 4 days, or 1, 2, 4, and 10 days were averaged. The rationale is that sorption is typically quite fast, requiring less than one day to approach an asymptote. That hypothesis is supported by the LANL data, in that after one day, oscillation in values were observed, but  $K_d$  values did not increase appreciably. The sorption averages were used in a second averaging operation, by including the results of the desorption experiments. In general, desorption and the averaged sorption  $K_d$ s are very similar or within about a factor of 3 or 4, except in a few cases. It is clear, however, that desorption is significantly slower. A third averaging was conducted to consider the results of experiments conducted in synthetic J13 water and actual J13 water. The reason for the different results in the two waters is not clear. For plutonium, since both Pu(IV) and Pu(V) may be present in Yucca Mountain, results from the goethite experiments were averaged. Goethite was selected rather than the more sorptive hematite, because goethite, as a less crystalline material, should more closely resemble corrosion-product colloids produced from waste degradation. The developed values are listed in Table XVI-6.

A second source of sorption data is compiled in the AMR focusing on transport properties in the unsaturated and saturated zones (CRWMS M&O 2000b), which also considers previously done Yucca-Mountain reviews by Meijer (1992) and others. Values developed for devitrified tuff and iron-(hydr)oxides in the saturated zone are listed in Table XVI-6. These ranges are generally comparably to values extracted from the NAGRA report (Table XVI-2). For sorption on colloids, it is likely to be conservative to use the large  $K_d$  values in the ranges.

#### **XVI.1.1.4 Recommendations**

Table XVI-7 summarizes recommended values, which have been extracted from the LANL data discussed above. Values for Sr, Cs, Pa, U, and Np were taken from the AMR discussing transport properties in the saturated and unsaturated zones (CRWMS M&O 2000b). The maximum  $K_d$  values from the ranges for devitrified tuff and iron-(hydr)oxides were used as an analog for colloids consisting of smectite and corrosion-product colloids, respectively. Values for Am were also used for Th, because of similar tendencies for sorption, not as an oxidation species analog. For Pu and Am, values were developed from Stenhouse (1995). Given the non-exact nature of developing these  $K_d$  values, a plus-or-minus one-order-of-magnitude uncertainty band can be assigned to each value.

#### **XVI.1.2 Irreversible Uptake**

The assumptions required for the linear sorption model described above are not met in two instances. First, evidence from HLW-glass degradation experiments shows that plutonium is irreversibly attached to smectite colloids generated during the experiments (CRWMS M&O 2000a). Second, evidence on plutonium sorption experiments with colloidal hematite, goethite, montmorillonite, and silica, show that the rate of desorption (backward rate) of Pu is significantly less than the rate of sorption (forward rate). Moreover, over a significant time period (up to 150 days in some experiments), the extents of desorption is significantly less than the extent of sorption. Special considerations must be made for these situations.

For the HLW-glass experiments, the conceptual model and abstraction developed below accounts for smectite colloids with "engulfed" plutonium and other radionuclides, by treating them as a separate colloid subtype, and by assuming that the engulfed radionuclides are an intrinsic part of the colloid, not in equilibrium with the aqueous system. For the non-ideal sorption behavior of plutonium, a larger  $K_d$  was selected based on the desorption experiments, pending further results from LANL.

Table XVI-1. Sorption Behavior of Key Radionuclides as a Function of Aqueous Chemical Conditions

Radionuclide Sorbate and Oxidation State(s) at YMP	Sorption Mechanisms	Redox Effects	Sorbate Speciation	Ionic Strength Effects	pH Effects	pCO <sub>2</sub> Effects
Sr(II)	Ion exchange in clay minerals; Surface complexation on minerals with pH-dependent surface charge	Not important	Sr <sup>2+</sup> ; in carbonate systems, may form SrCO <sub>3</sub> <sup>0</sup>	Sorption by ion exchange decreases with increasing IS because of surface competition of ions such as Na <sup>+</sup> , Ca <sup>2+</sup>	Change in pH from 6 to 9 results in slight increase in sorption	Sorption increases with increasing [CO <sub>3</sub> <sup>2-</sup> ], due to adsorption of carbonate complexes
Cs(I)	Ion exchange in clay minerals	Not important	Cs <sup>+</sup>	Sorption by ion exchange decreases with increasing IS because of surface competition of ions such as Na <sup>+</sup> , Ca <sup>2+</sup> , K <sup>+</sup>	Change in pH from 6 to 9 results in slight increase in sorption	Not important; Cs <sup>2+</sup> does not tend to complex with CO <sub>3</sub> <sup>2-</sup>
Th(IV)	Surface complexation	Not important	Sparsely soluble; Very strong hydrolysis; forms strong hydroxy carbonate complexes; Th(OH) <sub>3</sub> CO <sub>3</sub> <sup>-</sup>	Sorption decreases with increasing ionic strength because of surface competition of ions such as Na <sup>+</sup> , Ca <sup>2+</sup>		Sorption decreases with increasing [CO <sub>3</sub> <sup>2-</sup> ]
Pa(V)	Not ion exchange	Pa(IV) sorption greater than Pa(V) sorption	Strong hydrolysis behavior; PaO(OH) <sup>2+</sup> , PaO(OH) <sub>2</sub> <sup>+</sup>	Not important		
U(VI)		U(IV) sorption greater than U(VI) sorption	UO <sub>2</sub> (CO <sub>3</sub> ) <sub>2</sub> <sup>2-</sup> , UO <sub>2</sub> (CO <sub>3</sub> ) <sub>3</sub> <sup>4-</sup> , UO <sub>2</sub> CO <sub>3</sub> <sup>0</sup> , UO <sub>2</sub> (OH) <sub>3</sub> <sup>-</sup> , UO <sub>2</sub> (OH) <sub>2</sub> <sup>0</sup>		pH dependence of sorption similar to Am(III)	Sorption decreases with increasing [CO <sub>3</sub> <sup>2-</sup> ]
Np(V)			Strong hydrolysis			

Radionuclide Sorbate and Oxidation State(s) at YMP	Sorption Mechanisms	Redox Effects	Sorbate Speciation	Ionic Strength Effects	pH Effects	pCO <sub>2</sub> Effects
Pu(IV, V, VI)	At lower pH, cationic species sorb by cation exchange; at higher pH, anionic carbonate species sorb by exchange with surface hydroxyl or carbonate groups; neutral species sorb by surface complexation	Sorption of reduced species greater than oxidized species	Strong hydrolysis; forms strong carbonate complexes; Pu(IV) may form polynuclear complexes; Pu(OH) <sub>2</sub> (CO <sub>3</sub> ) <sub>2</sub> <sup>2-</sup> , Pu(OH) <sub>4</sub> <sup>0</sup>		pH dependence of sorption similar to Am(III)	
Am(III)	at lower pH cations sorb by cation exchange; Anionic carbonate complexes sorb through exchange of carbonate with surface hydroxyl groups on oxides	Not important	Strong hydrolysis; forms strong carbonate complexes; Am(OH)(CO <sub>3</sub> ) <sup>0</sup> , Am(OH)(CO <sub>3</sub> ) <sub>2</sub> <sup>2-</sup> , Am(CO <sub>3</sub> ) <sup>+</sup> , Am(CO <sub>3</sub> ) <sub>2</sub> <sup>-</sup>		Sorption highest at pH 7-8 due to neutral complexes, e.g., Am(OH) <sub>3</sub> <sup>0</sup> ; K <sub>d</sub> decreases above pH 9 because of anionic species	Anionic species (di-carbonato) at higher pH (8.6) results in decreased K <sub>d</sub>

Table XVI-2. YMP Groundwater Compositions, Compared to NAGRA Groundwater (and Porewater) Compositions

Parameters	Crystalline Rock		Valanginian Marl		Bentonite	YMP*
	West-area Water	East-area Water	NaCl Water	NaHCO <sub>3</sub> Water	Porewater	J-13
Na <sup>+</sup>	14000	8000	490000	20000	80000	1990
K <sup>+</sup>	200	100	700	51	170	129
Ca <sup>2+</sup>	400	300	4500	57	11	324
Cl <sup>-</sup>	4000	700	470000	300	300	201
HCO <sub>3</sub> <sup>-</sup>	5000	5000	4000	16000	52000	2,090 (TC)
SO <sub>4</sub> <sup>2-</sup>	3000	1000	10.7	100	4500	192
Eh (mV)	-180	-30	-125	-125	-400	na
pH	7.7	7.7	7.5	8.3	9	na
ionic strength (M)	0.02	0.01	0.2	0.02	0.08	na

Table XVI-3. Summary of Sorption Data Developed by NAGRA for Bentonite, Crystalline Rock, and Marl

Radionuclide Sorbate and Oxidation State(s) at YMP	NAGRA Database	NAGRA Rock K <sub>d</sub> (mL/g) (specific reference)	NAGRA Mineral K <sub>d</sub> (mL/g)
Sr(II)	461 entries; 39 references	1,000 (p. Sr-11)	smectite = 20; oxides, quartz = 0
Cs(I)	516 entries; 41 references	1,000 (p. Cs-11)	smectite = 2,000; oxides, quartz = 40
Th(IV)	79 entries; 22 references	5,000 p. Th-7)	smectite = 2,000; oxides, quartz = 1,000
Pa(V)	21 entries; 12 references	1,000 (p. Pa-3)	NAGRA uses Zr(IV) as analog for Pa(IV); use Np(V) for Pa(V) for YMP
U(VI)	382 entries; 32 references	5,000 (p. U-7)	smectite = 100; oxides, quartz = 20
Np(V)	389 entries; 53 references	5,000 (p. Np-8)	smectite = 100; oxides, quartz = 20
Pu(IV, V, VI)	298 entries; 25 references	5,000 (p. Pu-10)	smectite = 1,000; oxides, quartz = 200
Am(III)	198 entries; 34 references	5,000 (p. Am-9)	smectite = 10,000; oxides, quartz = 1,000

Table XVI-4. Summary of Sorption Data Developed by EPA (1999)

Radionuclide Sorbate and Oxidation State(s) at YMP	Database	Category selected: Smectite colloid $K_d$ ; Iron-(hydr)oxide colloid $K_d$	Range: Minimum to Maximum (geom. mean): Smectite $K_d$ (mL/g); Iron-(hydr)oxide $K_d$ (mL/g)
Sr(II)	63 entries (166 in Appendix)	high clay (20-60 wt%); pH 8-10; low clay (<4 wt%); pH 8-10	300 to 1,700 (714); 3 to 120 (19)
Cs(I)	177 $K_d$ values	high clay (20-60 wt%) low clay (<4 wt%)	80 to 26,700 (1,462); 30 to 9,000 (520)
Th(IV)	17 entries	pH 8-10; [Th] <math>10^{-9}</math> M	20 to 2,000 (200)
Pa(V)	not discussed, no good analog		
U(VI)	20 references	pH 8	0.4 to 250,000 (316)
Np(V)	not discussed, no good analog		
Pu(IV, V, VI)		high clay (51-70 wt%); 3-4 meq/L $\text{CO}_3^{2-}$ ; low clay (<4 wt%); 3-4 meq/L $\text{CO}_3^{2-}$	1,860 to 2,550 (2,178); 80 to 470 (194)
Am(III)	not discussed, no good analog		

Table XV. YMP-specific Data for Sorption of Plutonium and Americium on Colloids: Hematite, Goethite, Ca-montmorillonite, and Silica: (a) Pu(IV), (b) Pu(V), (c) Am(III)

sorbate = <sup>239</sup>Pu(IV)

source	mineral	[colloid] (mg/L)	sorption direction	time (d)	Kd (mL/g * 1000)		mean		J13 actual	J13 simulant
					J13 actual	J13 simulant				
A1	hematite	1	forward	1	270	18000				
A1	hematite	1	forward	2	570	1900				
A1	hematite	1	forward	4	1800	790				
A1	hematite	1	forward	arithmetic mean	880	6897	X	$K_{d,forward} / K_{d,backward}$	0.7	0.5
A5	hematite	1	backward	150	1200	13000	X	$K_{d,backward} / K_{d,forward}$	1.4	1.9
				arithmetic mean	1040	9948				5494

source	mineral	[colloid] (mg/L)	sorption direction	time (d)	Kd (mL/g * 1000)		mean		J13 actual	J13 simulant
					J13 actual	J13 simulant				
A2	goethite	1	forward	1	1.9	12				
A2	goethite	1	forward	2	2.3	7.1				
A2	goethite	1	forward	4	1.5	18				
A2	goethite	1	forward	arithmetic mean	1.9	12	X	$K_{d,forward} / K_{d,backward}$	0.9	0.3
A5	goethite	1	backward	150	2.1	49	X	$K_{d,backward} / K_{d,forward}$	1.1	4.0
				arithmetic mean	2.0	31				16

source	mineral	[colloid] (mg/L)	sorption direction	time (d)	Kd (mL/g * 1000)		mean		J13 actual	J13 simulant
					J13 actual	J13 simulant				
A3	Ca-montmorillonite	1	forward	1	5.3	180				
A3	Ca-montmorillonite	1	forward	2	3.7	240				
A3	Ca-montmorillonite	1	forward	4	3.5	140				
A3	Ca-montmorillonite	1	forward	10	3.3	190				
A3	Ca-montmorillonite	1	forward	arithmetic mean	4.0	188	X	$K_{d,forward} / K_{d,backward}$	2.8	64.7
A5	Ca-montmorillonite	1	backward	150	1.4	2.9	X	$K_{d,backward} / K_{d,forward}$	0.4	0.0
				arithmetic mean	2.7	95				49

source	mineral	[colloid] (mg/L)	sorption direction	time (d)	Kd (mL/g * 1000)		mean		J13 actual	J13 simulant
					J13 actual	J13 simulant				
A4	silica-PST-1	1	forward	1	3.4	7.7				
A4	silica-PST-1	1	forward	2	3.5	10				
A4	silica-PST-1	1	forward	4	4.0	16				
A4	silica-PST-1	1	forward	10	4.9	30				
A4	silica-PST-1	1	forward	arithmetic mean	4.0	16	X	$K_{d,forward} / K_{d,backward}$	1.4	2.8
A5	silica-PST-1	1	backward	150	2.8	5.7	X	$K_{d,backward} / K_{d,forward}$	0.7	0.4
				arithmetic mean	3.4	11				7.1

Table XVI-5. YMP-specific Data for Sorption of Plutonium and Americium on Colloids: Hematite, Goethite, Ca-montmorillonite, and Silica: (a) Pu(IV), (b) Pu(V), (c) Am(III)

sorbate = <sup>239</sup>Pu(V)

source	mineral	[colloid] (mg/L)	sorption direction	time (d)	Kd (mL/g * 1000)		mean			
					J13 actual	J13 simulant				
A1	hematite	1	forward	1	10	2100				
A1	hematite	1	forward	2	19	1300				
A1	hematite	1	forward	4	200	430				
A1	hematite	1	forward	arithmetic mean	76	1277	X	$K_{d,forward} / K_{d,backward}$	0.2	0.7
A5	hematite	1	backward	150	430	1800	X	$K_{d,backward} / K_{d,forward}$	5.6	1.4
B1	hematite	200	forward	1	23	150				
B1	hematite	200	forward	2	75	170				
B1	hematite	200	forward	4	97	700				
B1	hematite	200	forward	10	110	120				
B1	hematite	200	forward	arithmetic mean	94	330	X			
				arithmetic mean	200	1136				668

source	mineral	[colloid] (mg/L)	sorption direction	time (d)	Kd (mL/g * 1000)		mean			
					J13 actual	J13 simulant				
A2	goethite	1	forward	1	3.5	77				
A2	goethite	1	forward	2	6.0	760				
A2	goethite	1	forward	4	8.7	140				
A2	goethite	1	forward	arithmetic mean	6.1	326	X	$K_{d,forward} / K_{d,backward}$	0.3	3.0
A5	goethite	1	backward	150	18	110	X	$K_{d,backward} / K_{d,forward}$	3.0	0.3
				arithmetic mean	12	218				115

source	mineral	[colloid] (mg/L)	sorption direction	time (d)	Kd (mL/g * 1000)		mean			
					J13 actual	J13 simulant				
A3	Ca-montmorillonite	1	forward	1	4.2	8.3				
A3	Ca-montmorillonite	1	forward	2	5.1	13				
A3	Ca-montmorillonite	1	forward	4	6.4	26				
A3	Ca-montmorillonite	1	forward	10	10	47				
A3	Ca-montmorillonite	1	forward	arithmetic mean	6.4	24	X	$K_{d,forward} / K_{d,backward}$	0.4	3.4
A5	Ca-montmorillonite	1	backward	150	17	7.0	X	$K_{d,backward} / K_{d,forward}$	2.7	0.3
B1	Ca-montmorillonite	200	forward	1	0.8	1.1				
B1	Ca-montmorillonite	200	forward	2	1.0	1.2				
B1	Ca-montmorillonite	200	forward	4	4.0	1.7				
B1	Ca-montmorillonite	200	forward	10	5.8	6.5				
B1	Ca-montmorillonite	200	forward	arithmetic mean	2.9	2.6	X			
				arithmetic mean	8.8	11				10

Table XVI-3. YMP-specific Data for Sorption of Plutonium and Americium on Colloidal Hematite, Goethite, Ca-montmorillonite, and Silica: (a) Pu(IV), (b) Pu(V), (c) Am(III)

source	mineral	[colloid] (mg/L)	sorption direction	time (d)	Kd (mL/g * 1000)		mean
					J13 actual	J13 simulant	
A4	silica-PST-1	1	forward	1	0.6	0.4	
A4	silica-PST-1	1	forward	2	0.8	0.9	
A4	silica-PST-1	1	forward	4	1.5	1.8	
A4	silica-PST-1	1	forward	10	2.2	2.0	
A4	silica-PST-1	1	forward	arithmetic mean	1.3	1.3 X	$K_{d,forward} / K_{d,backward}$ 0.3 0.1
A5	silica-PST-1	1	backward	150	4.1	24 X	$K_{d,backward} / K_{d,forward}$ 3.2 18.9
B1	silica-PST-1	200	forward	1	5.5	10	
B1	silica-PST-1	200	forward	2	5.8	10	
B1	silica-PST-1	200	forward	4	6.7	12	
B1	silica-PST-1	200	forward	10	8.1	15	
B1	silica-PST-1	200	forward	arithmetic mean	6.5	12 X	
				arithmetic mean	4.0	12	8

sorbate = 241Am

source	mineral	[colloid] (mg/L)	sorption direction	time (d)	Kd (mL/g * 1000)		mean
					J13 actual	J13 simulant	
B2	hematite	200	forward	1	270	200	
B2	hematite	200	forward	2	200	510	
B2	hematite	200	forward	4	320	6200	
B2	hematite	200	forward	10	79	120	
B2	hematite	200	forward	arithmetic mean	217	1758 X	$K_{d,forward} / K_{d,backward}$ 4.3 9.3
B3	hematite	200	backward	42	51	190 X	$K_{d,backward} / K_{d,forward}$ 0.2 0.1
				arithmetic mean	134	974	554

source	mineral	[colloid] (mg/L)	sorption direction	time (d)	Kd (mL/g * 1000)		mean
					J13 actual	J13 simulant	
B2	Ca-montmorillonite	200	forward	1	24	46	
B2	Ca-montmorillonite	200	forward	2	65	110	
B2	Ca-montmorillonite	200	forward	4	100	100	
B2	Ca-montmorillonite	200	forward	10	14	23	
B2	Ca-montmorillonite	200	forward	arithmetic mean	51	70 X	$K_{d,forward} / K_{d,backward}$ 3.6 7.2
B3	Ca-montmorillonite	200	backward	42	14	10 X	$K_{d,backward} / K_{d,forward}$ 0.3 0.1
				arithmetic mean	32	40	36

source	mineral	[colloid] (mg/L)	sorption direction	time (d)	Kd (mL/g * 1000)		mean
					J13 actual	J13 simulant	
B2	Silica-PST-1	200	forward	1	7.4	5.0	
B2	Silica-PST-1	200	forward	2	21	32	
B2	Silica-PST-1	200	forward	4	4.6	20	
B2	Silica-PST-1	200	forward	10	12	5.6	
B2	Silica-PST-1	200	forward	arithmetic mean	11	16 X	$K_{d,forward} / K_{d,backward}$ 0.9 1.6
B3	Silica-PST-1	200	backward	42	12	10 X	$K_{d,backward} / K_{d,forward}$ 1.1 0.6
				arithmetic mean	12	13	12

Table XVI-6. Summary of Sorption Data

Radionuclide Sorbate and Oxidation State(s) at YMP	$K_d$ s from CRWMS M&O (2000b) (Table 16 – $K_d$ s for SZ units): Devitrified tuff (min – max) Iron-(Hydr)oxides (min – max)	CRWMS M&O (2000b) – Minimum $K_d$ approach (Section 6.4)	NAGRA Data Set (Stenhouse 1995)
Sr(II)	10 – 200 0 – 30	>100	not discussed
Cs(I)	20 – 1000 0 – 500	>100	not discussed
Th(IV)	(see Am)	?	not discussed
Pa(V)	0 – 100 500 – 1000	like Np(V)	not discussed
U(VI)	0 – 5 100 – 1000	quartz – 0.1 to 0.07 from pH 7 to 8.5 (Table 4)	not discussed
Np(V)	0 – 10 0 – 100	montmorillonite = 30; hematite = 1,800 (Figure 6)	not discussed
Pu(IV, V, VI)	5 – 150 1000 – 5000	hematite > montmorillonite > quartz; >10,000 (Table 1)	iron-(hydr)oxides = $7 \times 10^4$ ; Ca-montmorillonite = $3 \times 10^4$
Am(III)	100 – 2000 1000 – 5000	>100	hematite = $6 \times 10^5$ ; Ca-montmorillonite = $4 \times 10^4$

Table XVI-7. Recommendations for PA

Radionuclide Sorbate and Oxidation State(s) at YMP	Recommended $K_d$ (mL/g) Iron-(hydr)oxide Colloids Smectite Colloids	Source
Sr(II)	200 30	Maximum values developed in Conca's UZ transport AMR, for devitrified tuff and iron-(hydr)oxides, respectively, for saturated zone units.
Cs(I)	1000 500	as above
Th(IV)	(use same values as developed for Am)	as above
Pa(V)	100 1000	as above
U(VI)	5 1000	as above
Np(V)	10 100	as above
Pu(IV, V, VI)	70,000 30,000	Values from NAGRA data compendium (Stenhouse 1995)
Am(III)	600,000 40,000	Values from NAGRA data compendium (Stenhouse 1995)